Development of Efficient Carbon-Carbon Bond Forming Reactions Using a ppb to ppm Loading Amount of a Palladium NNC-Pincer Complex

Shun Ichii

The Graduate University for Advanced Studies,
SOKENDAI
Graduate School of Physical Sciences
Department of Functional Molecular Science

Table of Contents

General Introduction

Transition-metal-catalyzed organic transformations are indispensable means of chemical syntheses today, among which palladium-catalyzed reactions have been recognized as the most powerful methods in modern organic synthesis. Palladium-catalyzed reactions have been extensively studied since 1970s, and a variety of unique and useful carbon-carbon bond forming reactions including Mizoroki-Heck,[1] Negishi,[2] Migita-Kosugi-Stille,[3] Suzuki-Miyaura,[4] Sonogashira,[5] and Hiyama coupling reactions[6] have been developed so far. With the advent of "cross-coupling", the chemistry of sp^2 carbon-sp^2 carbon bond formation with haloarenes has seen an increase in interest and importance over the past several decades. Indeed, a wide variety of pharmaceuticals, bioactive compounds, functional materials, etc. have been efficiently synthesized by utilizing the cross-coupling reactions.[7] Because of these achievements, Richard F. Heck, Ei-ichi Negishi, and Akira Suzuki were awarded the 2010 Nobel Prize in Chemistry for developing palladium-catalyzed cross-coupling reactions.

However, despite the high synthetic utility, problems associated with the practical use of palladium lies in its toxicity and low-earth abundance. In general, a mol percent (parts-per-hundred)-level loading of a palladium complex is often required to promote the intended reactions with high efficiency under homogeneous conditions, where, especially for preparing pharmaceuticals as well as functional (electronic, optical, etc.) materials, palladium metal contaminants have to be removed from the products (e.g. the permissible level of Pd contaminants in oral drugs is 10 ppm or less[8]) resulting in complicated and costly

manipulations. Reducing the loading of palladium catalysts would solve these difficulties.

In this context, the development of efficient catalyst systems, which work at mol ppb (parts-per-billion) to mol ppm (parts-per-million) levels of palladium, i.e. 10^4–10^7 higher catalytic performance compared to the conventional mol percent catalysis, is highly desirable. To date, many research groups have focused on the development of catalyst systems which can work at ppb to ppm levels of palladium.[9] Representative examples are shown in below.

Palladacycles

An early discovery of palladium catalysis at parts per million levels is made by Herrmann and Beller *et al.*, who described the use of palladacycle **1** in 1995.[10]

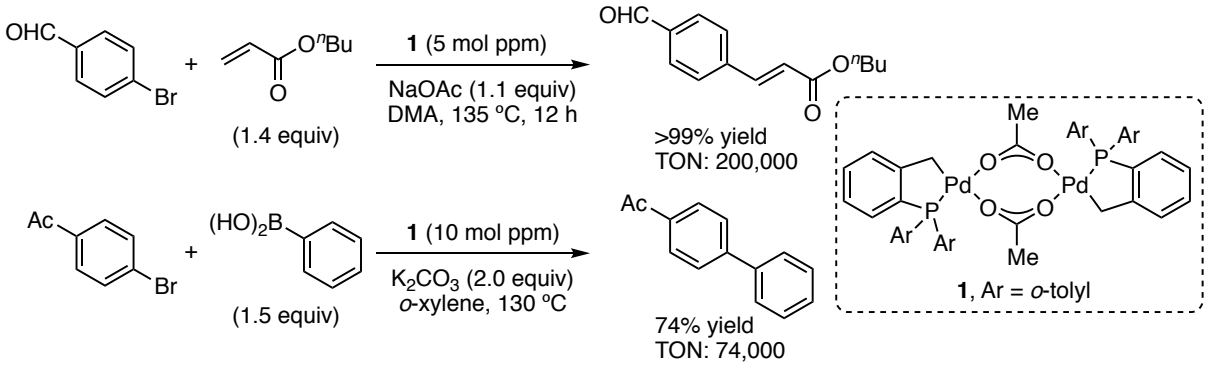

Scheme 1. Heck and Suzuki Reactions Catalyzed by Palladacyle **1**

5–10 mol ppm loading amounts of palladacycle **1** catalyzed the Mizoroki-Heck reaction[10a] and the Suzuki-Miyaura coupling reaction,[10b] where the total turnover number reached to 200,000 and 74,000, respectively (Scheme 1). Since the

discovery of Herrmann's catalyst, palladacycles have attracted a great deal of attention, and new palladacycle catalysts have been developed by many research groups. Examples of high-turnover palladacycles are shown in Scheme 2.

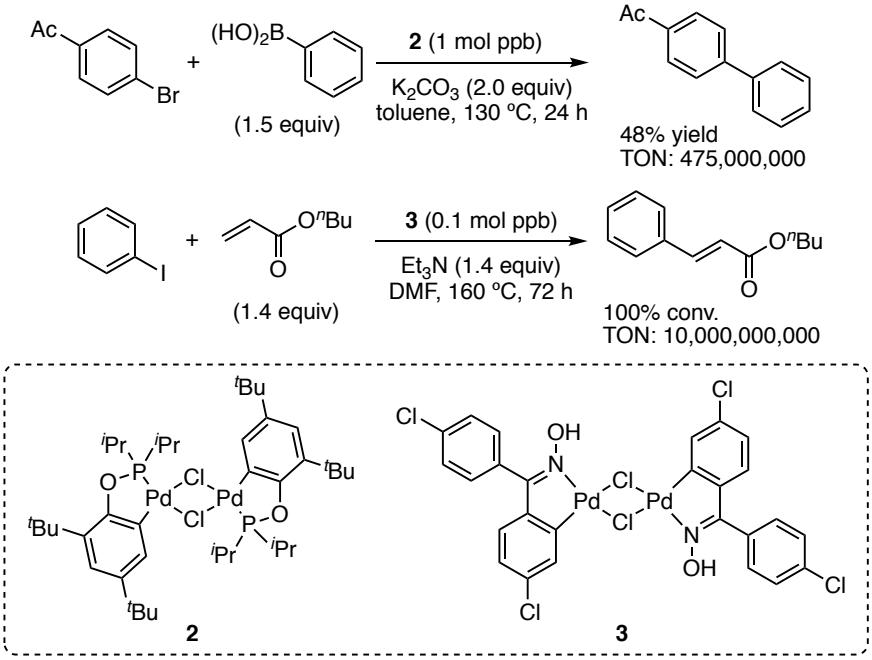

Scheme 2. High-Turnover Palladacycle Catalysts **2** and **3**

Bedford *et al.* reported the Suzuki coupling reaction of 4-bromoacetophenone with phenylboronic acid proceeded in the presence of a 1 mol ppb loading amount of bulky phosphinite-based palladacycle **2** to give the corresponding product in 48% yield (TON: 475,000,000).[11] The hydroxyoxime-derived palladacycle **3** developed by Nájera *et al.* achieved the extremely high turnover number of 10,000,000,000 in the Mizoroki-Heck reaction of iodobenzene with butyl acrylate.[12]

Phosphines and N-Heterocyclic Carbenes as Ligands

The use of phosphines and N-heterocyclic carbenes as ligands is also powerful strategies for reducing catalyst loadings. Phosphines and N-heterocyclic carbenes strongly bind to a metal center because of their high basicity, leading to the long lifetime of catalytically active species.

In 1995, Herrmann and co-workers described the use of an N-heterocyclic carbene **4** as the ligand for the Heck reaction; a 2 mol ppm loading amount of $Pd(dba)_2$/**4** complex gave 66% yield of the coupling product (Scheme 3).[13]

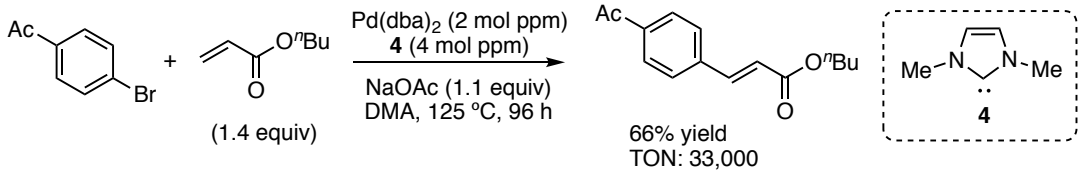

Scheme 3. The Heck Reaction Using an N-Heterocyclic Carbene Complex

Phosphines are one of the most common ligands in transition-metal catalysis, and some of them have led to reduce the catalyst loading at ppb to ppm levels. In a seminal study on the design of phosphine ligands, Buchwald and co-workers developed a bulky and electron-rich mono phosphine ligand **5** and reported its use in the Suzuki-Miyaura coupling reaction (Scheme 4).[14] The coupling of 4-bromoacetophenone with phenylboronic acid proceeded in the presence of palladium acetate (10 mol ppb) and **5** (20 mol ppb) to furnish the coupling product in 91% yield, where the turnover number reached to 91,000,000. Less reactive aromatic chlorides were also suitable substrates in this catalyst system.

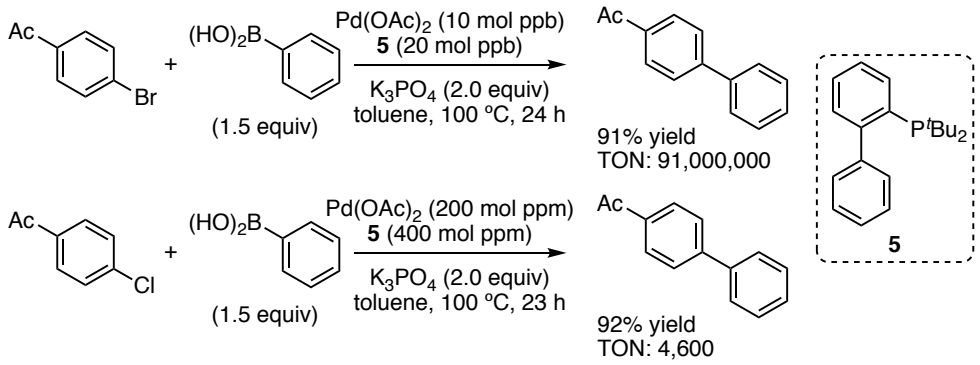

Scheme 4. Suzuki-Miyaura Coupling Using $Pd(OAc)_2$ and a phosphine ligand **5**

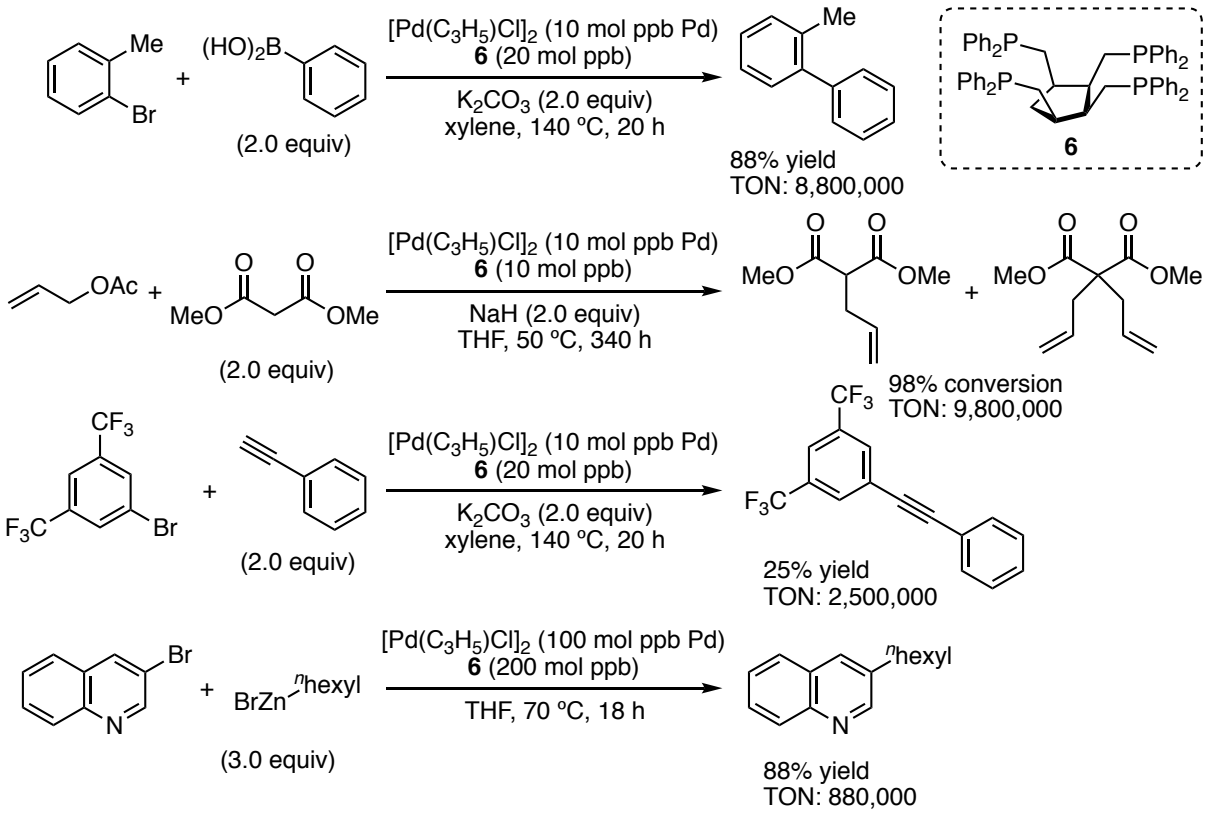

Scheme 5. C-C Bond Forming Reactions Using a Tetradentate Phosphine **6**

Dauset and Santelli and co-workers reported that a tetradentate phosphine ligand **6** is very effective in various palladium-catalyzed carbon-carbon bond forming reactions (Scheme 5).[15] Various coupling reactions including Suzuki-Miyaura,[15a]

allylic alkylation (Tsuji-Trost),[15b] and Sonogashira reactions[15c] efficiently proceeded in the presence of a 10 mol ppb loading amount of η^3-allylpalladium(II) chloride dimer and ligand **6**, and several millions of TON values were achieved in all cases. Additionally, this system was also applicable to the Negishi coupling reaction of an aryl bromides with an alkylzinc reagent using a catalyst loading of 100 mol ppb.[15d]

Stabilizing Agents of Palladium Nanoparticles

On the other hand, simple palladium sources are also capable of reducing the catalyst loading in the presence of stabilizing agents as additives (Scheme 6).

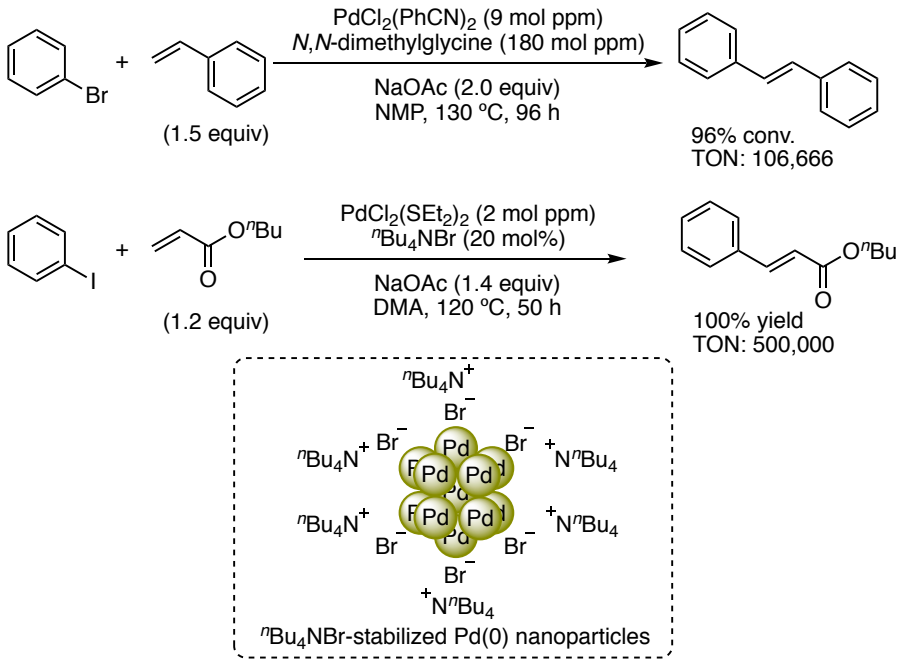

Scheme 6. Mizoroki-Heck Reactions Using Stabilizing Agents as Additives

Reetz *et al.* reported that a 9 mol ppm loading amount of

bis(benzonitrile)palladium(II) chloride efficiently promoted the Heck reaction of bromobenzene with styrene in the presence of *N,N*-dimethylglycine as a stabilizing agent.[16] Similarly, Dupont and co-workers found that tetrabutylammonium bromide ($^{n}Bu_4NBr$) also served as a stabilizer and used it in the Heck reaction of iodobenzene with butyl acrylate at a 2 mol ppm loading of palladium.[17] These stabilizing agents suppress the aggregation of palladium nanoparticles generated in situ from simple palladium sources.

Heterogeneous Catalysts

As mentioned above, carbon-carbon bond forming reactions employing an extremely low catalyst loading of homogeneous palladium catalysts have been energetically developed for a couple of decades. On the other hand, heterogeneous catalysts which can work at ppm levels have recently been described.[18]

Yamada, Uozumi, and co-workers reported that a solid catalyst **7**, prepared by the complexation of poly[(*N*-vinylimidazole)-*co*-(*N*-isopropylacrylamide)$_5$] with ammonium tetrachloropalladate, efficiently catalyzed several carbon-carbon bond forming reactions in aqueous media (Scheme 7).[19] A 66 mol ppm loading amount of **7** promoted the Suzuki-Miyaura coupling reaction using unactivated aryl chlorides as the substrates in water to give the corresponding biaryls quantitatively. The allylic arylations of allyl acetates with arylboronic acids also proceeded smoothly in the presence of 40 mol ppm of **7**. Furthermore, in the reaction of cinnamyl acetate with sodium tetraphenylborate, a 40 mol ppm loading amount

of this catalyst was recovered by filtration and reused five times without loss of its catalytic activity. The target product was obtained quantitively in all batches, where the total turnover number reached to 150,000. Additionally, ICP-AES experiments of the recovered catalyst revealed no leaching of palladium species from the catalyst **7**.

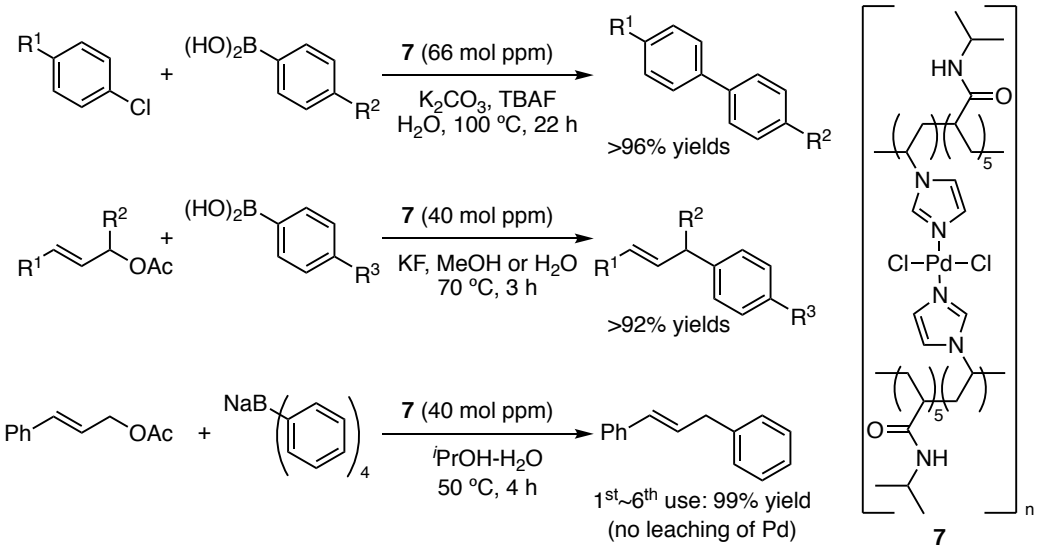

Scheme 7. C-C Bond Forming Reactions in Water Catalyzed by a Polymeric Palladium Catalyst **7**

Yamada, Uozumi, and co-workers also developed a silicon nanowire array-stabilized palladium nanoparticle catalyst **8** (Scheme 8).[20] The solid-supported palladium nanoparticle catalyst **8** showed the highest TON value of 2,000,000 for the Mizoroki-Heck reaction with heterogeneous catalysts. Moreover, this catalyst was applicable to a multi-gram scale synthesis of an antiasthmatic agent (Ozagrel).

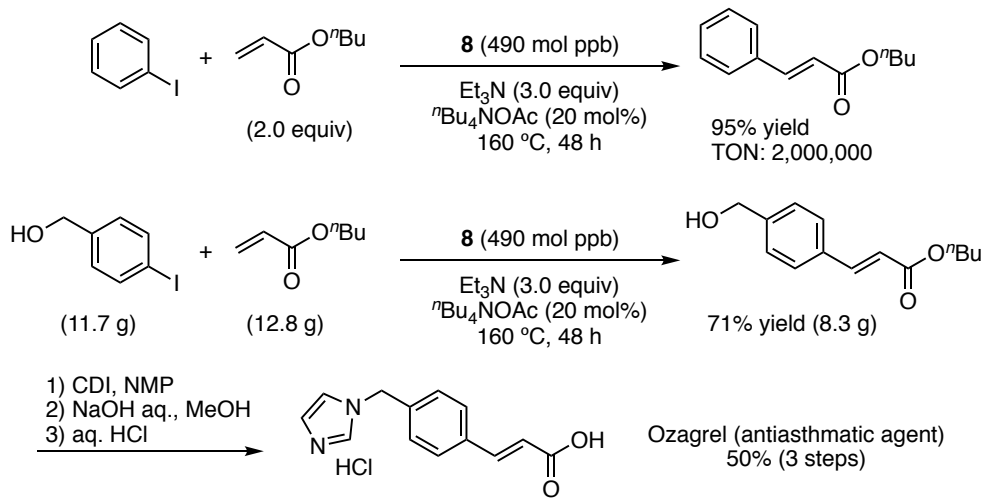

Scheme 8. Mizoroki-Heck Reaction with a Silicon Nanowire Array-Stabilized Palladium Nanoparticle Catalyst **8** and Its Use in the Synthesis of Ozagrel

Although many efficient ppm/ppb-catalytic systems have been reported as described above, the substrate scope as well as practical use of the catalyst systems remains limited. Clearly, while pioneering studies have been made, additional studies on ppm/ppb-catalytic palladium protocol are warranted.

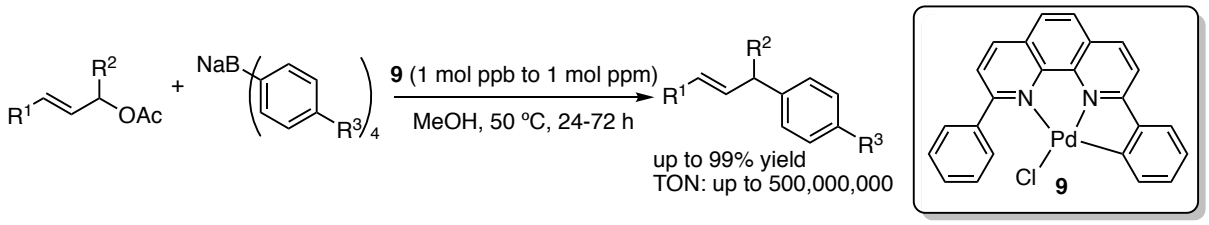

Scheme 9. Allylic Arylation Using 1 mol ppb to 1mol ppm of Pd NNC-Pincer Complex **9**

In this context, Uozumi *et al.* have recently reported that ppb to ppm loading amounts of a palladium NNC-pincer complex **9** catalyzed the allylic arylation of

allyl acetates with sodium tetraarylboronates to give the corresponding products in high yields. When the reaction was carried out with 1 mol ppb of **9**, the turnover number reached to 500,000,000 (Scheme 9).[21]

Inspired by this result, this author conjectured that the palladium NNC-pincer complex **9** might also show a high catalytic activity in other carbon-carbon bond forming reactions. Herein, this author developed efficient carbon-carbon bond forming reactions using ppb to ppm loading amounts of the palladium NNC-pincer complex for expansion of the versatility and usefulness of the catalyst.

This thesis is composed of Chapter 1–3 and General Conclusion.

In Chapter 1, a palladium NNC-pincer complex as an efficient catalyst precursor for the Mizoroki-Heck is described.

In Chapter 2, the Hiyama cross coupling reaction at parts per million levels of Pd is described.

In Chapter 3, mechanistic studies on the Hiyama cross coupling reaction at parts per million levels of Pd is described.

Finally, this author mentions General Conclusion of this thesis

References

(1) (a) T. Mizoroki, K. Mori, A. Ozaki *Bull. Chem. Soc. Jpn.* **1971**, *44*, 581. (b) R. F. Heck, J. P. Nolley, Jr. *J. Org. Chem.* **1972**, *37*, 2320–2322. (c) I. P. Beletskaya, A. V. Cheprakov *Chem. Rev.* **2000**, *100*, 3009–3066.

(2) (a) E. Negishi, A. O. King, N. Okukado *J. Org. Chem.* **1977**, *42*, 1821–1823. (b) E. Negishi *Acc. Chem. Res.* **1982**, *15*, 340–348. (c) P. Knochel, R. D. Singer *Chem. Rev.* **1993**, *93*, 2117–2188.

(3) (a) M. Kosugi, K. Sasazawa, Y. Shimizu, T. Migita *Chem. Lett.* **1977**, *6*, 301–302. (b) D. Milstein, J. K. Stille *J. Am. Chem. Soc.* **1978**, *100*, 3636–3638. (c) J. K. Stille *Angew. Chem. Int. Ed. Engl.* **1986**, *25*, 508–524.

(4) (a) N. Miyaura, K. Yamada, A. Suzuki *Tetrahedron Lett.* **1979**, *20*, 3437–3440. (b) N. Miyaura, T. Yanagi, A. Suzuki *Synth. Commun.* **1981**, *11*, 513–519. (c) N. Miyaura, A. Suzuki *Chem. Rev.* **1995**, *95*, 2457–2483

(5) (a) M. Kosugi, K. Sasazawa, Y. Shimizu, T. Migita *Chem. Lett.* **1977**, *6*, 301–302. (b) D. Milstein, J. K. Stille *J. Am. Chem. Soc.* **1978**, *100*, 3636–3638. (c) J. K. Stille *Angew. Chem. Int. Ed. Engl.* **1986**, *25*, 508–524.

(6) (a) Y. Hatanaka, T. Hiyama *J. Org. Chem.* **1988**, *53*, 918–920. (b) S. E. Denmark, J. H.-C. Liu, *Angew. Chem. Int. Ed.* **2010**, *49*, 2978–2986. (c) Y. Nakao, T. Hiyama, *Chem. Soc. Rev.* **2011**, *40*, 4893–4901. (d) T. Komiyama, Y. Minami, T. Hiyama, T. *ACS Catal.* **2017**, *7*, 631–651.

(7) (a) C. Torborg, M. Beller *Adv. Synth. Catal.* **2009**, *351*, 3027–3043. (b) J. Magano, J. R. Dunetz *Chem. Rev.* **2011**, *111*, 2177–2250. (c) A. F. P. Biajoli,

C. S. Schwalm, J. Limberger, T. S. Claudino, A. L. Monteiro *J. Braz. Chem. Soc.* **2014**, *25*, 2186–2214. (d) S. Xu, E. H. Kim, A. Wei, E.-i. Negishi *Sci. Technol. Adv. Mater.* **2014**, *15*, 044201 (23 pp).

(8) The ICH Q3D guidelines can be downloaded here: http://www.ich.org/products/guidelines/quality/article/qualityguidelines.html (accessed Jan 5, 2018).

(9) For a review on the high-turnover palladium catalysts, see: (a) V. Farina *Adv. Synth. Catal.* **2004**, *346*, 1553–1582. (b) D. Roy, Y. Uoumi *Adv. Synth. Catal.* **2018**, *360*, 602–625.

(10) (a) W. A. Herrmann, C. Brossmer, K. Öfele, C.-P. Reisinger, T. Priermeier, M. Beller, M. Fischer *Angew. Chem. Int. Ed.* **1995**, *34*, 1844–1848. (b) M. Beller, H. Fischer, W. A. Herrmann, K. Öfele, C. Brossmer *Angew. Chem. Int. Ed.* **1995**, *34*, 1848–1849.

(11) R. B. Bedford, S. L. Welch *Chem. Commun.* **2001**, 129–130.

(12) D. A. Alonso, C. Nájera, M. C. Pacheco *Adv. Synth. Catal.* **2002**, *344*, 172–183.

(13) W. A. Herrmann, M. Elison, J. Fischer, C. Köcher, G. R. Artus *Angew. Chem. Int. Ed.* **1995**, *34*, 2371–2374.

(14) J. P. Wolfe, R. A. Singer, B. H. Yang, S. L. Buchwald *J. Am. Chem. Soc.* **1999**, *121*, 9550–9561.

(15) (a) M. Feuerstein, H. Doucet, M. Santelli *Tetrahedron Lett.* **2001**, *42*, 6667–6670. (b) D. Laurenti, M. Feuerstein, G. Pépe, H. Doucet, M. Santelli *J. Org.*

Chem. **2001**, *66*, 1633–1637. (c) M. Feuerstein, F. Berthiol, H. Doucet, M. Santelli *Org. Biomol. Chem*. **2003**, *1*, 2235–2237. (d) I. Kondolff, H. Doucet, M. Santelli *Organometallics* **2006**, *25*, 5219–5222.

(16) M. T. Reetz, E. Westermann, R. Lohmer, G. Lohmer *Tetrahedron Lett.* **1998**, *39*, 8449–8452.

(17) A. S. Gruber, D. Pozebon, A. L. Monteiro, J. Dupont *Tetrahedron Lett.* **2001**, *42*, 7345–7348.

(18) For selected recent examples of supported high-turnover palladium catalysts, see: (a) Z. Dong, Z. Ye *Applied Catalysis A: General* **2015**, *489*, 61–71. (b) S. M. Sarkar, Md. L. Rahman, M. M. Yusoff *New J. Chem.* **2015**, *39*, 3564–3570.

(19) Y. M. A. Yamada, S. M. Sarkar, Y. Uozumi *J. Am. Chem. Soc.* **2012**, *134*, 3190–3198.

(20) Y. M. A. Yamada, Y. Yuyama, T. Sato, S. Fujikawa, Y. Uozumi *Angew. Chem. Int. Ed.* **2014**, *53*, 127–131.

(21) G. Hamasaka, F. Sakurai, Y. Uozumi *Chem. Commun.* **2015**, *51*, 3886–3888.

Chapter 1

A Palladium NNC-Pincer Complex as an Efficient Catalyst Precursor for the Mizoroki-Heck Reaction

Go Hamasaka, Shun Ichii, and Yasuhiro Uozumi

Adv. Synth. Catal. **2018**, *360*, 1833-1840

Introduction

The Mizoroki-Heck reaction is a palladium-catalyzed reaction of aryl halides with alkenes in the presence of a base to give the corresponding substituted olefins (Scheme 1a).

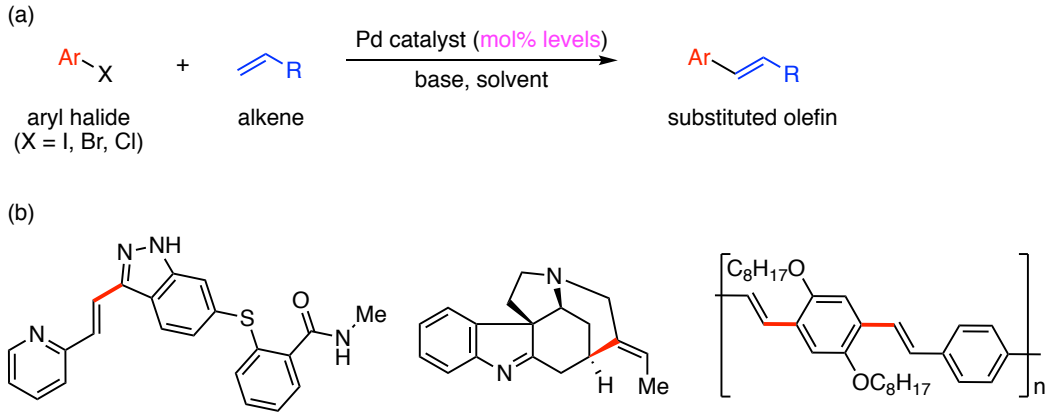

Scheme 1. the Mizoroki-Heck Reaction (a) general chemical equation (b) applications of the reaction

Since the groups of Mizoroki and Heck independently reported the palladium-catalyzed arylation of olefins in the early 1970s,[1] this reaction has been frequently used in the synthesis of natural products, pharmaceuticals, and functional materials because of its high synthetic utility (Scheme 1b).[2] Nevertheless, this reaction still requires a large amount of palladium catalyst (generally 1–10 mol%). Reducing the catalyst loading in this transformation is therefore an important research objective.

Palladium pincer complexes are attracting considerable attention from organic chemists because such catalysts display the required high level of activity in a

variety of catalytic reactions.[3] In particular, several palladium pincer complexes have been used in the Mizoroki–Heck reaction at ppb to ppm loadings.[4] In 1997, Milstein and co-workers reported that a 90 mol ppm loading amount of a palladium PCP-pincer complex **10** catalyzed the Mizoroki-Heck reaction of iodobenzene with methyl acrylate to give the corresponding methyl cinnamate in 95% yield (Scheme 2a).[5]

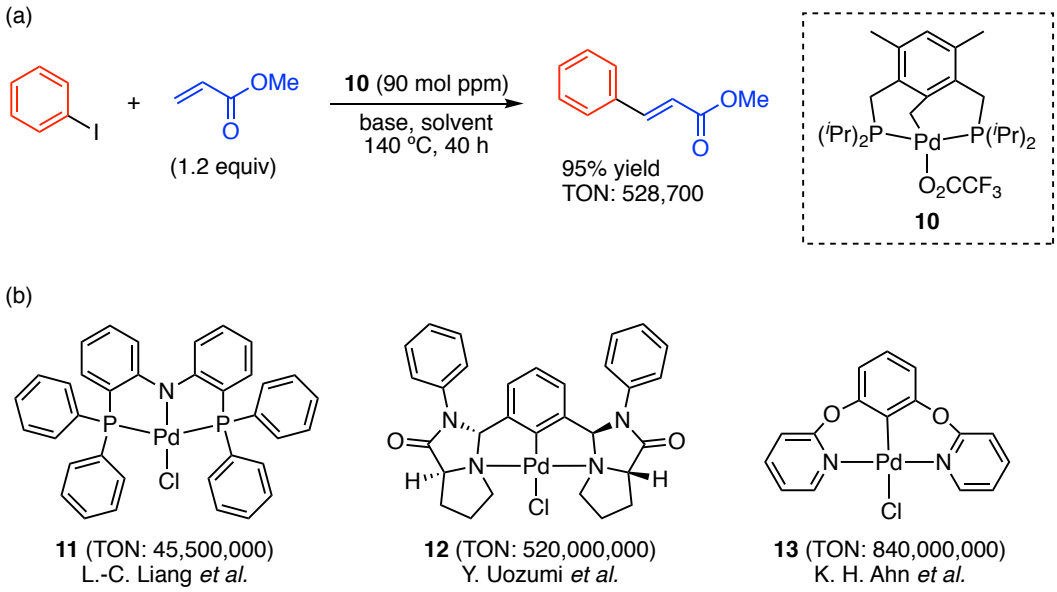

Scheme 2. Palladium Pincer Complexes for the Mizoroki-Heck Reaction (a) Milstein's work (b) high-turnover pincer complexes

Subsequently, various types of palladium pincer complexes which promote the Mizoroki-Heck reaction at ppb to ppm levels have been developed (Scheme 2b).[6] However, the substrate scopes of these catalyst systems are generally too narrow (less than 10 examples in most cases).

In this context, this author decided to apply the palladium-NNC pincer complex

9 to the Mizoroki-Heck reaction with broad substrate scope (38 examples). Moreover, some mechanistic studies were performed to identify a catalytically active species in this reaction system.

Results and Discussion

First, this author screened the reaction conditions for the reaction of iodobenzene (**14a**) with butyl acrylate (**15a**) in the presence of a 1 mol ppm loading of complex **9** at 140 ºC (Table 1).

Table 1. Screening of Bases and Solvents in the Mizoroki-Heck Reaction with 1 mol ppm Complex **9**[a]

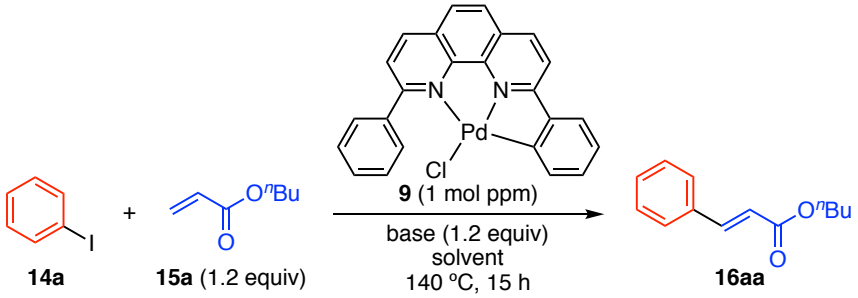

Entry	Base	Solvent	Yield (%)[b]
1	K_2CO_3	NMP	0
2	$NaHCO_3$	NMP	0
3	NaOAc	NMP	45
4	K_3PO_4	NMP	52
5	^{i}Pr$_2$NEt	NMP	23
6	^{n}Bu$_3$N	NMP	100 (99)[c]
7	^{n}Bu$_3$N	DMF	24
8	^{n}Bu$_3$N	DMA	28
9	^{n}Bu$_3$N	hexan-1-ol	24
10	^{n}Bu$_3$N	*m*-xylene	4
11	^{n}Bu$_3$N	PhCN	58
12	^{n}Bu$_3$N	EtO[(CH$_2$)$_2$O]$_2$Et	16

[a] *Reaction conditions*: **9** (1 mol ppm, 1.0×10^{-6} mmol), **14a** (1.0 mmol), **15a** (1.2 mmol), base (1.2 mmol), solvent (1.0 mL), 140 ºC, 15 h. [b] Determined by GC analysis with an internal standard (mesitylene). [c] Isolated yield.

When this author tested various bases in *N*-methylpyrrolidin-2-one (NMP), no reaction took place in the presence of potassium carbonate or sodium bicarbonate (Table 1, entries 1 and 2). When sodium acetate or potassium phosphate was used as the base, moderate yields of butyl cinnamate [**16aa**; butyl (2*E*)-3-phenylacrylate] were obtained (entries 3and 4). The reaction in the presence of *N*,*N*-diisopropylethylamine gave cinnamate **16aa** in 23% yield (entry 5). A quantitative yield of **16aa** was obtained in the presence of tributylamine as the base (entry 6). This author also screened various solvents [*N*,*N*-dimethylformamide (DMF), *N*,*N*-dimethylacetamide (DMA), hexan-1-ol, *m*-xylene, benzonitrile, and diethylene glycol diethyl ether] (entries 7–12), and this author found that NMP was the optimal solvent for this reaction.

This author also examined the catalytic activity of various other palladium catalysts in this reaction (Scheme 3). The cationic palladium NNC-pincer complex **17** showed a lower catalytic activity than complex **9**. Non-substituted, dimethyl, or monophenyl 1,10-phenanthroline palladium complexes **18**–**20** gave cinnamate **16aa** in 35–62% yield. A low yield (<10%) of **16aa** was obtained when the bipyridine-based complexes **21** and **22** were used as catalysts. The 1,10-phenanthroline framework is therefore effective in this reaction. The reaction with bis(acetonitrile)palladium dichloride (**23**) or palladium(II) acetate (**24**) afforded **16aa** in 64 and 70% yield, respectively. The catalytic activity of bis(triphenylphosphine)palladium(II) chloride (**25**) and palladium(II) chloride (**26**) were lower than those of **23** and **24**. Phosphine ligand did not enhance the

catalytic activity. This author also examined the reaction with Nájera's catalyst **27**,[7] which is known as an effective catalyst for the Mizoroki-Heck reaction, and this author obtained **16aa** in 58% yield. During the screening of the catalysts, complex **9** therefore showed the highest catalytic activity.

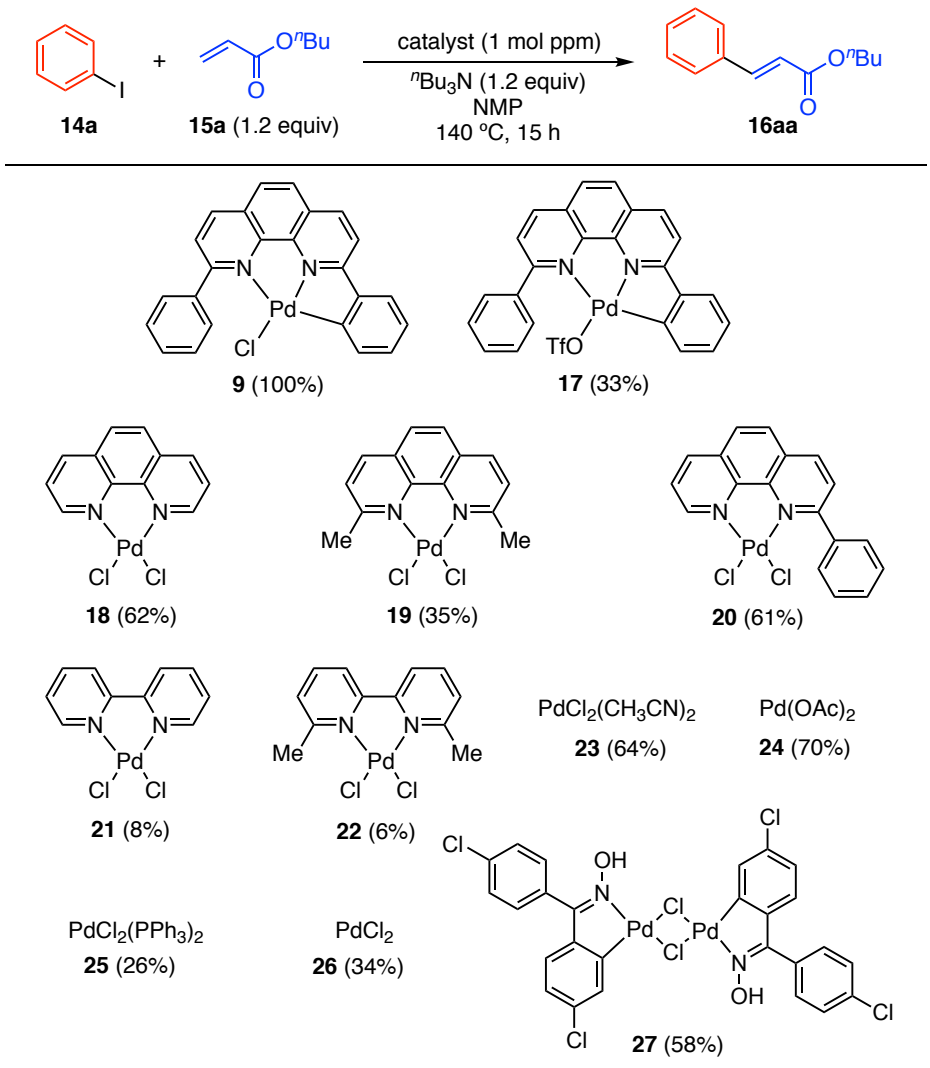

Scheme 3. Screening of Palladium Catalysts in the Mizoroki-Heck Reaction of Iodobenzene (**14a**) with Butyl Acrylate (**15a**)[a]

[a] *Reaction conditions*: catalyst (1 mol ppm, 1.0×10^{-6} mmol), **14a** (1.0 mmol), **15a** (1.2 mmol), $^{n}Bu_3N$ (1.2 mmol), NMP (1.0 mL), 140 °C, 15 h. The yields were determined by GC analysis with an internal standard (mesitylene).

Next, this author performed several experiments to identify the catalytically active species in this reaction. Initially, this author checked the time course of the yield of cinnamate **16aa** in the reaction of iodobenzene (**14a**) with butyl acrylate (**15a**) in the presence of a 1 mol ppm of complex **9** [Figure 1 and equation 1]. An induction period was observed in the initial stages of this reaction (up to 1 h), suggesting that the catalytic active species is generated in situ.

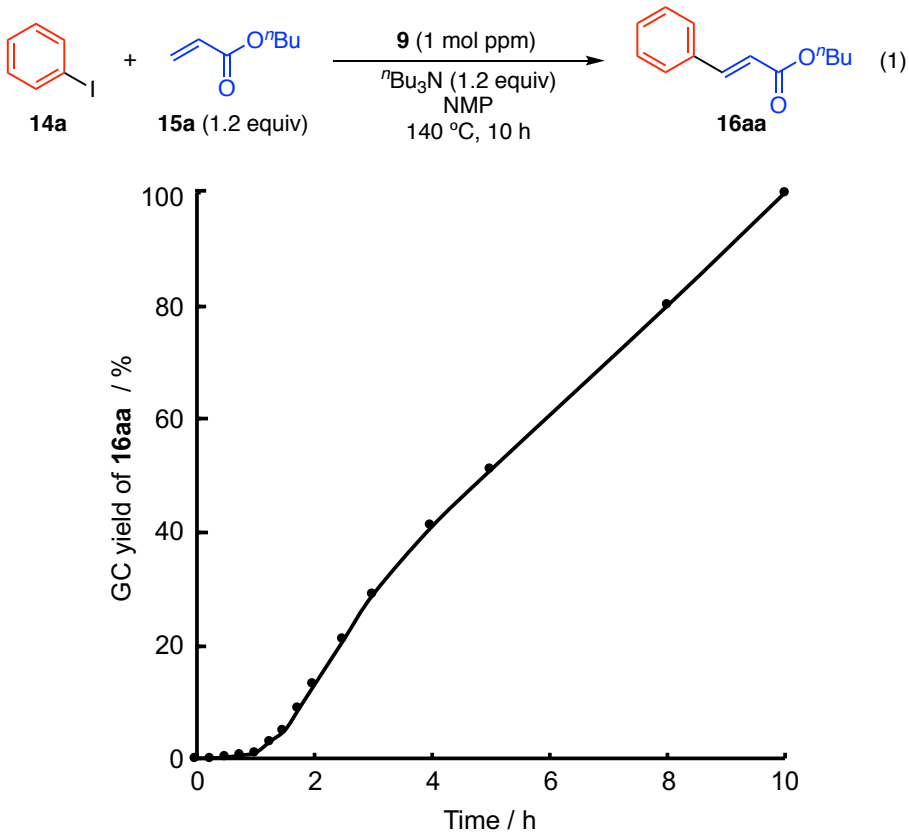

Figure 1. Time Course of the yield of the Reaction of Iodobenzene (**14a**) with Butyl Acrylate (**15a**) under the Standard Conditions (equation 1)

This author next conducted a transmission electron microscopy (TEM) analysis of the reaction mixture after the reaction. Palladium nanoparticles were observed

in the reaction mixture (Figure 2). The average size of these nanoparticles was estimated to be 2.2 ± 0.7 nm. These experimental results showed that complex **9** is a precursor of the actual catalytically active species in this reaction.

(a) (b)

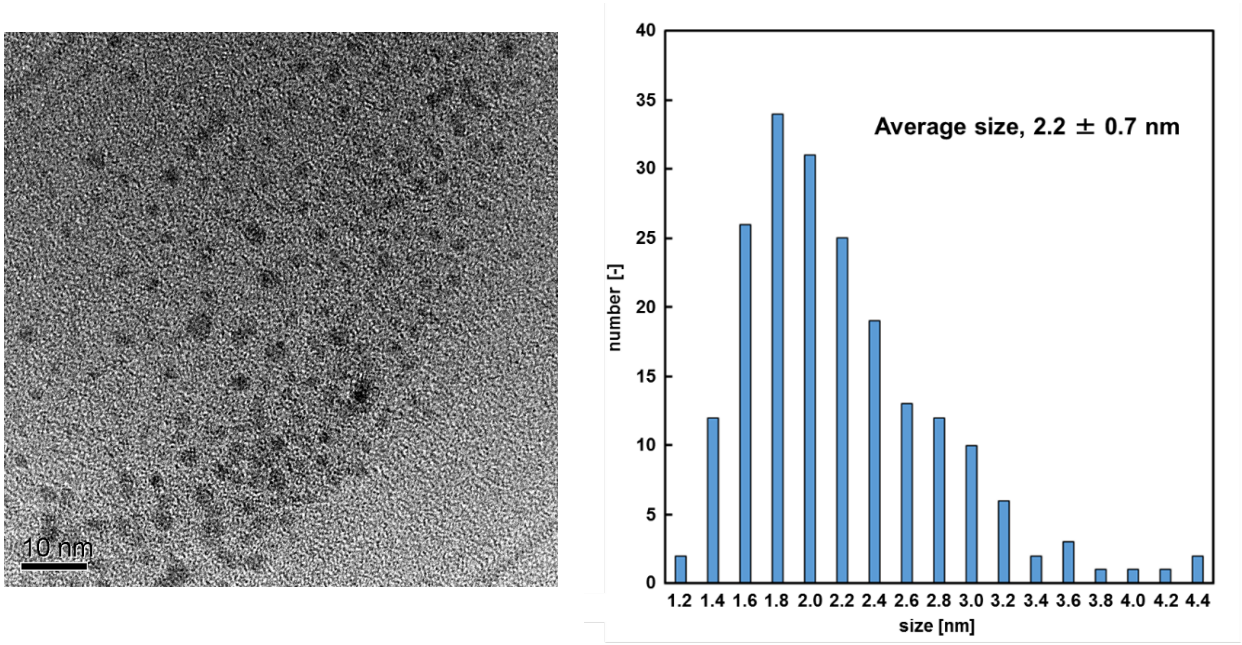

Figure 2. TEM Image of the Reaction Mixture (Table 1, entry 6) (a) A TEM image of the palladium nanoparticles (b) A histogram of the particle size distribution of the palladium nanoparticles (total counts = 200)

To obtain more information on the catalytic active species, a mercury-amalgamation test was carried out.[8] Under the standard reaction conditions (Table 1, entry 6), the addition of one drop of mercury to the reaction mixture at two hours, when the GC yield of **16aa** was 15%, significantly retarded the reaction,

which finally gave **16aa** in 19% GC yield after an additional eight hours [Figure 3 (blue line) and equation 2].

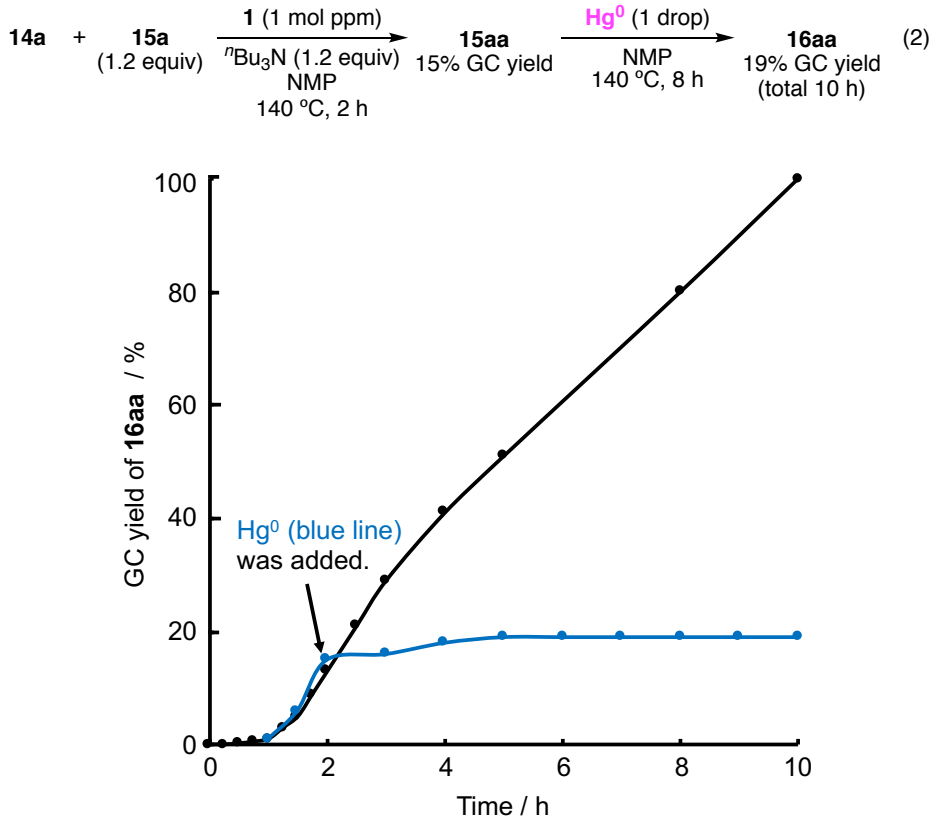

Figure 3. Time Course of the yield of the Reaction of Iodobenzene (**14a**) with Butyl Acrylate (**15a**) in the Presence of Hg^0. (black line; equation 1, blue line; equation 2)

If a ligandless palladium metal species (i.e., a ligandless monomeric palladium species and/or palladium cluster) is generated in situ, the reaction should be inhibited by the amalgamation of this species with Hg. This experimental result indicates that a ligandless palladium species is indeed the catalytically active species in this reaction. Although the TEM observations and the mercury-

amalgamation test suggested that the complex **9** is a precursor of the catalytically active species, it was unclear at this stage whether the catalytically active species consists of palladium clusters or monomeric palladium species.

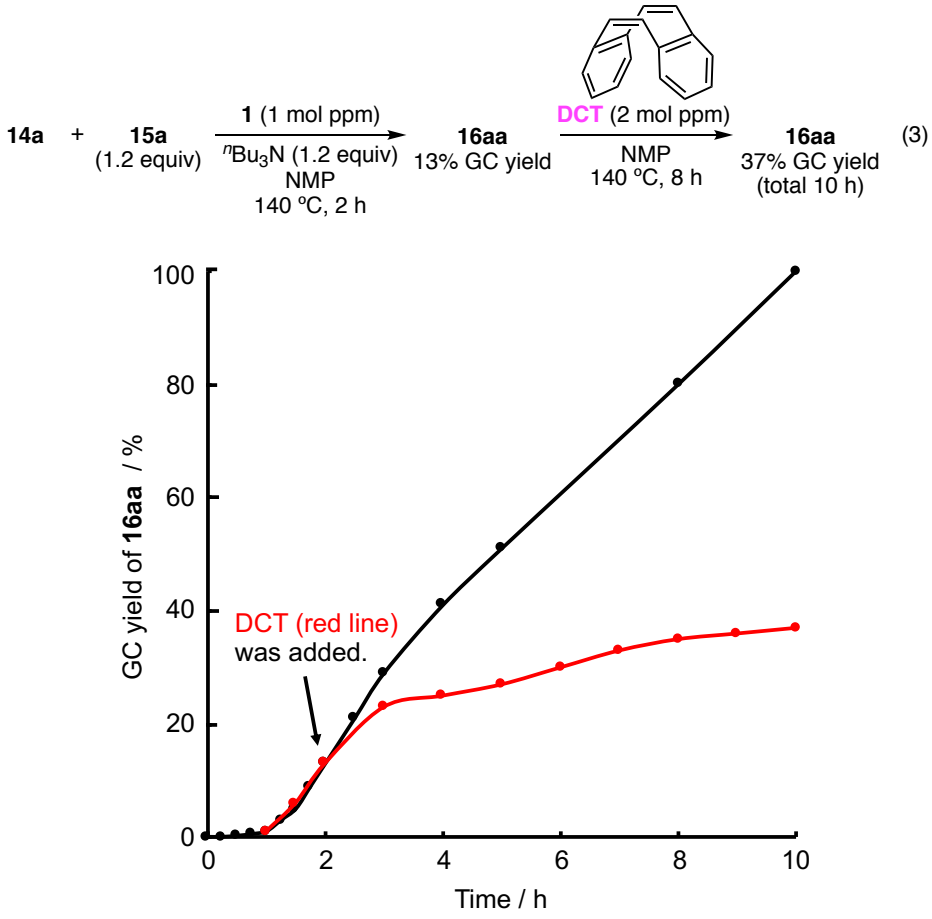

Figure 4. Time Course of the yield of the Reaction of Iodobenzene (**14a**) with Butyl Acrylate (**15a**) in the Presence of DCT. (black line; equation 1, red line; equation 3)

This author therefore performed a Crabtree test [the addition of dibenzo[*a*,*e*]cyclooctene (DCT)].[9] After starting the reaction under the standard conditions (Table 1, entry 6) for 2 h, when the yield of **16aa** was 13%, DCT was

added to the reaction mixture. A suppression of the reaction was then observed (Figure 4 (red line) and equation 3), and the desired product **16aa** was obtained in 37% GC yield after an additional 8 h. It has been reported that DCT coordinates to monomeric palladium species[10] to give a stable and catalytically inactive DCT-Pd complex [Figure 5(a)], whereas DCT cannot coordinate to palladium clusters because of its structural rigidity [Figure 5(b)]. Consequently, the result of the Crabtree test suggests that a monomeric palladium species is involved in this catalytic cycle. If palladium clusters were essential to promote the catalytic process, the Mizoroki-Heck reaction should proceed efficiently in the presence of DCT. Although palladium nanoparticles were observed by the TEM analysis, the Crabtree test suggested that monomeric palladium species are generated under the reaction conditions.

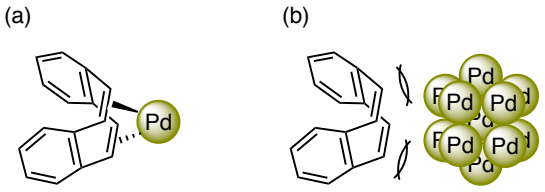

Figure 5. Schematic Structures of DCT (a) with Monomeric Pd Species, (b) with Pd Clusters

From these experimental results, the catalytic cycle shown in Scheme 4 is proposed. Palladium complex **9** is reduced under the thermal conditions to form the monomeric palladium(0) species **A** and/or palladium(0) clusters **E**. An equilibrium between **A** and **E** should exist under the reaction conditions. The

monomeric Pd(0) species **A** promotes the Mizoroki-Heck reaction, and a monomeric palladium(II) species **B** is generated through the reaction of **A** with the haloarene. The usual Mizoroki-Heck process then takes place, giving desired product along with regeneration of **A**. Therefore, complex **9** acts as a good precursor for the catalytically highly active palladium(0) species **A**.

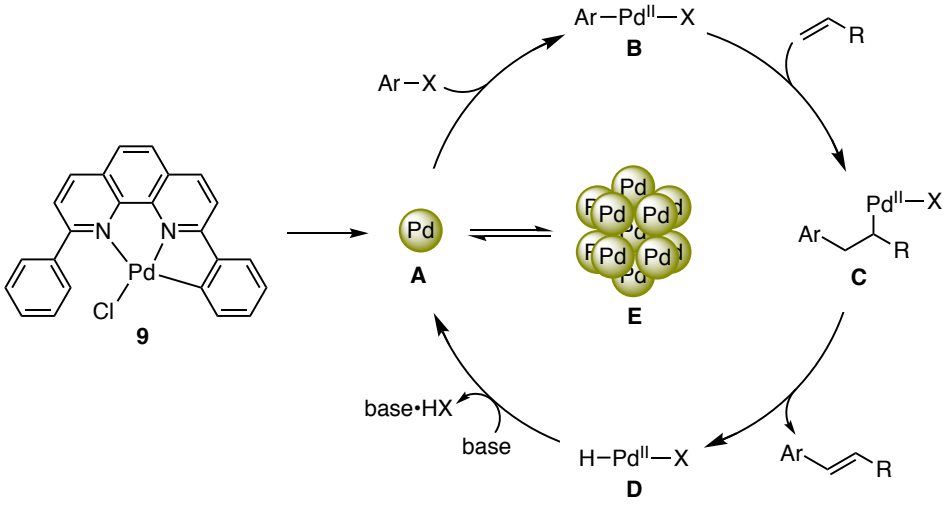

Scheme 4. Proposed Catalytic Cycle

Complex **9** was used in the Mizoroki-Heck reactions of a variety of aryl iodides with alkenes (Scheme 5). The reaction of *p*-, *m*-, and *o*-iodotoluenes (**14b**–**d**) with butyl acrylate (**15a**) in the presence of a 1 mol ppm loading of complex **9** gave the corresponding tolylacrylates **16ba**, **16ca**, and **16da** in high yields. The position of the methyl group on the aromatic ring did not affect the efficiency of the reaction. A variety of iodobenzenes substituted with electron-donating groups (**14e**–**g**) or electron-withdrawing groups (**14h**–**n**) gave the corresponding internal alkenes **16ea**–**na** in high yields.

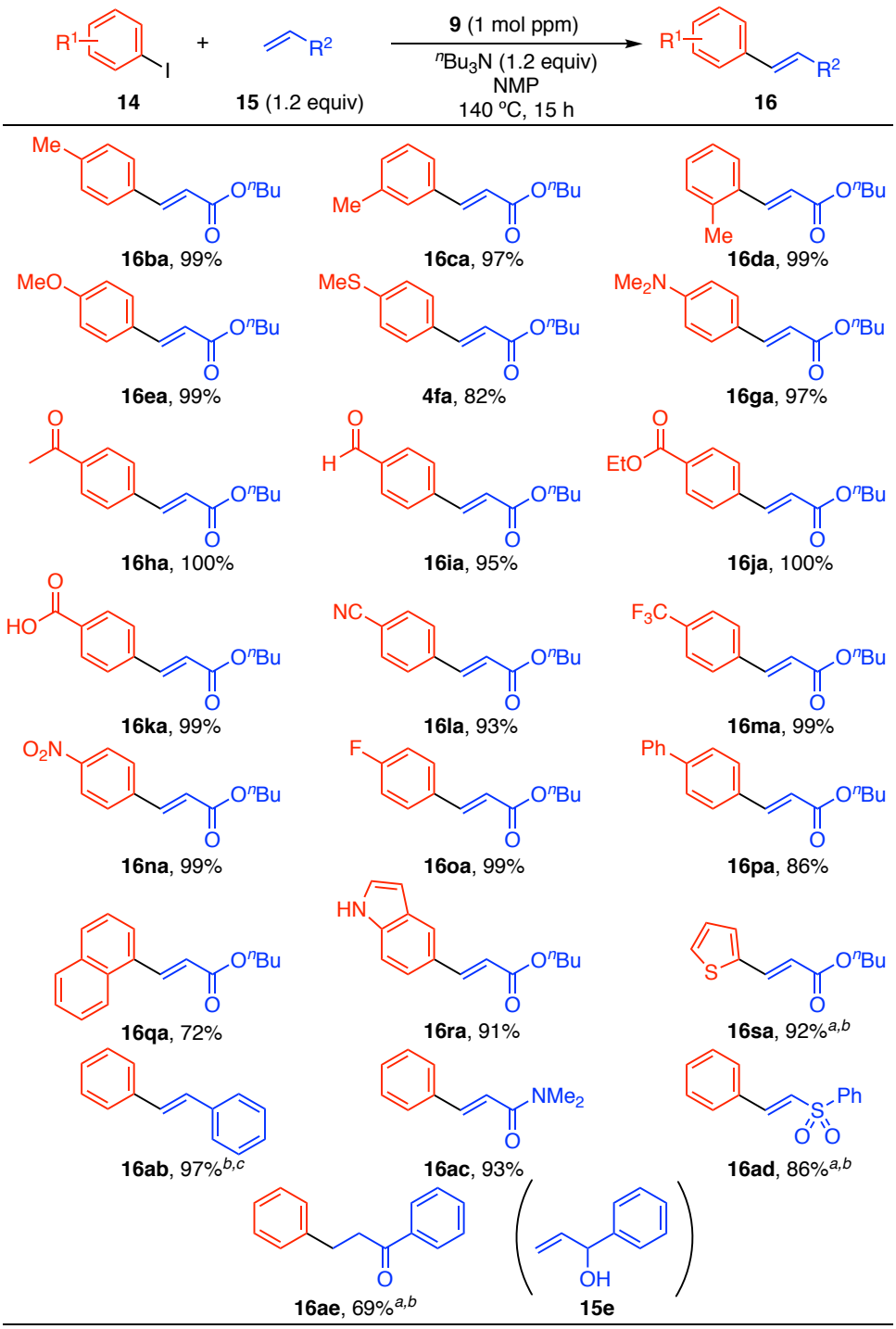

Scheme 5. Scope of the Mizoroki-Heck Reaction of Aryl Iodides **14** with Alkenes **15**

Reaction conditions: **9** (1 mol ppm, 1.0×10^{-6} mmol), **14** (1.0 mmol), **15** (1.2 mmol), $^{n}Bu_3N$ (1.2 mmol), NMP (1.0 mL), 140 ºC, 15 h. The yields refer to isolated products. [a] **9** (10 mol ppm, 1.0×10^{-5} mmol) [b] NaOAc (1.5 mmol) was used instead of $^{n}Bu_3N$. [c] Containing 9% of the α-arylated product.

This reaction system tolerated catalyst-poisoning functionalities such as methylsulfanyl (**16fa**) or dimethylamino (**16ga**) groups. The reactions of 1-fluoro-4-iodobenzene (**14o**), 4-iodobiphenyl (**14p**), and 1-iodonaphthalene (**14q**) with acrylate **15a** gave the corresponding alkenes **16oa**, **16pa**, and **16qa** in 99, 86, and 72% yield, respectively. In this catalytic system, iodoheteroarenes also underwent the reaction. Complex **9** catalyzed the reaction of 5-iodoindole (**14r**) with **15a** to give **4ra** in 91% yield. The reaction of 2-iodothiophene (**14s**), carried out in the presence of 10 mol ppm of complex **9** and NaOAc instead of Bu_3N, gave the desired alkene **16sa** in 92% yield. Next, this author examined the reaction with other terminal alkenes **15b**–**e**. Styrene (**15b**) and *N*,*N*-dimethylacrylamide (**15c**) gave the desired products **16ab** and **16ac**, respectively, in good yields. The reaction of iodobenzene (**14a**) with phenyl vinyl sulfone (**15d**) or 1-phenyl-prop-2-en-1-ol (**3e**) also proceeded in the presence of 10 mol ppm of complex **1** to afford **16ad** and **16ae** in 86 and 69% yield, respectively.

A ppm loading of complex **9** also catalyzed the Mizoroki-Heck reaction of aryl bromides (Scheme 6). The reaction of bromobenzene (**28a**) with butyl acrylate (**15a**) in the presence of a 10 mol ppm loading of complex **9** in NMP at 140 ºC for 48 hours gave alkene **16aa** in 99% isolated yield.[11, 12] 2-Bromonaphthalene (**28b**) and 1-bromopyrene (**28c**) also underwent the reaction to afford the corresponding alkenes **16ta** and **16ua** in 94 and 84% yield, respectively. The reaction of bromobenzenes **28h**, **28v**, and **28w**, containing electron-withdrawing groups, proceeded smoothly to give the corresponding acrylates **16ha**, **16va**, and **16wa** in

good yields. On the other hand, bromobenzenes **28b** and **28e**, containing electron-donating substituents, gave moderate yields of the corresponding products **16ba** and **16ea**. The reaction of 3-bromopyridine (**28x**) with **15a** also failed to proceed efficiently.

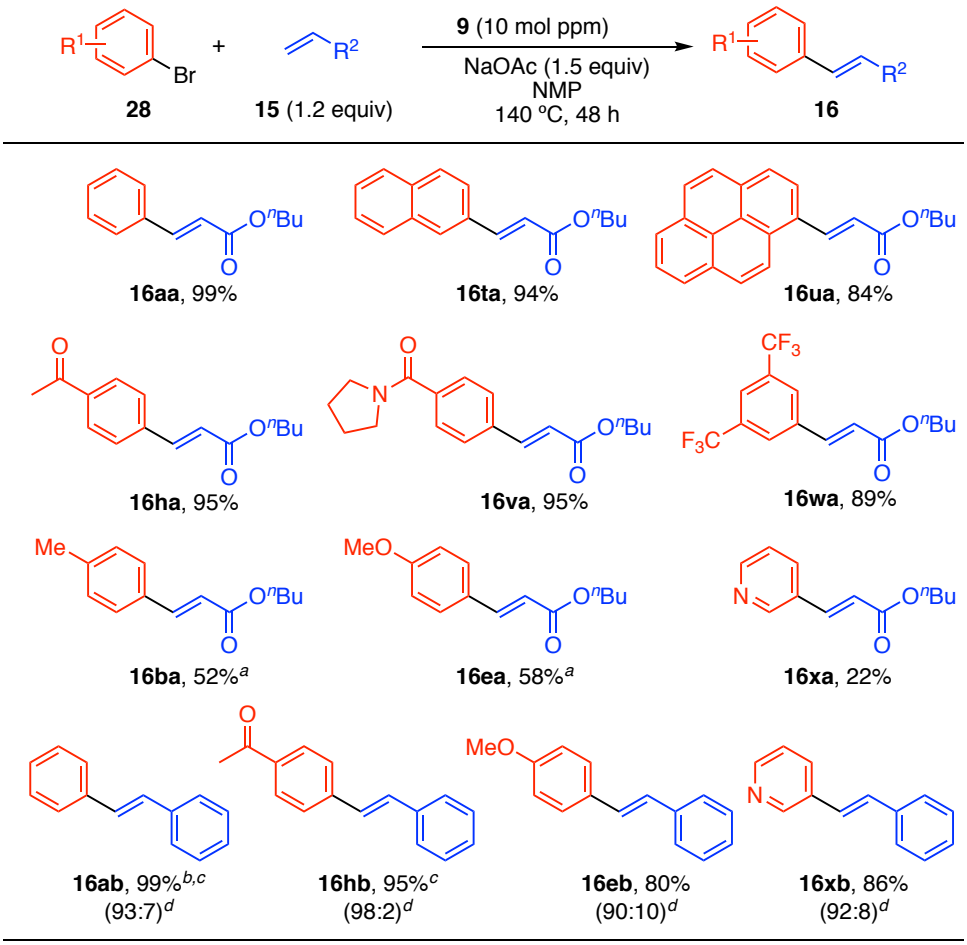

Scheme 6. Scope of the Mizoroki-Heck Reaction of Aryl Bromides **28** with Alkenes **15**

Reaction conditions: **9** (10 mol ppm, 1.0×10^{-5} mmol), **28** (1.0 mmol), **15** (1.2 mmol), NaOAc (1.5 mmol), NMP (1.0 mL), 140 °C, 48 h. The yields refer to isolated products. [a] 160 °C [b] **9** (1 mol ppm, 1.0×10^{-6} mmol) [c] 24 h. [d] The ratio of regioisomers (β arylation/α arylation) was determined by ^{1}H NMR.

When styrene (**15b**) was used as the coupling partner, the reaction efficiency increased dramatically. A lower catalyst loading (1 mol ppm) and a shorter reaction time (24 h) could be achieved in the reactions of bromobenzene (**28a**) and 4-bromoacetophenone (**28h**) with styrene (**15b**), giving the stilbenes **16ab** and **16hb** in 99 and 95% yield, respectively. Whereas the reactions of **28e** and **28x** with **15a** did not proceed efficiently, these compounds reacted efficiently with styrene (**15b**) to give **16eb** and **16xb**, respectively, in good yields.

To demonstrate that the pincer complex works at a ppb loading, this author examined the Mizoroki-Heck reaction of iodobenzene (**14a**) with butyl acrylate (**15a**) in the presence of a 1 mol ppb loading amount of complex **9** (scheme 7) under solvent-free conditions at 160 ºC for 72 h, and cinnamate **16aa** was obtained in 87% yield. In this case, the total turnover number reached to 870,000,000 and the turnover frequency was 3,356 s^{-1}.

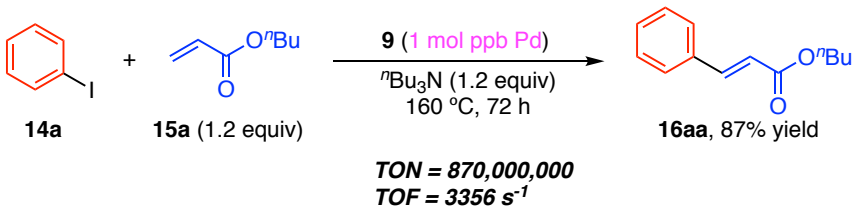

Scheme 7. The Mizoroki-Heck Reaction of Iodobenzene (**14a**) with Butyl Acrylate (**15a**) in the Presence of 1 mol ppb of Complex **9**

This author also applied the catalyst system to the reaction of a less-reactive aryl chloride. Thus, the reaction of 4-chloroacetophenone (**29**) with styrene (**15b**)

proceeded in the presence of 100 ppm loading of **9** in NMP at 160 ºC for 48 hours to give alkene **16hb** in 25% yield (Scheme 8).

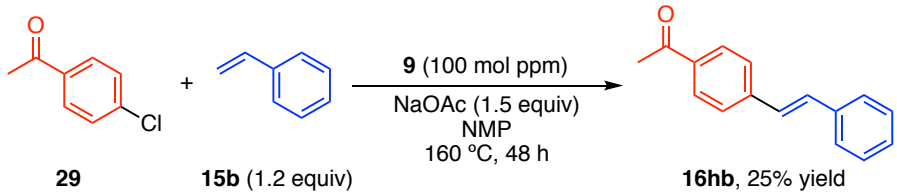

Scheme 8. The Mizoroki-Heck Reaction of 4-Chloroacetophenone (**29**) with Styrene (**15b**)

To demonstrate the utility of the catalytic system, this author used complex **9** in a ten-gram-scale synthesis of the UV-B sunscreen agent octinoxate (**16ef**; 2-ethylhexyl 4-methoxycinnamate)[13] (Scheme 9).

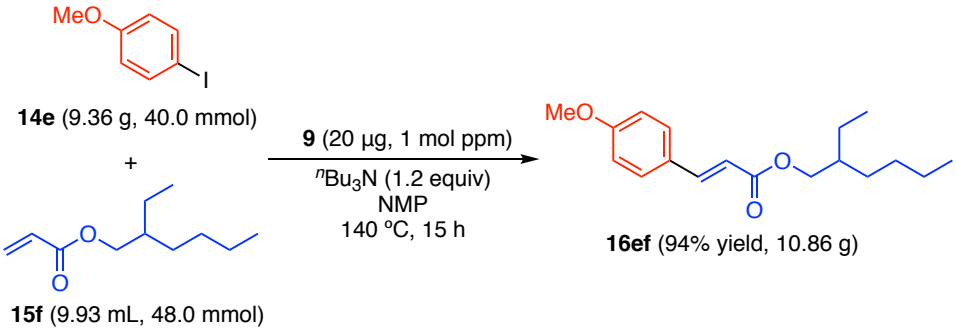

Scheme 9. Ten-Gram-Scale Synthesis of the UV-B Sunscreen Agent Octinoxate (**16ef**) in the Presence of 1 mol ppm Complex **9**

The reaction of 1-iodo-4-methoxybenzene (**14e**; 9.36 g, 40.0 mmol) with acrylate **15f** (9.93 mL, 48.0 mmol) in the presence of 1 mol ppm complex **9** (20

μg) and tributylamine in NMP at 140 ºC for 15 h gave 10.86 g (94%) of Octinoxate (**16ef**). The resulting product **16ef** was tested for metal contamination by ICP-AES analysis to detect palladium. This result indicated that the content of palladium in the product was below 1 weight ppm (< 1 μg Pd/g **16ef**).

Conclusion

In summary, this author has found that complex **9** is a good catalyst precursor for the Mizoroki-Heck reaction. The reaction of aryl halides with activated terminal alkenes in the presence of quite low loadings of complex **9** gave the desired coupling products in excellent yields. In the reaction of iodobenzene with butyl acrylate, the total turnover number and turnover frequency reached 870,000,000 and 3356 s^{-1}, respectively. Reaction rate analyses, transmission electron microscopic measurement of the reaction mixture, and catalyst poisoning tests suggested that the palladium NNC-pincer complex served as a precursor for the generation of a monomeric (single atomic) palladium species. The catalyst was applied in a ten-gram-scale synthesis of the UV-B sunscreen agent octinoxate (2-ethylhexyl 4-methoxycinnamate).

Experimental Section

General Methods. All reactions with oxygen- or moisture-sensitive reagents were performed under a nitrogen atmosphere, nitrogen gas was dried by passage through P_2O_5. Silica gel was purchased from Kanto chemical (Silica gel 60N, spherical neutral, particle size 40-50μm) or Yamazen corporation (Hi-FlashTM Column Silica gel 40 mm 60 Å). NMR spectra were recorded on a JEOL JNM ECS-400 spectrometer (396 MHz for ^{1}H, 100 MHz for ^{13}C). Chemical shifts are reported in δ (ppm) referenced to an internal tetramethylsilane standard for ^{1}H NMR. Chemical shifts of ^{13}C NMR are given related to solvent peak as an internal standard ($CDCl_3$: δ 77.0 or DMSO-*d*$_6$: δ 39.5). Chemical shifts of ^{19}F NMR are obtained related to CF_3CO_2H (δ -76.0) as an external standard. ^{1}H, ^{13}C and ^{19}F NMR spectra were recorded in $CDCl_3$ or DMSO-*d*$_6$ at 25 °C. GC-MS analyses were measured with an Agilent 6890 GC/5973N MS Detector. ESI-MS spectra were recorded on a JEOL JMS-T100LC spectrometer. Elemental analyses were performed on a J-SCIENCE LAB MICRO CORDER JM10. Transmission electron microscopy (TEM) images were obtained using a JEOL JEM-2100F operated at 200 kV. Commercially available chemicals (purchased from Sigma Aldrich, TCI, Kanto chemical, Wako Pure Chemical Industries, Nacalai tesque, and Merck) were used without further purification unless otherwise noted. *N*-methylpyrrolidone (NMP), butyl acrylate (**3a**) and tributylamine were distilled under reduced pressure prior to use. 4-iodo-*N*,*N*-dimethylaniline (**14g**),[14] 1-phenylallyl alcohol (**15e**), [15] palladium NNC-pincer complex **9**,[16] complexes **19**,[17]

20,[16] and **27**[18] were prepared according to literature procedures.

Typical Procedure for the Mizoroki-Heck Reaction of Aryl Iodides with Alkenes

A Schlenk tube and a stirrer bar were treated with aqua regia (1:3 concd aq HCl–concd aq HNO_3) for 30 min, washed sequentially with pure water and acetone, and dried with heating. The palladium complex **9** (0.47 mg, 0.001 mmol) was dissolved in NMP (10 mL), and the catalyst solution (10 μL, 1×10^{-6} mmol) was added to a mixture of PhI (**14a**; 203 mg, 1.0 mmol), butyl acrylate (**15a**; 0.17 mL, 1.2 mmol), and Bu_3N (0.28 mL, 1.2 mmol) in NMP (1.0 mL). The resulting solution was degassed by means of three freeze–pump–thaw cycles, and then stirred vigorously at 140 °C for 15 h under N_2. The mixture was then cooled to 25 °C, diluted with *t*-BuOMe (15 mL), transferred to a separatory funnel, and washed with 0.5 M aq HCl (20 mL). The aqueous layer was extracted with *t*-BuOMe (3 × 10 mL), and the extracts were combined, washed with brine (20 mL), and dried over Na_2SO_4. The resulting solution was concentrated under reduced pressure to give a crude product that was purified by chromatography [silica gel, hexane–EtOAc (20:1)] to give butyl (2*E*)-3-phenylacrylate (**16aa**) as a colorless oil; yield: 201 mg (0.99 mmol, 99%).

Typical Procedure for the Mizoroki-Heck Reaction of Aryl Bromides with Alkenes

A Schlenk tube and a stirrer bar were treated with aqua regia (1:3 concd aq HCl–concd aq HNO_3) for 30 min, washed sequentially with pure water and acetone, and dried with heating. The palladium complex **9** (0.47 mg, 0.001 mmol) was dissolved in NMP (10 mL), and the catalyst solution (100 μL, 1×10^{-5} mmol) was added to a mixture of PhBr (**28a**; 156 mg, 1.0 mmol), butyl acrylate (**15a**; 0.17 mL, 1.2 mmol), and sodium acetate (123 mg, 1.5 mmol) in NMP (0.9 mL). The resulting solution was degassed by means of three freeze–pump–thaw cycles, and then stirred vigorously at 140 °C for 48 h under N_2. The mixture was then cooled 25 °C, diluted with *t*-BuOMe (15 mL), transferred to a separatory funnel, and washed with 0.5 M aq HCl (20 mL). The aqueous layer was extracted with *t*-BuOMe (3 × 10 mL), and the extracts were combined, washed with brine (20 mL), and dried over Na_2SO_4. The resulting solution was concentrated under reduced pressure to give a crude product that was purified by chromatography [silica gel, hexane–EtOAc (20:1)] to give butyl (2*E*)-3-phenylacrylate (**16aa**) as a colorless oil; yield: 201 mg (0.99 mmol, 99%).

The Mizoroki-Heck Reaction of Iodobenzene with Butyl Acrylate in the Presence of 1 mol ppb Loading Amount of 9

A Schlenk tube and a stirrer bar were treated with piranha solution (3:1 concd H_2SO_4–30% aq H_2O_2) for 30 min, then rinsed with pure water and treated with aqua regia (1:3 concd aq HCl–concd. aq HNO_3) for 30 min. The treated Schlenk tube and stirrer bar were rinsed vigorously with pure water to remove acid

components then dried with heating. This reaction vessel was charged with dry Et_2O (5 mL), Et_3N (1 mL), and TMSCl (0.5 mL) under N_2 to cap any surface silanols on the glassware. After stirring at room temperature for 30 min, the mixture was removed by decantation and the vessel was washed with acetone and pure water, then dried with heating.

The palladium complex **9** (0.47 mg, 0.001 mmol) was dissolved in NMP (10 mL). The catalyst solution (10 μL; 1.0×10^{-6} mmol) was further diluted with NMP (10 mL). The resulting solution (10 μL, 1.0×10^{-9} mmol) was added to a mixture of PhI (**14a**; 203 mg, 1.0 mmol), butyl acrylate (**15a**; 0.17 mL, 1.2 mmol), and Bu_3N (0.28 mL, 1.2 mmol), and the resulting mixture was degassed by three freeze–pump–thaw cycles. The mixture was then stirred vigorously at 160 °C for 72 h under N_2. The mixture was then cooled to 25 °C, and purified by direct chromatography [silica gel, hexane–EtOAc (20:1)] to give butyl (2*E*)-3-phenylacrylate (**16aa**); yield: 177 mg (0.87 mmol, 87%).

Ten-Gram-Scale Synthesis of a Sunscreen Agent Octinoxate (16ef)

A Schlenk tube and a stirrer bar were cleaned with aqua regia (1:3 concd aq HCl–concd aq HNO_3) for 30 min, washed with sequentially with pure water and acetone, and dried with heating. The palladium complex **9** (0.47 mg, 0.001 mmol) was dissolved in NMP (10 mL). The catalyst solution (400 μL, 20 μg, 4.0×10^{-5} mmol) was added to a mixture of 4-iodoanisole (**14e**; 9.36 g, 40.0 mmol), 2-ethylhexyl acrylate (**15f**; 9.93 mL, 48.0 mmol), and Bu_3N (11.2 mL, 48.0 mmol)

in NMP (40 mL). The resulting solution was degassed by three freeze–pump–thaw cycles, and then stirred vigorously at 140 °C for 15 h under N_2. The mixture was then cooled to 25 °C, diluted with *t*-BuOMe (40 mL), and washed with 0.5 M aq HCl (60 mL). The aqueous layer was extracted with *t*-BuOMe (3 × 20 mL) and the extracts were combined, washed with brine (50 mL), and dried over Na_2SO_4. The resulting solution was concentrated under reduced pressure to give a crude product was that was purified by chromatography [silica gel, hexane–EtOAc (20:1)] to give 2-ethylhexyl (2*E*)-3-(4-methoxyphenyl)acrylate (**16ef**) as a color-less oil; yield: 10.86 g (37.6 mmol, 94%).

2-Ethylhexyl (2*E*)-3-(4-methoxyphenyl)acrylate (**16ef**) [CAS: 83834-59-7]: Colorless oil. ^{1}H NMR (396 MHz, $CDCl_3$): δ = 7.63 (d, *J* = 16.0 Hz, 1H), 7.49 (d, *J* = 8.8 Hz, 2H), 6.91 (d, *J* = 9.2 Hz, 2H), 6.32 (d, *J* = 16.0 Hz, 1H), 4.12–4.10 (m, 2H), 3.84 (s, 1H), 1.68–1.62 (m, 1H), 1.46–1.24 (m, 9H), 0.94–0.89 (m, 7H); ^{13}C NMR (100 MHz, $CDCl_3$): δ = 167.65, 161.37, 144.22, 129.77, 127.28, 115.88, 114.35, 66.88, 55.43, 38.95, 30.54, 29.04, 23.91, 23.08, 14.16, 11.11; EI-MS: *m/z* 290 (M^+).

Transmission Electron Microscopy (TEM) Analysis

A sample for TEM analysis was prepared as follows. After the Heck reaction of iodobenzene (**14a**) with butyl acrylate (**15a**), the reaction mixture was dropped onto a copper grid covered with a carbon membrane. The sample was rinsed with water and ethanol then dried under air. The resulting sample was then examined

by TEM.

Poisoning Tests

The palladium complex **9** (0.47 mg, 0.001 mmol) was dissolved in NMP (10 mL). The resulting catalyst solution (10 μL, 1×10^{-6} mmol) was added to a mixture of PhI (**14a**) (203 mg, 1.0 mmol), butyl acrylate (**15a**) (0.17 mL, 1.2 mmol), and Bu_3N (0.28 mL, 1.2 mmol) in NMP (1.0 mL). The resulting solution was degassed by three freeze–pump–thaw cycles, and then stirred vigorously at 140 °C for 2 h under N_2. Then one drop of Hg(0) or a 2 mol ppm solution of DCT in NMP was added under flowing N_2. The mixture was further stirred at 140 °C. Yields were determined by GC, with mesitylene as an internal standard.

Preparation of [2-(9-phenyl-1,10-phenanthrolin-2-yl)phenyl] palladium triflate (17)

To a suspension of **9** (47.2 mg, 0.1 mmol) in CH_2Cl_2 (8 mL) was added silver triflate (27.0 mg, 0.105 mmol). The reaction mixture was stirred in dark at room temperature for 12 h. The resulting suspension was through a pad of Celite®, and the filtrate was concentrated under reduced pressure to give **17** (51.4 mg, 0.087 mmol, 87%) as yellow solids.

Mp. >300.

^{1}H NMR (396 MHz, DMSO-d_6) δ 8.84 (d, J = 8.8 Hz, 1H), 8.80 (d, J = 8.8 Hz, 1H), 8.32 (d, J = 8.4 Hz, 1H), 8.23 (d, J = 8.4 Hz, 1H), 8.19-8.13 (m, 2H), 8.04

(d, J = 5.6 Hz, 1H), 7.75 (d, J = 7.6 Hz, 1H), 7.67-7.65 (m, 3H), 7.19-7.06 (m, 3H).

^{19}F NMR (372 MHz, DMSO-d_6) δ -78.29.

^{13}C NMR (100 MHz, DMSO-d_6) δ 163.16, 160.50, 150.48, 147.52, 145.54, 144.44, 139.58, 137.24, 132.49, 130.45, 130.34, 130.08, 129.17, 128.78, 127.91, 127.58, 126.99, 126.50, 126.01, 125.62, 122.20, 119.57.

IR (ATR): 3298, 3059, 1581, 1508, 1420, 1284, 1236, 1158, 1028, 857 cm^{-1}.

ESI-TOF-MS *m/z* 437 ([M-OTf]$^+$), 455 ([M-OTf+H_2O]$^+$).

Anal. Calcd for $C_{25}H_{15}F_3N_2O_3PdS\cdot H_2O$: C, 49.64: H, 2.83: N, 4.63%. Found: C, 49.54: H, 2.97: N, 4.56%.

Compound Data in the Mizoroki-Heck Reaction

Butyl (2*E*)-3-phenylacrylate (16aa)[19] [CAS: 52392-64-0]

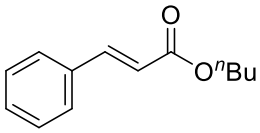

Colorless oil. ^{1}H NMR (396 MHz, $CDCl_3$) δ 7.69 (d, J = 16.0 Hz, 1H), 7.55-7.51 (m, 2H), 7.40-7.37 (m, 3H), 6.45 (d, J = 16.0 Hz, 1H), 4.21 (t, J = 6.8 Hz, 2H), 1.73-1.66 (m, 2H), 1.49-1.40 (m, 2H), 0.96 (t, J = 7.2 Hz, 3H). ^{13}C NMR (100 MHz, $CDCl_3$) δ 167.09, 144.52, 134.42, 130.18, 128.83, 128.02, 118.22, 64.40, 30.73, 19.17, 13.75. EI-MS m/z 204 (M$^+$).

Butyl (2*E*)-3-(4-methylphenyl)acrylate (16ba)[20] [CAS: 123248-21-5]

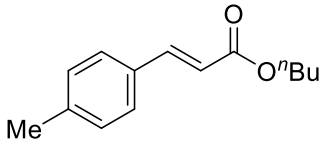

Colorless oil. ^{1}H NMR (396 MHz, $CDCl_3$) δ 7.66 (d, J = 16.2 Hz, 1H), 7.43 (d, J = 8.0 Hz, 2H), 7.19 (d, J = 8.0 Hz,

2H), 6.40 (d, *J* = 16.2 Hz, 1H), 4.21 (t, *J* = 6.8 Hz, 2H), 2.37 (s, 1H), 1.73-1.65 (m, 2H), 1.49-1.39 (m, 2H), 0.97 (t, *J* = 7.6 Hz, 3H). ^{13}C NMR (100 MHz, CDCl3) δ 167.31, 144.53, 140.59, 131.69, 129.56, 128.02, 117.14, 64.34, 30.77, 21.45, 19.18, 13.75. EI-MS m/z 218 (M^+).

Butyl (2*E*)-3-(3-methylphenyl)acrylate (16ca)[20] [CAS: 173593-27-6]

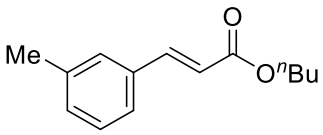

Colorless oil. ^{1}H NMR (396 MHz, $CDCl_3$) δ 7.64 (d, *J* = 16.0 Hz, 1H), 7.33-7.31 (m, 2H), 7.26 (t, *J* = 7.2 Hz, 1H), 7.18 (d, *J* = 8.0 Hz, 1H), 6.42 (d, *J* = 16.2 Hz, 1H), 4.20 (t, *J* = 6.8 Hz, 2H), 2.36 (s, 1H), 1.70-1.64 (m, 2H), 1.48-1.38 (m, 2H), 0.96 (t, *J* = 7.6 Hz, 3H). ^{13}C NMR (100 MHz, $CDCl_3$) δ 167.16, 144.70, 138.47, 134.36, 131.00, 128.71, 128.67, 125.20, 117.99, 64.35, 30.73, 21.28, 19.17, 13.73. EI-MS m/z 218 (M^+).

Butyl (2*E*)-3-(2-methylphenyl)acrylate (16da)[20] [CAS: 163977-61-5]

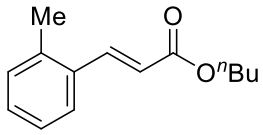

Colorless oil. ^{1}H NMR (396 MHz, $CDCl_3$) δ 7.96 (d, *J* = 16.0 Hz, 1H), 7.56-7.53 (m, 1H), 7.28-7.24 (m, 1H), 7.20 (t, *J* = 7.2 Hz, 2H), 6.35 (d, *J* = 16.0 Hz, 1H), 4.21 (t, *J* = 6.8 Hz, 2H), 2.43 (s, 1H), 1.72-1.65 (m, 2H), 1.48-1.38 (m, 2H), 0.96 (t, *J* = 7.6 Hz, 3H). ^{13}C NMR (100 MHz, $CDCl_3$) δ 167.14, 142.20, 137.58, 133.37, 130.73, 129.91, 126.33, 126.27, 119.23, 64.38, 30.73, 19.76, 19.17, 13.73. EI-MS *m/z* 218 (M^+).

Butyl (2*E*)-3-(4-methoxyphenyl)acrylate (16ea)[19] [CAS: 121725-19-7]

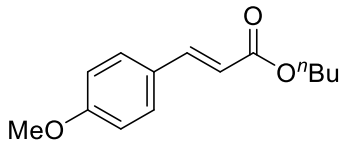

Colorless oil. ^{1}H NMR (396 MHz, $CDCl_3$) δ 7.63 (d, *J* = 16.0 Hz, 1H), 7.47 (d, *J* = 8.8 Hz, 2H), 6.90 (d, *J* = 8.8 Hz, 2H), 6.31 (d, *J* = 16.0 Hz, 1H), 4.19 (t, *J* = 6.8 Hz, 2H), 3.83 (s, 3H), 1.71-1.64 (m, 2H), 1.48-1.38 (m, 2H), 0.96 (t, *J* = 7.6 Hz, 3H). ^{13}C NMR (100 MHz, $CDCl_3$) δ 167.41, 161.25, 144.16, 129.63, 127.13, 115.69, 114.24, 64.38, 55.38, 30.76, 19.16, 13.72. EI-MS *m/z* 234 (M^+).

Butyl (2*E*)-3-(4-methylthiophenyl)acrylate (16fa) [CAS: none]

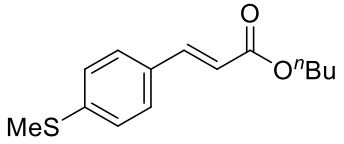

Colorless oil. ^{1}H NMR (396 MHz, $CDCl_3$) δ 7.63 (d, *J* = 16.0 Hz, 1H), 7.44 (d, *J* = 8.8 Hz, 2H), 7.23 (d, *J* = 8.8 Hz, 2H), 6.39 (d, *J* = 16.0 Hz, 1H), 4.20 (t, *J* = 6.8 Hz, 2H), 2.51 (s, 3H), 1.72-1.65 (m, 2H), 1.48-1.39 (m, 2H), 0.97 (t, *J* = 7.6 Hz, 3H). ^{13}C NMR (100 MHz, $CDCl_3$) δ 167.07, 143.81, 141.70, 130.81, 128.27, 125.78, 117.06, 64.26, 30.67, 19.10, 15.00, 13.67. IR (ATR): 2958, 1704, 1629, 1492, 1308, 1267, 1164, 1091, 979, 812 cm^{-1}. EI-MS *m/z* 250 (M^+). HR-ESI MS calcd for $C_{14}H_{18}O_2S$ *m/z* 250.1027, found 250.1016.

Butyl (2*E*)-3-(4-(dimethylamino)phenyl)acrylate (16ga)[19] [CAS: 173593-29-8]

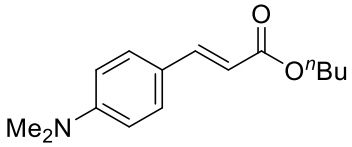

Colorless oil. ^{1}H NMR (396 MHz, $CDCl_3$) δ 7.62 (d, *J* = 16.0 Hz, 1H), 7.43 (d, *J* = 9.2 Hz, 2H), 6.67 (d, *J* = 8.8 Hz, 2H), 6.23 (d, *J* = 16.0 Hz, 1H), 4.19 (t, *J* = 6.8 Hz, 2H), 3.02 (s, 6H), 1.70-

1.66 (m, 2H), 1.47-1.41 (m, 2H), 0.96 (t, J = 7.6 Hz, 3H). ^{13}C NMR (100 MHz, $CDCl_3$) δ 167.96, 151.62, 145.00, 129.63, 122.18, 112.50, 111.72, 63.95, 40.08, 30.83, 19.19, 13.75. EI-MS *m/z* 247 (M^+).

Butyl (2*E*)-3-(4-acetylphenyl)acrylate (16ha)[21] [CAS: 173464-57-8]

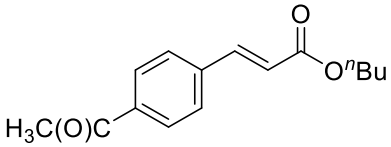

Colorless oil. ^{1}H NMR (396 MHz, $CDCl_3$) δ 7.98 (d, J = 8.8 Hz, 2H), 7.70 (d, J = 16.0 Hz, 1H), 7.62 (d, J = 8.4 Hz, 2H), 6.53 (d, J = 16.0 Hz, 1H), 4.23 (t, J = 6.8 Hz, 2H), 2.62 (s, 3H), 1.74-1.67 (m, 2H), 1.49-1.40 (m, 2H), 0.97 (t, J = 7.6 Hz, 3H). ^{13}C NMR (100 MHz, $CDCl_3$) δ 197.33, 166.58, 142.95, 138.76, 137.90, 128.82, 128.09, 120.79, 64.67, 30.69, 26.68, 19.15, 13.72. EI-MS *m/z* 246 (M^+).

Butyl (2*E*)-3-(4-formylphenyl)acrylate (16ia)[19] [CAS: 169479-49-6]

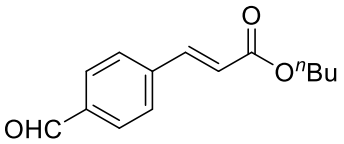

Colorless oil. ^{1}H NMR (396 MHz, $CDCl_3$) δ 10.02 (s, 1H), 7.89 (d, J = 8.4 Hz, 2H), 7.71-7.66 (m, 3H), 6.54 (d, J = 16.0 Hz, 1H), 4.22 (t, J = 6.8 Hz, 2H), 1.72-1.65 (m, 2H), 1.48-1.38 (m, 2H), 0.96 (t, J = 7.6 Hz, 3H). ^{13}C NMR (100 MHz, $CDCl_3$) δ 191.44, 166.42, 142.75, 140.09, 137.06, 130.12, 128.45, 121.43, 64.72, 30.67, 19.14, 13.70. EI-MS *m/z* 232 (M^+).

Butyl (2*E*)-3-(4-(ethoxycarbonyl)phenyl)acrylate (16ja)[22] [CAS: 1221682-74-1]

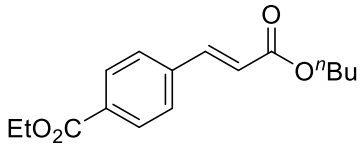

Colorless oil. ^{1}H NMR (396 MHz, $CDCl_3$) δ 8.06 (d, *J* = 8.4 Hz, 2H), 7.70 (d, *J* = 16.0 Hz, 1H), 7.59 (d, *J* = 8.0 Hz, 2H), 6.52 (d, *J* = 16.0 Hz, 1H), 4.39 (q, *J* = 7.2 Hz, 2H), 4.23 (t, *J* = 6.8 Hz, 2H), 1.74-1.66 (m, 2H), 1.49-1.39 (m, 5H), 0.97 (t, *J* = 7.6 Hz, 3H). ^{13}C NMR (100 MHz, $CDCl_3$) δ 166.60, 165.92, 143.12, 138.51, 131.61, 129.99, 127.80, 120.52, 64.59, 61.15, 30.67, 19.13, 14.25, 13.67. EI-MS *m/z* 276 (M^+).

Butyl (2*E*)-3-(4-carboxylphenyl)acrylate (16ka)[23] [CAS: 605644-02-8]

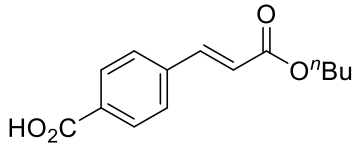

White solids. ^{1}H NMR (396 MHz, DMSO) δ 7.91 (d, *J* = 8.0 Hz, 2H), 7.81 (d, *J* = 8.4 Hz, 2H), 7.66 (d, *J* = 16.4 Hz, 1H), 6.72 (d, *J* = 16.0 Hz, 1H), 4.12 (t, *J* = 6.8 Hz, 2H), 1.62-1.55 (m, 2H), 1.37-1.31 (m, 2H), 0.87 (t, *J* = 7.6 Hz, 3H). ^{13}C NMR (100 MHz, DMSO) δ 167.54, 166.76, 143.87, 138.85, 132.75, 130.46, 129.20, 121.20, 64.67, 30.98, 19.40, 14.34. EI-MS *m/z* 248 (M^+).

Butyl (2*E*)-3-(4-cyanophenyl)acrylate (16la)[21] [CAS: 172418-41-6]

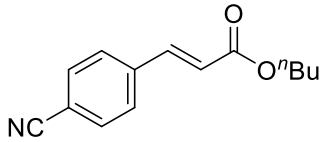

White solids. ^{1}H NMR (396 MHz, $CDCl_3$) δ 7.68-7.59 (m, 5H), 6.51 (d, *J* = 16.4 Hz, 1H), 4.22 (t, *J* = 6.8 Hz, 2H), 1.72-1.65 (m, 2H), 1.47-1.38 (m, 2H), 0.95 (t, *J* = 7.6 Hz, 3H). ^{13}C NMR (100

MHz, $CDCl_3$) δ 166.21, 142.06, 138.70, 132.60, 128.33, 121.83, 118.34, 113.27, 64.80, 30.63, 19.12, 13.69. EI-MS *m/z* 229 (M^+).

Butyl (2*E*)-3-(4-(trifluoromethyl)phenyl)acrylate (16ma)[19] [CAS: 220466-27-3]

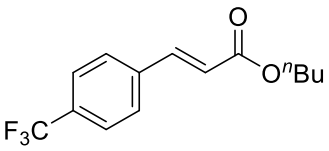

Colorless oil. ^1H NMR (396 MHz, $CDCl_3$) δ 7.69 (d, *J* = 16.0 Hz, 1H), 7.66-7.62 (m, 4H), 6.52 (d, *J* = 16.0 Hz, 1H), 4.23 (t, *J* = 6.8 Hz, 2H), 1.74-1.67 (m, 2H), 1.49-1.40 (m, 2H), 0.97 (t, *J* = 7.6 Hz, 3H). ^{13}C NMR (100 MHz, $CDCl_3$) δ 166.42, 142.58, 137.79, 131.61 (q, *J* = 32.6 Hz), 128.09, 125.77, 122.42, 120.79, 64.64, 30.66, 19.12, 13.64. EI-MS *m/z* 272 (M^+).

Butyl (2*E*)-3-(4-nitrophenyl)acrylate (16na)[19] [CAS: 131061-15-9]

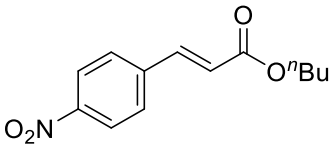

White solids. ^1H NMR (396 MHz, $CDCl_3$) δ 8.26 (d, *J* = 8.8 Hz, 2H), 7.73-7.67 (m, 3H), 6.57 (d, *J* = 16.0 Hz, 1H), 4.24 (t, *J* = 6.8 Hz, 2H), 1.74-1.67 (m, 2H), 1.49-1.40 (m, 2H), 0.97 (t, *J* = 7.6 Hz, 3H). ^{13}C NMR (100 MHz, $CDCl_3$) δ 166.06, 148.36, 141.51, 140.52, 128.56, 124.08, 122.51, 64.83, 30.60, 19.10, 13.66. EI-MS *m/z* 249 (M^+).

Butyl (2*E*)-3-(4-fluorophenyl)acrylate (16oa)[19] [CAS: 131061-12-6]

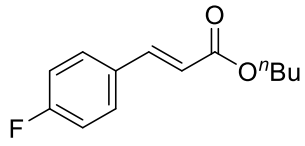

Colorless oil. ^1H NMR (396 MHz, $CDCl_3$) δ 7.64 (d, *J* = 16.0 Hz, 1H), 7.54-7.49 (m, 2H), 7.08 (t, *J* = 8.8 Hz, 2H),

6.37 (d, *J* = 16.0 Hz, 1H), 4.21 (t, *J* = 6.8 Hz, 2H), 1.73-1.65 (m, 2H), 1.49-1.39 (m, 2H), 0.97 (t, *J* = 7.6 Hz, 3H). ^{13}C NMR (100 MHz, $CDCl_3$) δ 167.04, 163.90 (d, *J* = 252 Hz), 143.29, 130.73, 129.95 (d, *J* = 8.6 Hz), 118.07, 116.07 (d, *J* = 22.0 Hz), 64.53, 30.81, 19.25, 13.81. EI-MS *m/z* 222 (M^+).

Butyl (2*E*)-3-(4-biphenyl)acrylate (16pa)[21] [CAS: 444108-93-4]

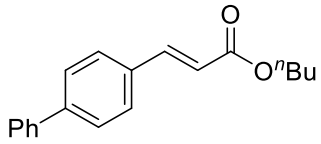

White solids. ^{1}H NMR (396 MHz, $CDCl_3$) δ 7.72 (d, *J* = 16.0 Hz, 1H), 7.62-7.59 (m, 6H), 7.46 (t, *J* = 7.6 Hz, 1H), 7.47-7.42 (m, 1H), 6.50-6.46 (d, *J* = 16.0 Hz, 1H), 4.22 (t, *J* = 6.8 Hz, 2H), 1.72-1.67 (m, 2H), 1.48-1.42 (m, 2H), 0.98 (t, *J* = 7.6 Hz, 3H). ^{13}C NMR (100 MHz, $CDCl_3$) δ 167.13, 144.05, 142.92, 140.11, 133.37, 128.86, 128.51, 127.80, 127.48, 127.00, 118.07, 64.43, 30.75, 19.18, 13.74. EI-MS *m/z* 280 (M^+).

Butyl (2*E*)-3-(1-naphthyl)acrylate (16qa)[19] [CAS: 123230-71-7]

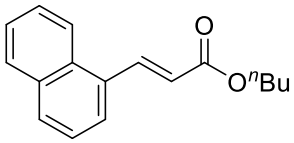

Colorless oil. ^{1}H NMR (396 MHz, $CDCl_3$) δ 7.72 (d, *J* = 16.4 Hz, 1H), 7.64-7.59 (m, 6H), 7.48 (t, *J* = 7.6 Hz, 2H), 7.38 (tt, *J* = 7.6, 1.2 Hz, 1H), 6.48 (d, *J* = 16.4 Hz, 1H), 4.26 (t, *J* = 6.8 Hz, 2H), 1.76-1.69 (m, 2H), 1.51-1.42 (m, 2H), 0.98 (t, *J* = 7.6 Hz, 3H). ^{13}C NMR (100 MHz, $CDCl_3$) δ 166.96, 141.53, 133.60, 131.76, 131.34, 130.40, 128.67, 126.79, 126.16, 125.40, 124.94, 123.34, 120.87, 64.50, 30.76, 19.20, 13.75. EI-MS *m/z* 254 (M^+).

Butyl (2*E*)-3-(5-indolyl)acrylate (16ra)[24] [CAS: 1621184-10-8]

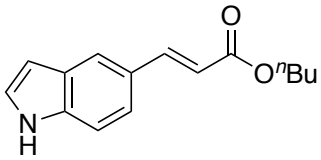

White solids. ^{1}H NMR (396 MHz, $CDCl_3$) δ 8.30 (brs, 1H), 7.84-7.80 (m, 2H), 7.38 (m, 2 H), 7.23 (t, *J* = 6.4 Hz, 1H), 6.59-6.57 (m, 1H), 6.41 (d, *J* = 16.4 Hz, 1H), 4.21 (t, *J* = 6.8 Hz, 2H), 1.73-1.66 (m, 2H), 1.49-1.39 (m, 2H), 0.96 (t, *J* = 7.6 Hz, 3H). ^{13}C NMR (100 MHz, $CDCl_3$) δ 167.97, 146.54, 136.97, 128.03, 126.28, 125.37, 122.33, 121.36, 121.03, 114.80, 111.60, 103.21, 64.21, 30.74, 19.14, 13.70. EI-MS *m/z* 243 (M^+).

Butyl (2*E*)-3-(2-thienyl)acrylate (16sa)[25] [CAS: 479413-24-6]

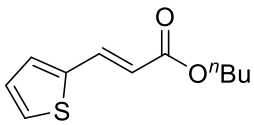

Colorless oil. ^{1}H NMR (396 MHz, $CDCl_3$) δ 7.76 (d, *J* = 15.6 Hz, 1H), 7.35 (d, *J* = 7.6 Hz, 1H), 7.23 (d, *J* = 3.6 Hz, 1H), 7.05-7.04 (m, 1H), 6.23 (d, *J* = 16.4 Hz, 1H), 4.18 (t, *J* = 6.8 Hz, 2H), 1.70-1.63 (m, 2H), 1.47-1.37 (m, 2H), 0.94 (t, *J* = 7.6 Hz, 3H). ^{13}C NMR (100 MHz, $CDCl_3$) δ 166.91, 139.55, 136.95, 130.79, 128.28, 128.01, 116.99, 64.37, 30.72, 19.14, 13.71. EI-MS *m/z* 210 (M^+).

Butyl (2*E*)-3-(2-naphthyl)acrylate (16ta)[26] [CAS: 124182-61-2]

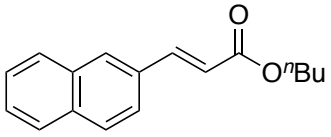

Colorless oil. ^{1}H NMR (396 MHz, $CDCl_3$) δ 7.93 (s, 1H), 7.86-7.81 (m, 4H), 7.67 (dd, *J* = 8.4, 1.2 Hz, 1H), 7.52-7.48 (m, 2H), 6.55 (d, *J* = 16.0 Hz, 1H), 4.23 (t, *J* = 6.8 Hz, 2H), 1.74-1.67 (m, 2H), 1.50-1.41 (m, 2H), 0.97 (t, *J* = 7.6 Hz, 3H). ^{13}C NMR (100 MHz, $CDCl_3$) δ

166.84, 144.31, 133.94, 133.02, 131.68, 129.66, 128.39, 128.30, 127.52, 126.92, 126.42, 123.21, 118.15, 64.17, 30.60, 19.03, 13.59. EI-MS *m/z* 254 (M^+).

Butyl (2*E*)-3-(1-pyrenyl)acrylate (**16ua**) [CAS: 1544738-96-6]

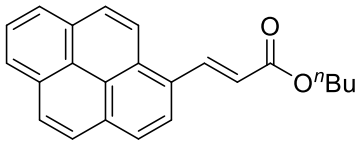

Yellow solids. ^{1}H NMR (396 MHz, $CDCl_3$) δ 8.82 (d, *J* = 16.0, 1H), 8.47 (d, *J* = 9.6, 1H), 8.27 (d, *J* = 8.4 Hz, 1H), 8.23-8.10 (m, 5H), 8.06-8.01 (m, 2H), 6.71 (d, *J* = 16.0 Hz, 1H), 4.31 (t, *J* = 6.8 Hz, 2H), 1.80-1.73 (m, 2H), 1.55-1.46 (m, 2H), 1.01 (t, *J* = 7.6 Hz, 3H). ^{13}C NMR (100 MHz, $CDCl_3$) δ 167.09, 140.98, 132.24, 130.93, 130.30, 129.25, 128.13, 128.10, 127.74, 126.95, 125.89, 125.63, 125.45, 124.63, 124.38, 124.18, 123.67, 121.99, 119.77, 64.40, 30.77, 19.19, 13.75. EI-MS *m/z* 328 (M^+).

Butyl (2*E*)-3-(4-pyrrolidinylcarbonylphenyl)acrylate (**16va**) [CAS: none]

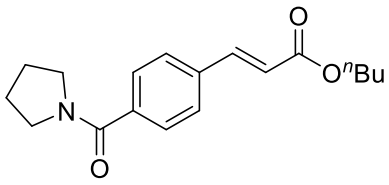

Colorless oil. ^{1}H NMR (396 MHz, $CDCl_3$) δ 7.68 (d, *J* = 16.0, 1H), 7.57-7.53 (m, 4H), 6.48 (d, *J* = 16.4 Hz, 1H), 4.22 (t, *J* = 6.8 Hz, 2H), 3.66 (t, *J* = 7.0 Hz, 2H), 3.44 (t, *J* = 6.8 Hz, 2H), 2.01-1.94 (m, 2H), 1.92-1.88 (m, 2H), 1.73-1.66 (m, 2H), 1.49-1.40 (m, 2H), 0.97 (t, *J* = 7.6 Hz, 3H). ^{13}C NMR (100 MHz, $CDCl_3$) δ 168.83, 166.79, 143.44, 138.57, 135.74, 127.83, 127.67, 119.46, 64.53, 49.50, 46.21, 30.69, 26.36, 24.38, 19.14, 13.70. IR (ATR): 2959, 2874, 1708, 1619, 1421, 1310, 1168, 983, 837, 750 cm^{-1}. EI-MS *m/z* 301 (M^+). HR-ESI MS calcd for $C_{18}H_{23}NO_3$ m/z 301.1677, found 301.1674.

Butyl (2*E*)-3-(3,5-bis(trifluoromethyl)phenyl)acrylate (16wa)[19] [CAS: 360550-36-3]

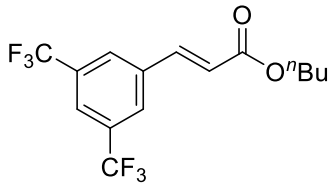

Colorless oil. ^{1}H NMR (396 MHz, $CDCl_3$) δ 7.94 (s, 2H), 7.88 (s, 1H), 7.71 (d, *J* = 16.0 Hz, 1H), 6.58 (d, *J* = 16.4 Hz, 1H), 4.24 (t, *J* = 6.8 Hz, 2H), 1.74-1.67 (m, 2H), 1.50-1.40 (m, 2H), 0.98 (t, *J* = 7.6 Hz, 3H). ^{13}C NMR (100 MHz, $CDCl_3$) δ 165.91, 140.84, 136.59, 132.39 (q, *J* = 134 Hz), 127.10, 123.27 (t, *J* = 11.6 Hz), 123.01 (q, *J* = 1096 Hz), 121.62, 64.88, 30.65, 19.13, 13.61. EI-MS *m/z* 340 (M^+).

Butyl (2*E*)-3-(3-pyridyl)acrylate (16xa)[19] [CAS: 360550-39-6]

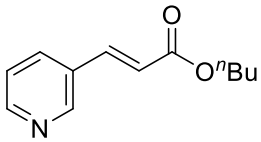

Colorless oil. ^{1}H NMR (396 MHz, $CDCl_3$) δ 8.75 (d, *J* = 1.6 Hz, 1H), 8.61 (dd, *J* = 3.6, 1.6 Hz, 1H), 7.85 (dt, *J* = 7.6, 2.0 Hz, 1H), 7.67 (d, *J* = 16.8 Hz, 1H), 7.35-7.32 (m, 1H), 6.52 (d, *J* = 16.4 Hz, 1H), 4.23 (t, *J* = 6.8 Hz, 2H), 1.74-1.67 (m, 2H), 1.49-1.40 (m, 2H), 0.97 (t, *J* = 7.6Hz, 3H). ^{13}C NMR (100 MHz, $CDCl_3$) δ 166.36, 150.91, 149.67, 140.77, 134.13, 130.15, 123.68, 120.42, 64.65, 30.65, 19.13, 13.68. EI-MS *m/z* 205 (M^+).

***trans*-Stilbene (16ab)**[21] [CAS: 103-30-0]

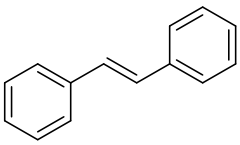

White solids. ^{1}H NMR (396 MHz, $CDCl_3$) δ 7.52 (d, *J* = 7.2 Hz, 4H), 7.36 (t, *J* = 7.6 Hz, 4H), 7.29-7.25 (m, 2H), 7.12 (s, 2H). ^{13}C NMR (100 MHz, $CDCl_3$) δ 137.27, 128.65, 127.59, 126.47. EI-MS *m/z* 180

(M^+).

(2*E*)-3-Phenyl-*N*,*N*-dimethylacrylamide (16ac)[27] [CAS: 17431-39-9]

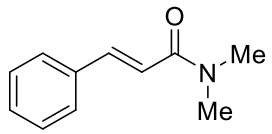

Colorless oil. ^{1}H NMR (396 MHz, $CDCl_3$) δ 7.68 (d, *J* = 15.6 Hz, 1H), 7.55-7.52 (m, 2H), 7.40-7.33 (m, 3H), 6.90 (d, *J* = 16.0 Hz, 1H), 3.18 (s, 3H), 3.08 (s, 3H). ^{13}C NMR (100 MHz, $CDCl_3$) δ 166.63, 142.29, 135.33, 129.49, 128.73, 127.75, 117.37, 37.40, 35.91. EI-MS *m/z* 175 (M^+).

(2*E*)-(2-Phenylethenyl)sulfonylbenzene (16ad)[28] [CAS: 16212-06-9]

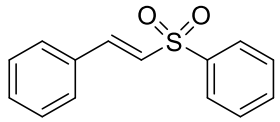

White solids. ^{1}H NMR (396 MHz, $CDCl_3$) δ 7.97-7.94 (m, 2H), 7.70 (d, *J* = 15.6 Hz, 1H), 7.65-7.61 (m, 1H), 7.58-7.54 (m, 2H), 7.50-7.48 (m, 2H), 7.43-7.38 (m, 3H), 6.87 (d, *J* = 15.6 Hz, 1H). ^{13}C NMR (100 MHz, $CDCl_3$) δ 142.44, 140.59, 133.35, 132.25, 131.19, 129.68, 129.30, 129.04, 128.85, 128.53, 128.16, 127.80, 127.59, 127.16. EI-MS *m/z* 244 (M^+).

3-Phenylpropiophenone (16ae)[29] [CAS: 1083-30-3]

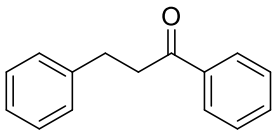

Colorless oil. ^{1}H NMR (396 MHz, $CDCl_3$) δ 7.96 (d, *J* = 7.3 Hz, 2H), 7.56 (t, *J* = 7.3 Hz, 1H), 7.46 (t, *J* = 7.3 Hz, 2H), 7.32-7.25 (m, 4H), 7.23-7.19 (m, 1H), 3.31 (t, *J* = 7.8 Hz, 2H), 3.08 (t, *J* = 7.6 Hz, 2H). ^{13}C NMR (100 MHz, $CDCl_3$) δ 199.20, 141.26, 136.78, 133.05, 128.58,

128.50, 128.40, 128.01, 126.11, 40.43, 30.08. EI-MS *m/z* 210 (M^+).

***trans*-4-Acetylstilbene (16jb)**[23] [CAS: 20488-42-0]

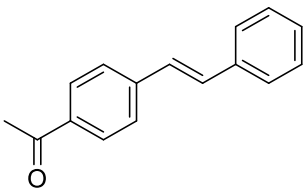

White solids. ^{1}H NMR (396 MHz, $CDCl_3$) δ 7.97 (d, *J* = 8.8 Hz, 2H), 7.60 (d, *J* = 8.4 Hz, 2H), 7.56 (d, *J* = 8.0 Hz, 2H), 7.38 (t, *J* = 7.2 Hz, 2H), 7.31 (t, *J* = 7.2 Hz, 1H), 7.24 (d, *J* = 16.4 Hz, 1H), 7.15 (d, *J* = 16.4 Hz, 1H), 2.62 (s, 3H). ^{13}C NMR (100 MHz, $CDCl_3$) δ 197.50, 141.97, 136.64, 135.88, 131.42, 128.85, 128.77, 128.29, 127.39, 126.79, 126.46, 26.59. EI-MS *m/z* 222 (M^+).

***trans*-4-Methoxylstilbene (16eb)**[20] [CAS: 1694-19-5]

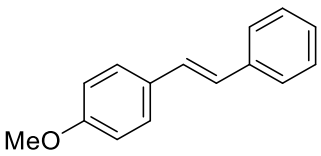

White solids. ^{1}H NMR (396 MHz, $CDCl_3$) δ 7.49 (d, *J* = 8.8 Hz, 2H), 7.45 (d, *J* = 8.8 Hz, 2H), 7.34 (t, *J* = 8.0 Hz, 2H), 7.23 (t, *J* = 7.6 Hz, 1H), 7.06 (d, *J* = 16.4 Hz, 1H), 6.97 (d, *J* = 16.4 Hz, 1H), 6.90 (d, *J* = 8.8 Hz, 2H), 3.83 (s, 3H). ^{13}C NMR (100 MHz, $CDCl_3$) δ 159.23, 137.58, 130.06, 128.59, 128.14, 127.67, 127.36, 127.15, 126.53, 126.20, 114.07, 55.24. EI-MS *m/z* 210 (M^+).

(*E*)-3-(2-Phenylethenyl)pyridine (16xb)[21] [CAS: 5097-91-6]

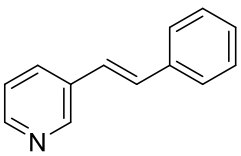

White solids. ^{1}H NMR (396 MHz, $CDCl_3$) δ 8.73 (sd, *J* = 2.0 Hz, 1H), 8.48 (dd, *J* = 4.4, 2.0 Hz, 1H), 7.83 (dt, *J* = 8.0, 2.0 Hz, 1H), 7.54 (d, *J* = 8.8 Hz, 2H), 7.38 (t, *J* = 7.2 Hz, 2 H), 7.31-7.26 (m, 2H), 7.17

(d, J = 17.2 Hz, 1H), 7.07 (d, J = 16.4 Hz, 1H). ^{13}C NMR (100 MHz, $CDCl_3$) δ 148.53, 136.59, 132.94, 132.61, 130.77, 128.76, 128.20, 126.63, 124.84, 123.51. EI-MS *m/z* 180 (M^+).

References

(1) (a) T. Mizoroki, K. Mori, A. Ozaki *Bull. Chem. Soc. Jpn.* **1971**, *44*, 581. (b) R. F. Heck, J. P. Nolley, Jr. *J. Org. Chem.* **1972**, *37*, 2320–2322. (c) I. P. Beletskaya, A. V. Cheprakov *Chem. Rev.* **2000**, *100*, 3009–3066.

(2) (a) J. G. de Vries, *Can. J. Chem.* **2001**, *79*, 1086–1092. (b) A. B. Dounay, L. E. Overman, *Chem. Rev.* **2003**, *103*, 2945–2964. (c) K. C. Nicolaou, P. G. Bulger, D. Sarlah, *Angew. Chem. Int. Ed.* **2005**, *44*, 4442–4489. (d) C. Torborg, M. Beller, *Adv. Synth. Catal.* **2009**, *351*, 3027–3043. (e) P. Michel, *Platinum Metals Rev.* **2013**, *57*, 272–280.

(3) (a) M. Albrecht, G. van Koten *Angew. Chem. Int. Ed.* **2001**, *40*, 3750–3781. (b) M. E. van der Boom, D. Milstein *Chem. Rev.* **2003**, *103*, 1759–1792. (c) J. T. Singleton *Tetrahedron*, **2003**, *59*, 1837–1857. (d) K. J. Szabó *Synlett*, **2006**, 811–824. (e) D. Benito-Garagorri, K. Kirchner *Acc. Chem. Res.* **2008**, *41*, 201–213. (f) N. Selander, K. J. Szabó *Dalton Trans.* **2009**, 6267–6279. (g) N. Selander, K. J. Szabó *Chem. Rev.* **2011**, *111*, 2048–2076. (h) *Organometallic Pincer Chemistry*; G. van Koten, D. Milstein, Eds.; Topics in Organometallic Chemistry; Vol. 40; Springer: Heidelberg, **2013**.

(4) For reports on the Mizoroki–Heck reaction with palladium pincer complexes at ppm loadings, see: (a) F. Miyazaki, K. Yamaguchi, M. Shibasaki *Tetrahedron Lett.* **1999**, *40*, 7379–7383. (b) D. Morales-Morales, C. Grause, K. Kasaoka, R. Redón, R. E. Cramer, C. M. Jensen *Inorg. Chim. Acta*, **2000**, *300–302*, 958–963. (c) S. Sjövall, O. F. Wendt, C. Andersson *J. Chem. Soc.,*

Dalton Trans. **2002**, 1396–1400. (d) I. G. Jung, S. U. Son, K. H. Park, K.-C. Chung, J. W. Lee, Y. K. Chung *Organometallics* **2003**, *22*, 4715–4720. (f) M.-H. Huang, L.-C. Liang *Organometallics* **2004**, *23*, 2813–2816. (e) C. S. Consorti, G. Ebeling, F. R. Flores, F. Rominger, J. Dupont *Adv. Synth. Catal.* **2004**, *346*, 617–624. (f) K. Takenaka, M. Minakawa, Y. Uozumi *J. Am. Chem. Soc.* **2005**, *127*, 12273–12281. (g) J. L. Bolliger, O. Blacque, C. M. Frech *Chem.–Eur. J.* **2008**, *14*, 7969–7977. (h) Q.-L. Luo, J.-P. Tan, Z.-F. Li, Y. Qin, L. Ma, D.-R. Xiao *Dalton Trans.* **2011**, *40*, 3601–3609.

(5) M. Ohff, A. Ohff, M. E. van der Boom, D. Milstein, *J. Am. Chem. Soc.* **1997**, *119*, 11687–11688.

(6) (a) M.-H. Huang, L.-C. Liang, *Organometallics* **2004**, *23*, 2813–2816. (b) K. Takenaka, Y. Uozumi, *Adv. Synth. Catal.* **2004**, *346*, 1693–1696. (c) M. S. Yoon, D. Ryu, J. Kim, K. H. Ahn, *Organometallics* **2006**, *25*, 2409–2411.

(7) D. A. Alonso, C. Nájera, C. Pacheco *Adv. Synth. Catal.* **2002**, *344*, 172–183.

(8) G. M. Whitesides, M. Hackett, R. L. Brainard, J.-P. P. M. Lavalleye, A. F. Sowinski, A. M. Izumi, S. S. Moore, D. W. Brown, E. M. Staudt *Organometallics* **1985**, *4*, 1819–1830.

(9) (a) D. R. Anton, R. H. Crabtree *Organometallics* **1983**, *2*, 855–859. (b) C. S. Consorti, F. R. Flores, J. Dupont *J. Am. Chem. Soc.* **2005**, *127*, 12054–12065.

(10) In ref. 9, it was reported that DCT coordinates to homogeneous platinum metal to form stable and catalytically inactive complexes. To discuss the mechanism of our catalytic system briefly, we consider homogeneous

palladium as a monomeric palladium species.

(11) No reaction of **16a** with **3a** took place in the presence of Bu_3N.

(12) When $Pd(OAc)_2$ was used as the catalyst, the reaction of **16a** with **3a** proceeded to give **4aa** in 51% yield. The catalytic activity of complex **1** was superior to that of $Pd(OAc)_2$ in this reaction.

(13) For information on octinoxate, see: http://www.smartskincare.com/skinprotection/sunblocks/sunblock_octinoxate.html (accessed Jan 5, 2018)

(14) V. Hrobáriková, P. Hrobárik, P. Gajdos, I. Fitilis, M. Fakis, P. Persephonis, P. Zahradnik *J. Org. Chem.* **2010**, *75*, 3053–3068.

(15) A. J. Musacchio, L. Q. Nguyen, G. H. Beard, R. R. Knowles *J. Am. Chem. Soc.* **2014**, *136*, 12217–12220.

(16) G. Hamasaka, F. Sakurai, Y. Uozumi *Chem. Commun*. **2015**, *51*, 3886–3888.

(17) F. Ragaini, M. Gasperini, S. Cenini, L. Arnera, A. Caselli, P. Macchi, N. Casati *Chem. Eur. J.* **2009**, *15*, 8064–8077.

(18) D. A. Alonso, C. Nájera, M. C. Pacheco *Adv. Synth. Catal.* **2002**, *344*, 172–183.

(19) M. Feuerstein, H. Doucet, M. Santelli *J. Org. Chem.* **2001**, *66*, 5923–5925.

(20) G. Xie, P. Chellan, J. Mao, K. Chibale, G. S. Smith *Adv. Synth. Catal.* **2010**, *352*, 1641–1647.

(21) X. Cui, Z. Li, C.-Z. Tao, Y. Xu, J. Li, L. Liu, Q.-X. Guo *Org. Lett*. **2006**, *8*, 2467–2470.

(22) S. Yu, Z. Zhang, Z. Yu, Y. Shang *Appl. Organometal. Chem.* **2014**, *28*, 657–2460.

(23) M.-K. Zhu, J.-F. Zhao, T.-P. Loh *Org. Lett*. **2011**, *13*, 6308–6311.

(24) A. K. Verma, A. K. Danodia, R. K. Saunthwal, M. Patel, D. Choudhary *Org. Lett.* **2015**, *17*, 3658–3661.

(25) W. Fu, Y. Feng, Z. Fang, Q. Chen, T. Tang, Q. Yu, T. Tang *Chem. Commun.* **2016**, *52*, 3115–3118.

(26) G.-W. Wang, T. Miao *Chem. Eur. J.* **2011**, *17*, 5787–5790.

(27) N. Deibl, R. Kempe *J. Am. Chem. Soc.* **2016**, *138*, 10786–10789.

(28) X. Li, Y. Xu, W. Wu, C. Jiang, C. Qi, H. Jiang *Chem. Eur. J.* **2014**, *20*, 7911–7915.

(29) A. Briot, C. Baehr, R. Brouillard, A. Wagner, C. Mioskowski *J. Org. Chem.* **2004**, *69*, 1374–1377.

(30) G. Meng, M. Szostak *Angew. Chem. Int. Ed.* **2015**, *54*, 14518–14522.

Chapter 2

The Hiyama Coupling Reaction at Parts Per Million Levels of Pd

Shun Ichii, Go Hamasaka and Yasuhiro Uozumi

Chem. Asian J. **2019**, *14*, 3850-3854

Introduction

Palladium-catalyzed cross-coupling reactions are recognized as an indispensable class of organic transformations in modern synthetic chemistry.[1] A variety of organometallic reagents have been utilized in C–C bond-forming processes, including organomagnesium (Kumada–Tamao–Corriu),[2] organozinc (Negishi),[3] organotin (Migita–Kosugi–Stille),[4] organoboron (Suzuki–Miyaura),[5] and organosilicon compounds (Hiyama).[6] Among these, the Suzuki–Miyaura cross-coupling reaction of organoboron reagents is the most widely employed in the fields of pharmaceuticals, agrochemicals, and materials chemistry,[7] because it generally proceeds with excellent functional-group tolerance under mild conditions without producing hazardous waste. Despite these advantages of the Suzuki–Miyaura reaction, Hiyama cross-coupling has emerged as a viable alternative for efficient C–C bond-forming processes, because of the striking features of organosilicon compounds, such as their low toxicity, low cost, and ready availability and because of the rich natural abundance of silicon as an element (Scheme 1).

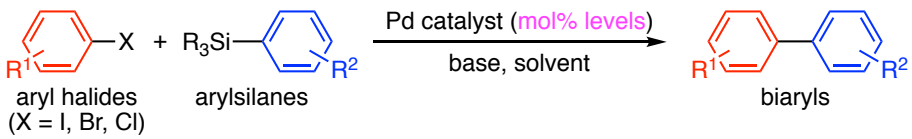

The use of silicon compounds as organometallic reagents

Advantages: low toxicity, low cost, ready availability, rich natural abundance of silicon

Disadvantages: less reactive (high catalyst loading, hursh conditions)

Scheme 1. General Chemical Equation of the Hiyama Cross-Coupling Reaction

However, organosilicon compounds are generally less reactive than organoboron compounds owing to the low degree of polarization of the Si–C bond. Consequently, high loadings of palladium catalyst (mol% levels) are inevitably required to bring about efficient Hiyama coupling reactions, leading to serious problems of contamination of the resulting products by toxic palladium metal.[8] This drawback has limited the range of industrial applications of the Hiyama coupling reaction.

Although many types of organosilicon reagents have been developed to permit the Hiyama coupling processes to proceed under milder conditions with wide functional-group tolerance (Scheme 2),[6c,6d,9] the reduction of the catalyst loading to ppm levels remains a challenging research objective.[10]

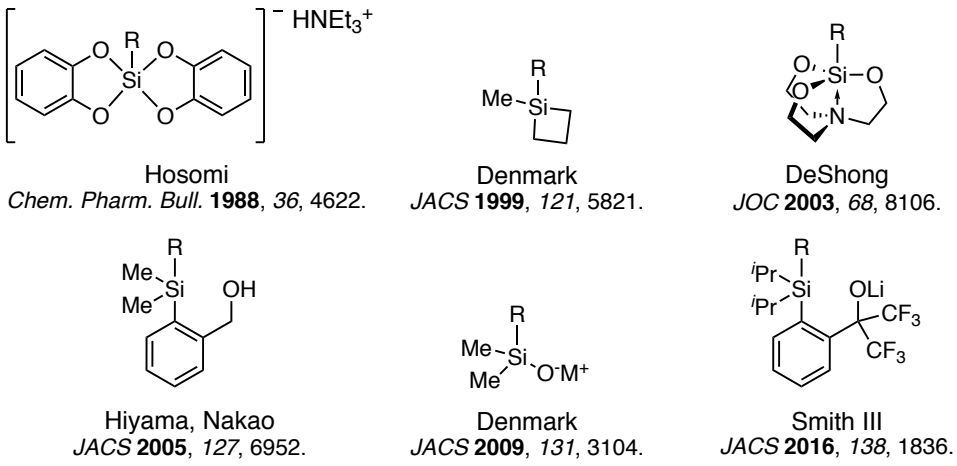

Scheme 2. Development of Organosilicon Reagents to Realize Efficient Hiyama Coupling

In this context, the development of efficient and general methods for the Hiyama

coupling reaction with ppm loadings of the relevant palladium catalysts is highly desired.

This author discovered that a palladium NNC-pincer complex **9** efficiently catalyzed the Heck reaction at ppb to ppm levels of catalyst loading (Chapter 1). Encouraged by this successful result, this author attempted to apply this catalytic system to the Hiyama coupling reaction at an extremely low catalyst loading.

Results and Discussion

First, this author performed the optimization of the reaction conditions (Table 1). 4-Bromotoluene (**30a**) and trimethoxy(phenyl)silane (**31a**) were chosen as substrates, and the reaction was initially performed under typical Hiyama coupling conditions by using palladium(II) acetate and PPh_3 as the catalyst system and tetrabutylammonium fluoride (TBAF) as the base in DMF (Table 1).[11] The reaction in the presence of 1.0 mol% of the catalyst gave the coupling product **32aa** in 86% yield (Table 1, entry 1), whereas reducing the catalyst loading to 0.1 mol% significantly lowered the yield of **32aa** to 2% only (entry 2). This result clearly showed the difficulty involved in reducing the catalyst loading under the classical Hiyama coupling conditions. During the screening of various solvents, this author found that glycol solvents were very effective in this transformation. When ethylene glycol or propylene glycol was employed as the solvent, the yield increased to 45 and 69%, respectively (Table 1, entries 3 and 4).[12] Moreover, potassium fluoride (KF) was found to be a more suitable base, affording the desired product in a higher yield (entries 5 and 6). Under these reaction conditions, the catalyst loading was successfully reduced to 100 mol ppm without a decrease in the yield (entry 7). However, in the reaction at a 10 mol ppm loading of the catalyst, then yield of **32aa** fell markedly to 3%, even on prolonging the reaction time to 12 hours (entry 8). This author therefore decided to apply the palladium NNC-pincer complex **9** in the Hiyama coupling reaction. When the reaction was

carried out in the presence of a 10 mol ppm loading of **9**, the yield improved significantly to 65% (entry 9).

Table 1. Optimization of the Conditions for the Hiyama Coupling Reaction[a]

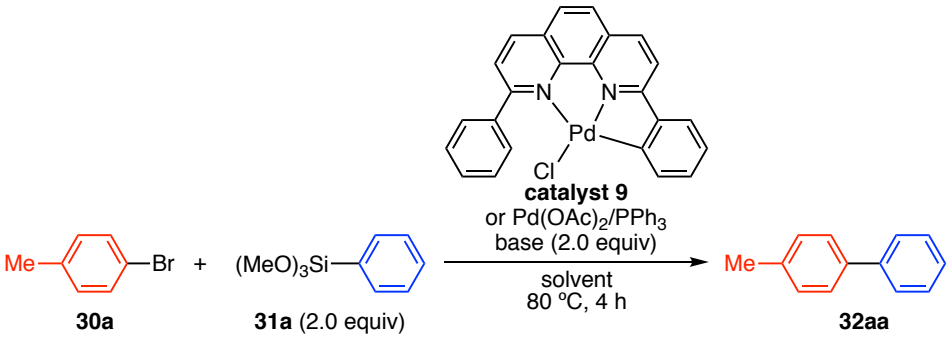

30a **31a** (2.0 equiv) **32aa**

Entry	Catalyst	Pd loading	Base	Solvent	Yield (%)
1	$Pd(OAc)_2/PPh_3$[b]	1.0 mol%	TBAF	DMF	86
2	$Pd(OAc)_2/PPh_3$[b]	0.1 mol%	TBAF	DMF	2
3	$Pd(OAc)_2/PPh_3$[b]	0.1 mol%	TBAF	ethylene glycol	45
4	$Pd(OAc)_2/PPh_3$[b]	0.1 mol%	TBAF	propylene glycol	69
5	$Pd(OAc)_2/PPh_3$[b]	0.1 mol%	KF	ethylene glycol	73
6	$Pd(OAc)_2/PPh_3$[b]	0.1 mol%	KF	propylene glycol	>99
7	$Pd(OAc)_2/PPh_3$[b]	100 mol ppm	KF	propylene glycol	97
8[c]	$Pd(OAc)_2/PPh_3$[b]	10 mol ppm	KF	propylene glycol	3
9[c]	**9**	10 mol ppm	KF	propylene glycol	65
10[c,d]	**9**	10 mol ppm	KF	propylene glycol	96
11[c,d]	**9**	5 mol ppm	KF	propylene glycol	86
12[c,d,e]	**9**	5 mol ppm	KF	propylene glycol	>99

[a] *Reaction conditions*: **30a** (0.5 mmol), **31a** (1.0 mmol), base (1.0 mmol), solvent (1.0 mL), 80 ºC, 4 h. Yields were determined by GC with mesitylene as the internal standard. [b] $Pd(OAc)_2/PPh_3$ (1:2) [c] 12 h. [d] **31a** (0.6 mmol, 1.2 equiv) + KF (1.5 mmol, 3.0 equiv) were used. [e] 100 °C.

Furthermore, the yield increased further on changing the amount of **31a** to 1.2 equivalents and that of KF to 3.0 equivalents (entry 10). Finally, the reaction proceeded in quantitative yield with a 5 mol ppm loading of **9** when the reaction temperature was raised to 100 °C (entry 12).

This author also investigated the effect of solvents and bases in the Hiyama coupling reaction of 4-bromotoluene (**30a**) and trimethoxy(phenyl)silane (**31a**) in the presence of 0.1 mol% of complex **9** (Table 2). First, the effect of solvents was examined using potassium fluoride as the base. When common solvents (toluene and dioxane) and simple alcoholic solvents (EtOH and ^{i}PrOH) were used, no reaction took place (entries 1-4). Ethylene glycol (S1) afforded the target product **32aa** in 68% yield (entry 5), whereas its mono- or di-methylated ethers (S2 and S3) were completely ineffective (entries 6 and 7), thus indicating that solvents containing a 1,2-diol unit are essential in this transformation. Other glycol solvents (S4, S5 and S6) were also tested, and propylene glycol (S4) was found to be the best solvent, giving **32aa** in >99% yield (entry 8). The use of 1,3-diol (S7) and a triol (S8) resulted in low yields of the product (entries 11 and 12). Next, this author examined the effect of bases using propylene glycol (S4) as the solvent. Other fluoride salts including NaF, CsF, and TBAF were less effective than KF, affording product **32aa** in 26–81% yield (entries 13-15). When strong bases such as potassium carbonate, potassium phosphate and potassium hydroxide were used, moderate yields of the product were obtained (entries 16-18). In these cases, the hydrodebromination of **30a** simultaneously proceeded to give toluene as a by-

product. The use of mild bases such as potassium acetate and triethylamine resulted in low conversion of substrates (entries 19 and 20).

Table 2. Effect of Solvents and Bases in the Hiyama Coupling Reaction Using 0.1 mol% of **9**

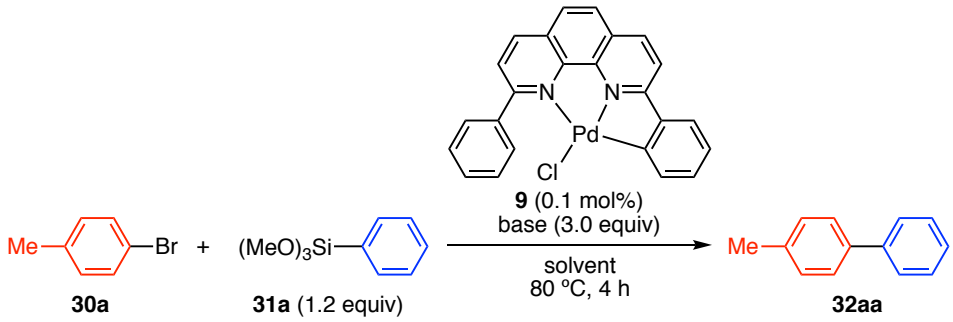

30a **31a** (1.2 equiv) **32aa**

Entry	Base	Solvent	Yield (%)	Entry	Base	Solvent	Yield (%)
1	KF	toluene	0	11	KF	S7	1
2	KF	dioxane	0	12	KF	S8	35
3	KF	EtOH	0	13	NaF	S4	26
4	KF	*i*PrOH	0	14	CsF	S4	81
5	KF	S1	68	15	TBAF	S4	35
6	KF	S2	0	16	K_2CO_3	S4	52
7	KF	S3	0	17	K_3PO_4	S4	54
8	KF	S4	>99	18	KOH	S4	10
9	KF	S5	61	19	KOAc	S4	10
10	KF	S6	<1	20	Et_3N	S4	0

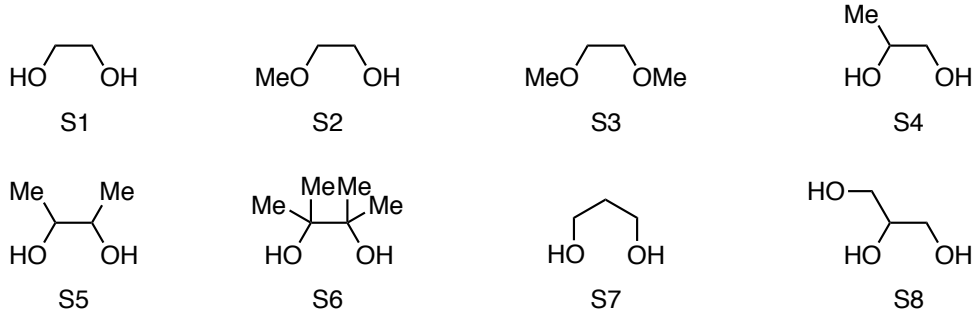

Next, this author explored the effects of other palladium complexes in the Hiyama coupling reaction under the optimized conditions (Scheme 3).

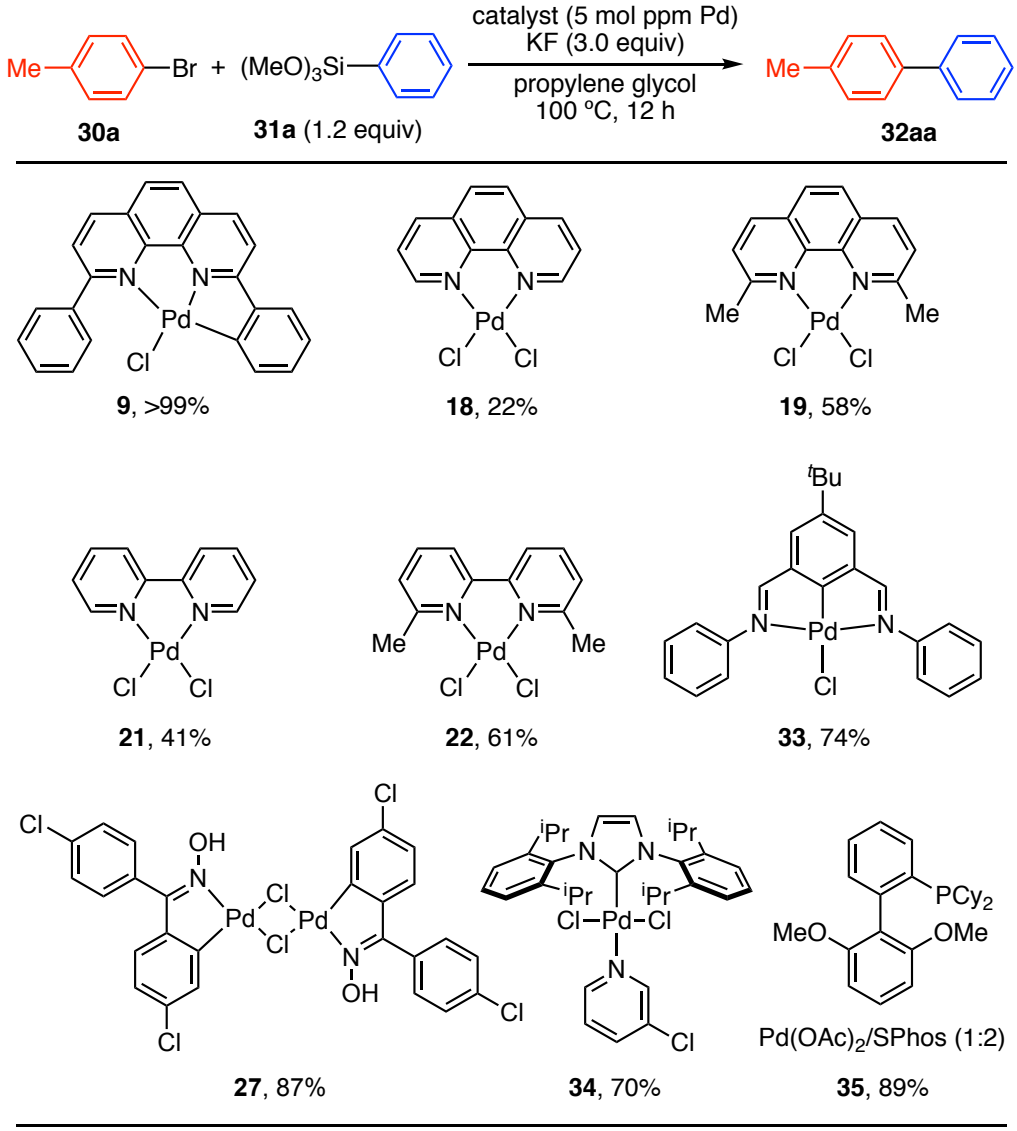

Scheme 3. The Hiyama Coupling Reaction in the Presence of Various Palladium Complexes

1,10-Phenanthroline and 2,9-dimethyl-1,10-phenanthroline palladium complexes **18** and **19** afforded the biaryl **32aa** in yields of 22 and 58%,

respectively. Similar results were obtained when the 2,2'-bipyridine palladium complexes **21** and **22** were used as catalysts. The palladium NCN-pincer complex **33**, previously developed by Uozumi and co-workers, gave product **32aa** in 74% yield. Moreover, Nájera's catalyst **27**,[13] PEPPSI-IPr **34**,[14] and $Pd(OAc)_2$/SPhos ligand **35**,[15] which are representative catalysts for various coupling reactions, gave **32aa** in yields of 70–89%. Therefore, the catalytic performance of **9** was superior to that of other palladium complexes in this transformation.

With the optimized conditions in hand, this author next investigated the scope of the reaction of various aryl bromides with trimethoxy(phenyl)silane (**31a**) (Scheme 4). Bromobenzenes **30** bearing an electron-donating substituent (methoxy, hydroxy, or *N,N*-dimethylamino) coupled efficiently with trimethoxy(phenyl)silane (**31a**) in the presence of a 5 mol ppm loading of complex **9** in propylene glycol to give the corresponding biaryls **32ba**, **32ca**, and **32da** in high yields. The reactions of substrates with halo or carbonyl groups also proceeded well to furnish products **32fa**–**32ma** in good yields. Under the reaction conditions, the chloro group in **32fa** remained completely intact. Unfortunately, bromobenzenes bearing highly electron-withdrawing substituents, such as cyano or nitro groups, were less reactive in this transformation; higher catalyst loadings (100 mol ppm to 0.1 mol%) were required to promote the reaction efficiently, and the coupling products **32na** and **32pa** were then obtained in yields of 95 and 93%, respectively. 4-Bromobenzonitrile substituted with an electron-donating 3-methoxy group coupled smoothly to furnish **32oa**, even with a 5 mol ppm loading

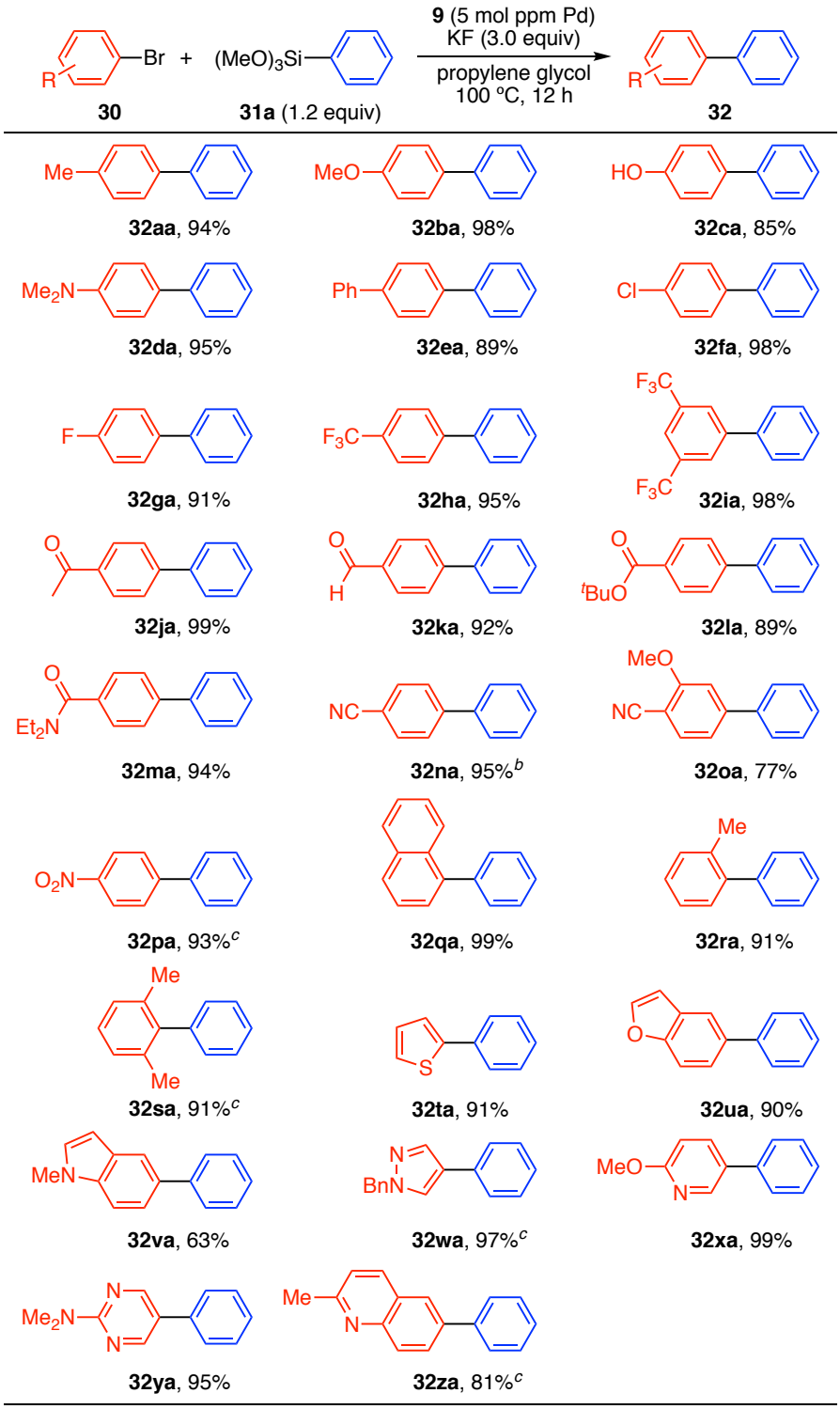

Scheme 4. Scope of Aryl Bromides[a]

[a] *Reaction conditions*: **9** (2.5×10^{-6} mmol), **30** (0.5 mmol), **31a** (0.6 mmol), KF (1.5 mmol), propylene glycol (1.0 mL), 100 °C, 12 h. Isolated yields are reported. [b] **9** (0.1 mol%). [c] **9** (100 mol ppm).

of **9**. Sterically hindered 1-naphthyl and 2-tolyl bromides were also compatible with this reaction. However, 2-bromo-1,3-dimethylbenzene required a 100 mol ppm loading of the catalyst to afford the corresponding product **32sa** in a reasonable yield. Notably, heteroaromatic bromides, including thiophene, benzofuran, indole, pyrazole, pyridine, pyrimidine, and quinoline bromides, were also suitable substrates, affording the corresponding products **32ta**–**32za** in high yields.

Next, this author focused on the scope with respect to aryl- or alkenyl(triethoxy)silanes (Scheme 5). Aryl- or (alkenyl)triethoxysilanes were chosen as silicon reactants instead of trimethoxysilanes because of their ready availability. Indeed, triethoxy(phenyl)silane exhibited a similar reactivity to that of **30a**, affording the coupling product **32aa** in 91% yield. Electron-rich and electronically neutral arylsilanes such as anisyl-, benzodioxolyl-, morpholinylphenyl-, naphthyl-, pyrenyl-, or (fluorophenyl)silanes coupled efficiently with 4-bromotoluene (**30a**) in the presence of a 5 mol ppm loading of the catalyst to give the corresponding biaryls **32ab**–**32ah** in yields of 72 to 99%. On the other hand, electron-deficient aryl(triethoxy)silanes **31l**, **31j**, and **31k** were less reactive owing to their low nucleophilicity, so that a 100 mol ppm loading of the catalyst was required to promote their coupling reactions efficiently. Additionally, alkenyl(triethoxy)silanes also served as good substrates in the transformation, providing the desired products **32qm** and **32an** in high yields.

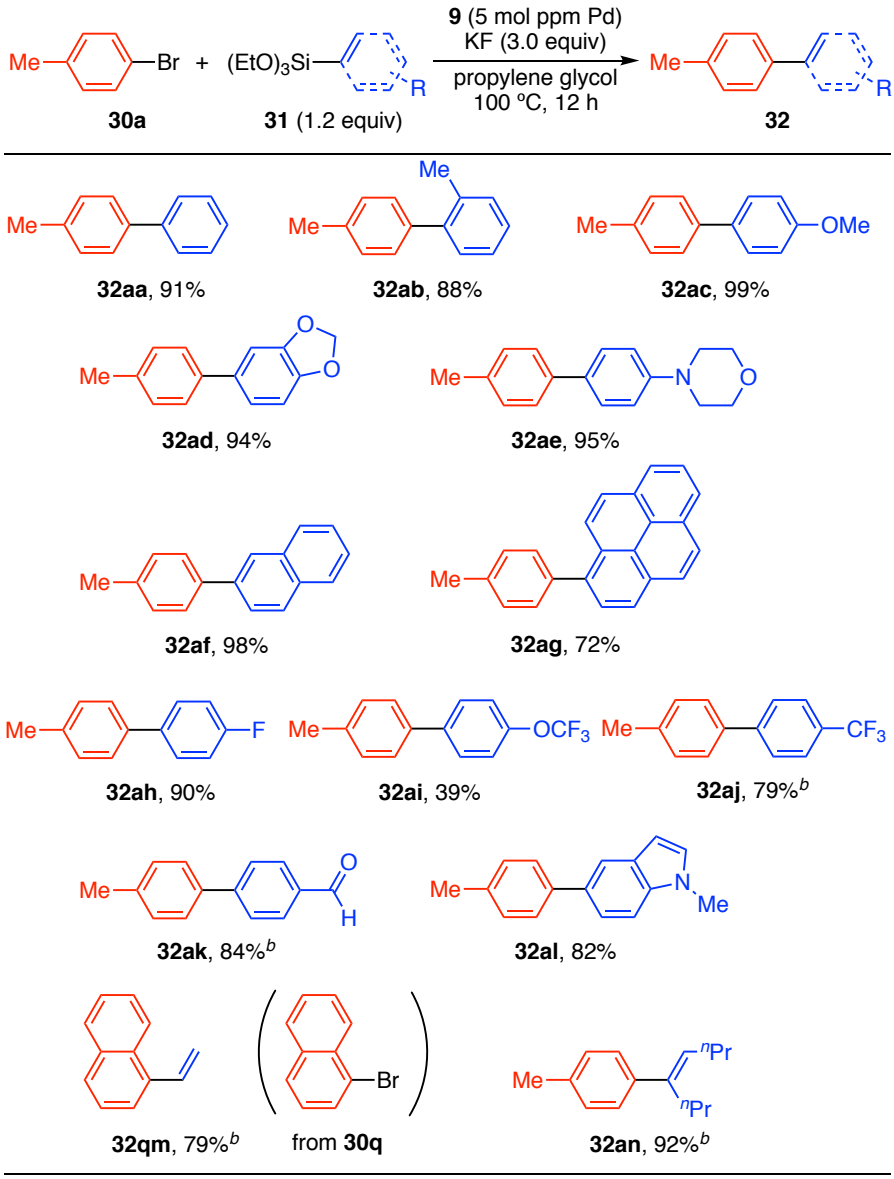

Scheme 5. Scope of Aryl- and Alkenyl(triethoxy)silanes[a]

[a] *Reaction conditions*: **9** (2.5×10^{-6} mmol), **30a** (0.5 mmol), **31** (0.6 mmol), KF (1.5 mmol), propylene glycol (1.0 mL), 100 °C, 12 h. Isolated yields are reported. [b] **9** (100 mol ppm).

To further demonstrate the utility of the reaction system, this author examined several of its synthetic applications (Schemes 6 and 7). This method was applied to a synthesis of the topical retinoid adapalene (**38**)[16] on about a seven-gram scale.

The target molecule was successfully synthesized in 93% yield without chromatographic purification (Scheme 6).

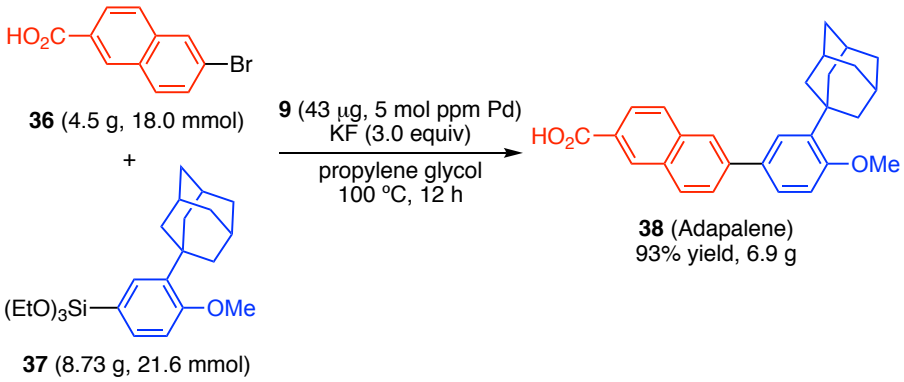

Scheme 6. Multigram-Scale Synthesis of Adapalene (**38**) in the Presence of a 5 mol ppm of **9**

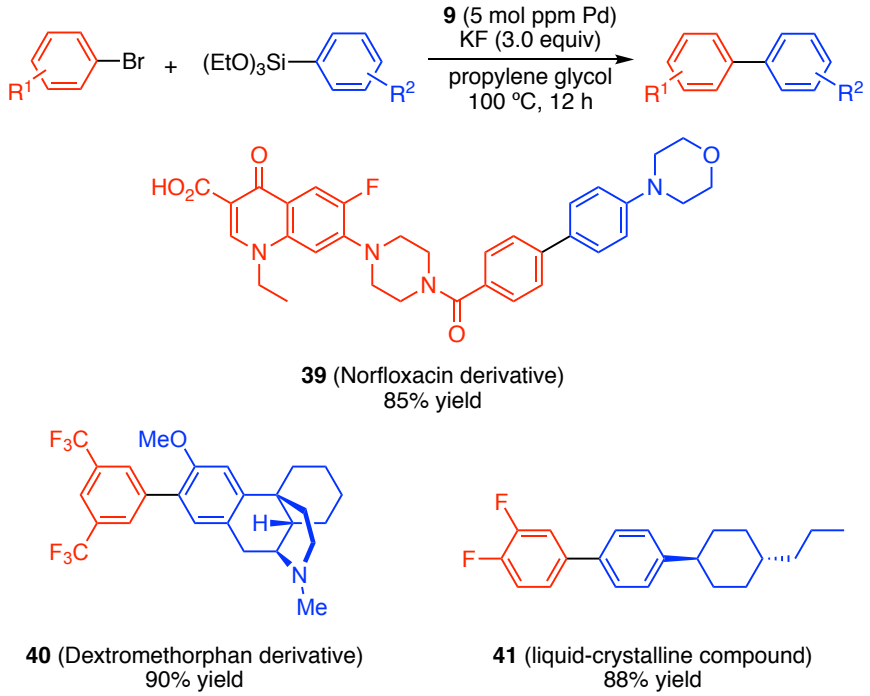

Scheme 7. Functionalization of Drug Molecules (Norfloxacin and Dextromethorphan) and Synthesis of a Liquid-Crystalline Compound **41**

Moreover, this method was applicable to the derivatization of drug molecules. The reaction of an aryl bromide-tethered norfloxacin[17] with 4-[4-(triethoxysilyl)phenyl]morpholine proceeded nicely to furnish the derivative **39** in 85% yield. A triethoxysilylated dextromethorphan[18] also coupled readily with 1-bromo-3,5-bis(trifluoromethyl)benzene to give product **40** in 90% yield. Additionally, the liquid-crystalline compound **41**[19] was also synthesized under the same reaction conditions (Scheme 7).

Conclusion

In summary, this author has developed a simple, efficient, and general method for performing the Hiyama coupling reaction at ppm levels of a Pd catalyst. A palladium NNC-pincer complex at a 5 mol ppm loading efficiently catalyzed the Hiyama coupling reaction of aromatic bromides with aryltrialkoxysilanes in the presence of potassium fluoride in propylene glycol at 100 ºC to furnish the corresponding biaryls in up to 99% yield with wide functional group tolerance including a variety of heteroaromatics. To demonstrate the further utility of the reaction system, this method was applied to a multi-gram scale synthesis of adapalene and a synthesis of a liquid-crystalline compound, as well as to the derivatization of triethoxysilylated dextromethorphan and an aryl bromide-tethered norfloxacin.

Experimental Section

General Methods. All reactions with oxygen- or moisture-sensitive reagents were performed under a nitrogen atmosphere, nitrogen gas was dried by passage through P_2O_5. Silica gel was purchased from Kanto chemical (Silica gel 60N, spherical neutral, particle size 40-50μm) or Yamazen corporation (Hi-FlashTM Column Silica gel 40 mm 60 Å). NMR spectra were recorded on a JEOL JNM ECS-400 spectrometer (396 MHz for ^{1}H, 100 MHz for ^{13}C). Chemical shifts are reported in δ (ppm) referenced to an internal tetramethylsilane standard for ^{1}H NMR. Chemical shifts of ^{13}C NMR are given related to solvent peak as an internal standard ($CDCl_3$: δ 77.0 or DMSO-d_6: δ 39.5). Chemical shifts of ^{29}Si NMR were obtained related to tetramethylsilane (δ -0.0) as an external standard. ^{1}H, ^{13}C and ^{29}Si NMR spectra were recorded in $CDCl_3$ or DMSO-d_6 at 25 °C. GC and GC-MS analyses were performed with an Agilent 6850 series II GC and an Agilent 6890 GC/5973N MS Detector, respectively. Commercially available chemicals (purchased from Sigma-Aldrich, TCI, Kanto chemical, Wako Pure Chemical Industries, Nacalai tesque, and Merck) were used without further purification unless otherwise noted. Propylene glycol was distilled under reduced pressure prior to use. Palladium NNC-pincer complex **9**,[20] 4-bromo-2-methoxybenzonitrile,[21] 4-bromo-1-(phenylmethyl)pyrazole,[22] 5-bromo-2-methoxypyridine,[23] 4-triethoxysilylbenzaldehyde[24] were prepared according to literature procedures.

Typical Procedure for the Hiyama Coupling Reaction

The palladium complex **9** (0.23 mg, 5×10^{-4} mmol) was dissolved in CH_2Cl_2 (1 mL), and the catalyst solution (5 μL, 2.5×10^{-6} mmol) was added to a mixture of 4-bromotoluene (**30a**; 85 mg, 0.5 mmol), phenyltrimethoxysilane (**31a**; 0.11 mL, 0.6 mmol), and KF (87 mg, 1.5 mmol) in propylene glycol (1.0 mL) under N_2 flow. The resulting solution was stirred vigorously at 100 °C for 12 h under N_2. The mixture was then cooled to 25 °C, diluted with *t*-BuOMe (10 mL), transferred to a separatory funnel, and washed with H_2O (10 mL). The aqueous layer was extracted with *t*-BuOMe (2 × 5 mL), and the extracts were combined, washed with brine (20 mL), and dried over Na_2SO_4. The resulting solution was concentrated under reduced pressure to give a crude product that was purified by chromatography [silica gel, hexane] to give 4-methylbiphenyl (**32aa**; 79 mg, 0.47 mmol); yield:94%.

[CAS: 644-08-6] Colorless solid. ^{1}H NMR (396 MHz, $CDCl_3$) δ 7.58 (dt, J = 8.0, 1.6 Hz, 2H), 7.49 (dt, J = 8.4, 1.6 Hz, 2H), 7.44-7.40 (m, 2H), 7.32 (tt, J = 7.2, 1.6 Hz, 1H), 7.26-7.24 (m, 2H), 2.40 (s, 3H). ^{13}C NMR (100 MHz, $CDCl_3$) δ 141.12, 138.32, 136.99, 129.45, 128.69, 126.95, 21.09. EI-MS *m/z* 168 (M^+).

Procedures for the Synthetic Applications

Procedure for the Gram-Scale Synthesis of Adapalene (**38**)[25]

The palladium complex **9** (0.23 mg, 5×10^{-4} mmol) was dissolved in CH_2Cl_2 (1 mL), and the catalyst solution (180 μL, 9.0×10^{-5} mmol) was added to a mixture

of 6-bromo-2-naphthoic acid (4.50 g, 18.0 mmol), 3-adamantyl-4-methoxyphenyltriethoxysilane (8.73 g, 21.6 mmol), and KF (3.13 g, 54.0 mmol) in propylene glycol (56.0 mL) under N_2 flow. The resulting solution was stirred vigorously at 100 °C for 12 h under N_2. After the mixture was cooled to 25 °C, 0.25 M aqueous HCl (150 mL) was added with vigorous stirring. The resulting precipitate was filtered and washed with H_2O (3 × 20 mL) followed by Et_2O (3 × 20 mL). The solid residue was dissolved in THF (150 mL), and insoluble materials were removed by filtration. The resulting filtrate was concentrated under reduced pressure to give Adapalene (**38**) (6.92 g, 16.7 mmol) as a pure form; yield 93%. [CAS: 106685-4-09] Colorless solid. ^{1}H NMR (396 MHz, DMSO-d_6) δ 8.60 (s, 1H), 8.23 (s, 1H), 8.16 (d, J = 7.6 Hz, 1H), 8.08 (d, J = 8.0 Hz, 1H), 7.98 (d, J = 8.4 Hz, 1H), 7.90 (d, J = 8.4 Hz, 1H), 7.66 (d, J = 8.4 Hz, 1H), 7.58 (s, 1H), 7.13 (d, J = 8.4 Hz, 1H), 3.87 (s, 3H), 2.14 (s, 6H), 2.07 (s, 3H), 1.76 (s, 6H). ^{13}C NMR (100 MHz, DMSO-d_6) δ 167.92, 159.09, 140.69, 138.53, 135.94, 131.99 131.38, 130.17, 130.30, 128.82, 129.09, 126.43, 125.96, 125.56, 124.55, 113.21, 55.84, 37.03, 28.87.

Procedure for the Synthesis of a Norfloxacin Derivative (**39**)

The palladium complex **9** (0.23 mg, 5 × 10^{-4} mmol) was dissolved in CH_2Cl_2 (1 mL), and the catalyst solution (5 μL, 2.5 × 10^{-6} mmol) was added to a mixture of an aryl bromide-tethered Norfloxacin (250 mg, 0.5 mmol), 4-morphorinophenyltriethoxysilane (195 mg, 0.6 mmol), and KF (87 mg, 1.5 mmol)

in propylene glycol (2.0 mL) under N_2 flow. The resulting solution was stirred vigorously at 100 °C for 12 h under N_2. After the mixture was then cooled to 25 °C, H_2O (5 mL) was added. The mixture was neutralized by adding aqueous solution of HCl (1.0 M) until the pH value reached 6.0. The aqueous mixture was transferred into a separatory funnel, extracted with DCM (3 × 10 mL), and the extracts were combined, washed with brine (30 mL), and dried over Na_2SO_4, and concentrated under reduced pressure. The resulting residue was stirred in EtOH (2 mL) with refluxing for 5 min, then the residue was cooled to 0 ºC, filtered off, rinsed with cold EtOH (2 × 1 mL), followed by dried under reduced pressure to give the titled product **39** (248 mg, 0.43 mmol) in 85% yield.

[CAS: none] Colorless solid. Mp. >300 ºC (decomp.). ^{1}H NMR (396 MHz, $CDCl_3$) δ 8.69 (s, 1H), 8.11 (d, *J* = 13.2 Hz, 1H), 7.63 (d, *J* = 8.0 Hz, 2H), 7.55 (d, *J* = 9.2 Hz, 2H), 7.51 (d, *J* = 8.4 Hz, 2H), 7.00 (d, *J* = 8.4 Hz, 2H), 6.87 (d, *J* = 7.6 Hz, 1H), 4.32 (q, *J* = 7.6 Hz, 2H), 4.00 (br, 4H), 3.89 (t, *J* = 4.8 Hz, 4H), 3.34 (br, 4H), 3.23 (t, *J* = 4.8 Hz, 4H), 1.60 (t, *J* = 6.8 Hz, 3H). ^{13}C NMR (100 MHz, $CDCl_3$) δ 177.05, 170.60, 166.98, 151.09, 147.30, 142.84, 137.06, 132.82, 131.96, 131.15, 127.87, 126.53, 121.40, 115.68, 113.31, 113.08, 108.71, 104.23, 66.83, 50,19, 49.73, 48.93, 14.51. IR (ATR): 3054, 2833, 1719, 1624, 1485, 1370, 1213, 1115, 1007, 925 cm^{-1}. HRMS (FAB, *m/z*, MH^+) calcd for $C_{33}H_{34}FN_4O_5$ 585.2513, found 585.2533.

Procedure for the Synthesis of a Dextromethorphan Derivative (**40**)

The palladium complex **9** (0.23 mg, 5×10^{-4} mmol) was dissolved in CH_2Cl_2 (1 mL), and the catalyst solution (5 μL, 2.5×10^{-6} mmol) was added to a mixture of triethoxysilylDextromethorphan (217 mg, 0.5 mmol), 3,5-bis(trifluoromethyl)-1-bromobenzene (174 mg, 0.6 mmol), and KF (87 mg, 1.5 mmol) in propylene glycol (1.0 mL) under N_2 flow. The resulting solution was stirred vigorously at 100 °C for 12 h under N_2. The mixture was then cooled to 25 °C, diluted with *t*-BuOMe (10 mL), transferred to a separatory funnel, and washed with H_2O (10 mL). The aqueous layer was extracted with *t*-BuOMe (2 × 5 mL), and the extracts were combined, washed with brine (20 mL), and dried over Na_2SO_4. The resulting solution was concentrated under reduced pressure to give a crude product that was purified by chromatography [silica gel, DCM/EtOH/Et_3N (90:8:2)] to give a Dextromethorphan derivative (**40**); yield 88%.

[CAS: none] Colorless solid. Mp. 129 ºC. ^{1}H NMR (396 MHz, $CDCl_3$) δ 8.02 (s, 2H), 7.80 (s, 1H), 7.07 (s, 1H), 6.88 (s, 1H), 3.81 (s, 3H), 3.04 (d, *J* = 18.4 Hz, 1H), 2.86-2.84 (m, 1H), 2.63 (dd, *J* = 18.0, 5.6 Hz, 1H), 2.50-2.39 (m, 5H), 2.13 (td, *J* = 12.4, 3.2 Hz, 1H), 1.87 (dt, *J* = 12.8, 2.8 Hz, 1H), 1.80 (td, *J* = 12.0, 5.2 Hz, 1H), 1.71-1.68 (m, 1H), 1.61-1.58 (m, 1H), 1.49-1.32 (m, 5H), 1.22-1.12 (m, 1H). ^{13}C NMR (100 MHz, $CDCl_3$) δ 154.93, 142.79, 140.49, 131.03 (q, *J* = 32.6 Hz), 130.57, 129.69, 129.58, 124.91, 123.56 (q, *J* = 270.2 Hz), 120.22, 108.12, 57.79, 55.65, 47.21, 45.42, 42.82, 42.00, 37.52, 36.76, 26.76, 26.51, 23.28, 22.27.

IR (ATR): 2924, 2856, 1612, 1505, 1372, 1271, 1176, 1119, 1048, 892 cm^{-1}. HRMS (FAB, *m/z*, MH^+) calcd for $C_{26}H_{28}F_6NO$ 484.2075, found 484.2080.

Procedure for the Synthesis of a Liquid Crystalline Compound (**41**)[26]

The palladium complex **9** (0.23 mg, 5×10^{-4} mmol) was dissolved in CH_2Cl_2 (1 mL), and the catalyst solution (5 μL, 2.5×10^{-6} mmol) was added to a mixture of 4-(*trans*-4-propylcyclohexyl)phenyltriethoxysilane (182 mg, 0.5 mmol), 3,4-difluoro-1-bromobenzene (114 mg, 0.6 mmol), and KF (87 mg, 1.5 mmol) in propylene glycol (1.0 mL) under N_2 flow. The resulting solution was stirred vigorously at 100 °C for 12 h under N_2. The mixture was then cooled to 25 °C, diluted with *t*-BuOMe (10 mL), transferred to a separatory funnel, and washed with H_2O (10 mL). The aqueous layer was extracted with *t*-BuOMe (2 × 5 mL), and the extracts were combined, washed with brine (20 mL), and dried over Na_2SO_4. The resulting solution was concentrated under reduced pressure to give a crude product that was purified by chromatography [silica gel, hexane] to give a liquid crystalline compound (**41**); yield 88%.

[CAS: 85312-59-0] Colorless solid. ^1H NMR (396 MHz, $CDCl_3$) δ 7.43 (d, *J* = 8.0 Hz, 2H), 7.38-7.33 (m, 1H), 7.28-7.25 (m, 3H), 7.21-7.14 (m, 1H), 2.50 (tt, *J* = 12.0, 3.2 Hz, 1H), 1.90 (t, *J* = 13.2 Hz, 4H), 1.52-1.42 (m, 2H), 1.38-1.26 (m, 3H), 1.25-1.19 (m, 2H), 1.13-1.01 (m, 2H), 0.91 (t, *J* = 7.2 Hz, 3H). ^{13}C NMR (100 MHz, $CDCl_3$) δ 151.30 (dd, *J* = 75.7, 12.4 Hz), 148.84 (dd, *J* = 76.7, 12.5

Hz), 147.70, 138.28, 136.61, 127.42, 126.80, 122.73, 117.38 (d, J = 17.3 Hz), 115.73 (d, J = 17.3 Hz), 44.27, 39.69, 36.99, 34.29, 33.51, 20.03, 14.41.

Compound Data in the Hiyama Coupling Reaction

4-methylbiphenyl (**32aa**)[27] [CAS: 644-08-6]

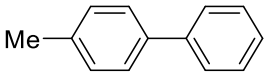

Colorless solid. ^{1}H NMR (396 MHz, $CDCl_3$) δ 7.58 (dt, J = 8.0, 1.6 Hz, 2H), 7.49 (dt, J = 8.4, 1.6 Hz, 2H), 7.44-7.40 (m, 2H), 7.32 (tt, J = 7.2, 1.6 Hz, 1H), 7.26-7.24 (m, 2H), 2.40 (s, 3H). ^{13}C NMR (100 MHz, $CDCl_3$) δ 141.12, 138.32, 136.99, 129.45, 128.69, 126.95, 21.09. EI-MS *m/z* 168 (M^+).

4-methoxylbiphenyl (**32ba**)[27] [CAS: 613-37-6]

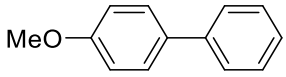

Colorless solid. ^{1}H NMR (396 MHz, $CDCl_3$) δ 7.57-7.52 (m, 4H), 7.44-7.40 (m, 2H), 7.31 (tt, J = 7.6, 1.2 Hz, 1H), 6.99 (dt, J = 9.2, 2.4 Hz, 2H) 3.86 (s, 3H). ^{13}C NMR (100 MHz, $CDCl_3$) δ 159.09, 140.79, 133.74, 128.70, 128.14, 126.72, 126.64, 114.17, 55.33. EI-MS *m/z* 184 (M^+).

4-hydroxybiphenyl (**32ca**)[28] [CAS: 92-69-3]

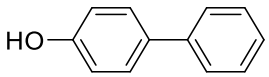

Colorless solid. ^{1}H NMR (396 MHz, $CDCl_3$) δ 7.55-7.53 (m, 2H), 7.50-7.47 (m, 2H), 7.44-7.39 (m, 2H), 7.31 (tt, J = 7.6, 1.2 Hz, 1H) 4.78 (s, 1H). ^{13}C NMR (100 MHz, $CDCl_3$) δ 154.99, 140.71, 134.02, 128.72, 128.38, 126.70, 115.61. EI-MS *m/z* 170 (M^+).

4-dimethylaminobiphenyl (**32da**)[29] [CAS: 1137-79-7]

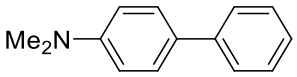 Colorless solid. ^{1}H NMR (396 MHz, $CDCl_3$) δ 7.57-7.54 (m, 2H), 7.53-7.49 (m, 2H), 7.27-7.23 (m, 1H), 6.83-6.79 (m, 2H) 2.99 (s, 6H). ^{13}C NMR (100 MHz, $CDCl_3$) δ 149.94, 141.19, 129.21, 128.62, 127.68, 126.27, 125.96, 112.74, 40.57. EI-MS *m/z* 197 (M^+).

p-terphenyl (**32ea**)[30] [CAS: 92-94-4]

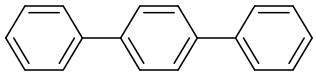 Colorless solid. ^{1}H NMR (396 MHz, $CDCl_3$) δ 7.68 (s, 4H), 7.66-7.63 (m, 4H), 7.47 (tt, *J* = 8.0, 1.6 Hz, 4H), 7.36 (tt, *J* = 9.2, 1.2 Hz, 2H). ^{13}C NMR (100 MHz, $CDCl_3$) δ 140.67, 140.10, 128.80, 127.49, 127.33, 127.03. EI-MS *m/z* 230 (M^+).

4-chlorobiphenyl (**32fa**)[27] [CAS: 2051-62-9]

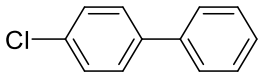 Colorless solid. ^{1}H NMR (396 MHz, $CDCl_3$) δ 7.57-7.50 (m, 4H), 7.47-7.39 (m, 4H), 7.36 (tt, *J* = 7.2, 1.6 Hz, 1H). ^{13}C NMR (100 MHz, $CDCl_3$) δ 139.97, 139.63, 133.34, 128.87, 128.37, 127.57, 126.96. EI-MS *m/z* 188 (M^+).

4-fluorobiphenyl (**32ga**)[31] [CAS: 324-72-3]

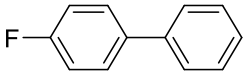 Colorless solid. ^{1}H NMR (396 MHz, $CDCl_3$) δ 7.56-7.51 (m, 4H), 7.45-7.40 (m, 2H), 7.36-7.32 (m, 1H), 7.15-7.09 (m, 2H). ^{13}C NMR (100 MHz, $CDCl_3$) δ 162.42 (d, *J* = 247.2 Hz), 140.22, 137.31, 128.79, 128.66 (d, *J* = 7.6 Hz), 127.23, 126.99, 115.59 (d, *J* = 22.0 Hz). EI-MS *m/z* 172 (M^+).

4-trifluoromethylbiphenyl (**32ha**)[27] [CAS: 398-36-7]

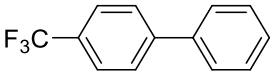 Colorless solid. ^{1}H NMR (396 MHz, $CDCl_3$) δ 7.70 (s, 4H), 7.62-7.59 (m, 2H), 7.51-7.46 (m, 2H), 7.43-7.39 (m, 1H). ^{13}C NMR (100 MHz, $CDCl_3$) δ 144.70, 139.75, 129.47, 129.15, 128.97, 128.17, 127.40, 127.26, 125.68, 122.94. EI-MS *m/z* 222 (M^+).

3,5-bis(trifluoromethyl)biphenyl (**32ia**)[32] [CAS: 336621-50-2]

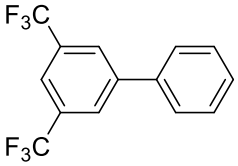 Colorless solid. ^{1}H NMR (396 MHz, $CDCl_3$) δ 8.01 (s, 2H), 7.86 (s, 1H), 7.63-7.59 (m, 2H), 7.54-7.49 (m, 2H), 7.47-7.43 (m, 1H). ^{13}C NMR (100 MHz, $CDCl_3$) δ 143.31, 138.23, 132.08 (q, *J* = 33.5 Hz), 129.27, 128.87, 127.23, 124.75, 122.01, 120.90 (m). EI-MS *m/z* 290 (M^+).

4-acetylbiphenyl (**32ja**)[27] [CAS: 92-91-1]

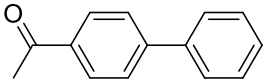 Colorless solid. ^{1}H NMR (396 MHz, $CDCl_3$) δ 8.04 (dt, *J* = 8.4, 2.0 Hz, 2H), 7.69 (dt, *J* = 8.8, 2.0 Hz, 2H), 7.65-7.62 (m, 2H), 7.50-7.45 (m, 2H), 7.43-7.38 (m, 1H), 2.64 (s, 3H). ^{13}C NMR (100 MHz, $CDCl_3$) δ 197.76, 145.74, 139.82, 135.79, 128.93, 128.89, 128.21, 127.24, 127.19, 26.67. EI-MS *m/z* 196 (M^+).

4-formylbiphenyl (**32ka**)[31] [CAS: 3218-36-8]

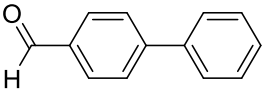 Colorless solid. ^{1}H NMR (396 MHz, $CDCl_3$) δ 10.06 (s, 1H), 7.96 (dt, *J* = 8.8, 2.0 Hz, 2H), 7.76 (dt, *J* = 8.4, 2.0 Hz, 2H), 7.66-7.63 (m, 2H),

7.51-7.46 (m, 2H), 7.44-7.40 (m, 1H). ^{13}C NMR (100 MHz, $CDCl_3$) δ 191.89, 147.11, 139.62, 135.11, 130.21, 128.95, 128.42, 127.61, 127.30. EI-MS *m/z* 182 (M^+).

4-(*tert*-butoxycarbonyl)biphenyl (**32la**)[33] [CAS: 220333-86-8]

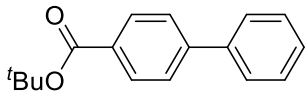

Colorless oil. ^{1}H NMR (396 MHz, $CDCl_3$) δ 8.06-8.04 (m, 2H), 7.64-7.60 (m, 2H), 7.48-7.44 (m, 2H), 7.40-7.36 (m, 1H), 1.61 (s, 9H). ^{13}C NMR (100 MHz, $CDCl_3$) δ 165.64, 145.10, 140.13, 130.73, 129.89, 129.36, 128.86, 128.13, 127.98, 127.23, 126.85. EI-MS *m/z* 254 (M^+).

4-(*N,N*-diethylaminocarbonyl)biphenyl (**32ma**)[34] [CAS: 204706-70-7]

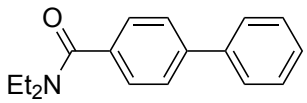

Colorless oil. ^{1}H NMR (396 MHz, $CDCl_3$) δ 7.61 (t, *J* = 7.2 Hz, 4H), 7.48-7.44 (m, 4H), 7.37 (t, *J* = 7.2 Hz, 1H), 3.57-3.33 (m, 4H), 1.26-1.16 (m, 6H) ^{13}C NMR (100 MHz, $CDCl_3$) δ 171.10, 141.97, 140.37, 136.04, 128.82, 127.63, 127.10, 126.82, 43.31, 39.23, 14.25, 12.86. EI-MS *m/z* 253 (M^+).

4-cyanobiphenyl (**32na**)[29] [CAS: 2920-38-9]

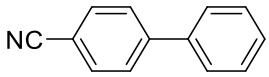

Colorless solid. ^{1}H NMR (396 MHz, $CDCl_3$) δ 7.75-7.68 (m, 4H), 7.61-7.58 (m, 2H), 7.51-7.46 (m, 2H), 7.45-7.41 (m, 1H). ^{13}C NMR (100 MHz, $CDCl_3$) δ 145.63, 139.13, 132.57, 129.08, 128.63, 127.70, 127.20, 118.93, 110.85. EI-MS *m/z* 179 (M^+).

4-cyano-3-methoxybiphenyl (**32oa**)[35] [CAS: 408339-01-5]

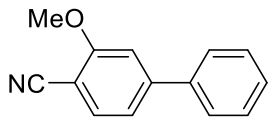

Colorless solid. ^{1}H NMR (396 MHz, $CDCl_3$) δ 7.61 (d, *J* = 7.6 Hz, 1H), 7.59-7.56 (m, 2H), 7.50-7.45 (m, 2H), 7.44-7.39 (m, 1H), 7.45-7.41 (m, 1H), 7.21 (dd, *J* = 8.4, 1.6 Hz, 1H), 7.13 (d, *J* = 1.2 Hz, 1H), 3.99 (s, 3H). ^{13}C NMR (100 MHz, $CDCl_3$) δ 161.47, 147.69, 139.55, 133.92, 129.01, 128.70, 127.23, 119.69, 116.60, 109.95, 100.35, 56.01. EI-MS *m/z* 209 (M^+).

4-nitrobiphenyl (**32pa**)[27] [CAS: 92-93-3]

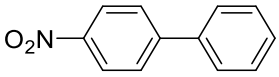

Colorless solid. ^{1}H NMR (396 MHz, $CDCl_3$) δ 8.31 (dt, *J* = 9.2, 2.4 Hz, 2H), 7.76-7.73 (m, 2H), 7.65-7.62 (m, 2H), 7.53-7.48 (m, 2H), 7.47-7.43 (m, 1H). ^{13}C NMR (100 MHz, $CDCl_3$) δ 147.54, 146.98, 138.67, 129.10, 128.87, 127.73, 127.32, 124.04. EI-MS *m/z* 199 (M^+).

1-phenylnaphthalene (**32qa**)[27] [CAS: 605-02-7]

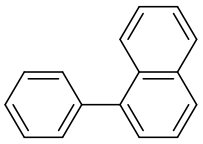

Colorless oil. ^{1}H NMR (396 MHz, $CDCl_3$) δ 7.92-7.89 (m, 2H), 7.88-7.85 (d, *J* = 8.4 Hz, 1H), 7.55-7.47 (m, 6H), 7.46-7.40 (m, 3H). ^{13}C NMR (100 MHz, $CDCl_3$) δ 140.72, 140.22, 133.75, 131.58, 130.06, 128.24, 127.60, 127.21, 126.90, 125.99, 125.75, 125.36. EI-MS *m/z* 204 (M^+).

2-methylbiphenyl (**32ra**)[27] [CAS: 643-58-3]

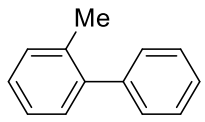

Colorless oil. ^{1}H NMR (396 MHz, $CDCl_3$) δ 7.43-7.38 (m, 2H), 7.35-7.31 (m, 3H), 7.27-7.22 (m, 4H), 2.27 (s, 3H). ^{13}C NMR (100 MHz, $CDCl_3$) δ 141.91, 135.33, 130.28, 129.78, 129.17, 128.03, 127.22, 126.73, 125.74, 20.46. EI-MS *m/z* 168 (M^+).

2,6-dimethylbiphenyl (**32sa**)[29] [CAS: 3976-34-9]

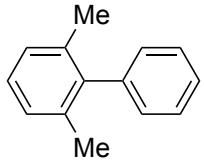

Colorless liquid. ^{1}H NMR (396 MHz, $CDCl_3$) δ 7.42 (t, *J* = 8.0 Hz, 2H), 7.33 (t, *J* = 7.6 Hz, 1H), 7.18-7.10 (m, 5H), 2.03 (s, 6H). ^{13}C NMR (100 MHz, $CDCl_3$) δ 141.85, 141.05, 136.05, 129.00, 128.39, 127.24, 126.99, 126.58, 20.84. EI-MS *m/z* 182 (M^+).

2-phenylthiophene (**32ta**)[30] [CAS: 825-55-8]

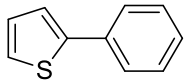

Colorless oil. ^{1}H NMR (396 MHz, $CDCl_3$) δ 7.63-7.60 (m, 2H), 7.40-7.36 (m, 2H), 7.32-7.25 (m, 3H), 7.08 (dd, *J* = 6.0, 4.5 Hz, 1H). ^{13}C NMR (100 MHz, $CDCl_3$) δ 144,38, 134.35, 128.85, 127.97, 127.42, 125.91, 124.77, 123.03. EI-MS *m/z* 160 (M^+).

5-phenylbenzofuran (**32ua**)[36] [CAS: 35664-71-2]

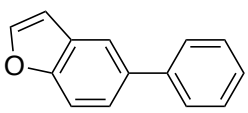

Colorless solid. ^{1}H NMR (396 MHz, $CDCl_3$) δ 7.79 (d, *J* = 1.6 Hz, 1H), 7.66 (d, *J* = 2.4 Hz, 1H), 7.63-7.60 (m, 2H), 7.58-7.51 (m, 2H), 7.47-7.43 (m, 2H), 7.37-7.32 (m, 1H). ^{13}C NMR (100 MHz, $CDCl_3$) δ

154.51, 145.55, 141.63, 136.45, 128.72, 127.91, 127.44, 126.85, 123.95, 119.69, 111.47, 106.78. EI-MS *m/z* 194 (M^+).

1-methyl-5-phenylindole (**32va**)[37] [CAS: 352197-74-1]

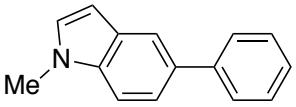

Colorless solid. ^{1}H NMR (396 MHz, $CDCl_3$) δ 7.84 (d, *J* = 1.6 Hz, 1H), 7.65 (dd, *J* = 7.2, 1.2 Hz, 2H), 7.48 (dd, *J* = 8.8, 1.6 Hz, 1H), 7.43 (t, *J* = 8.0 Hz, 2H), 7.38 (d, *J* = 8.4 Hz, 1H), 7.30 (tt, *J* = 7.6, 0.8 Hz, 1H), 7.07 (d, *J* = 3.2 Hz, 1H), 6.53 (d, *J* = 2.8 Hz, 1H), 3.81 (s, 1H). ^{13}C NMR (100 MHz, $CDCl_3$) δ 142.60, 136.22, 132.83, 129.46, 128.92, 128.60, 127, 37, 126.22, 121.38, 119.39, 109.40, 101.30, 32.93. EI-MS *m/z* 207 (M^+).

4-phenyl-1-benzylpyrazole (**32wa**)[38] [CAS: 700360-08-3]

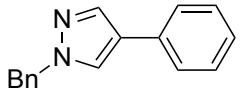

Colorless solid. ^{1}H NMR (396 MHz, $CDCl_3$) δ 7.83 (s, 1H), 7.62 (d, *J* = 1.2 Hz, 1H), 7.47 (tt, *J* = 8.4, 1.6 Hz, 2H), 7.39-7.33 (m, 5H), 7.28-7.26 (m, 2H), 7.22 (tt, *J* = 7.2, 1.6 Hz, 1H), 7.35 (s, 2H). ^{13}C NMR (100 MHz, $CDCl_3$) δ 137.00, 136.38, 132.50, 128.87, 128.81, 128.14, 127.72, 126.39, 126.14, 125.48, 123.51, 56.24. EI-MS *m/z* 234 (M^+).

2-methoxy-5-phenylpyridine (**32xa**)[39] [CAS: 53698-47-8]

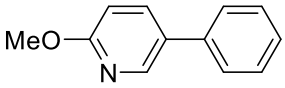

Colorless oil. ^{1}H NMR (396 MHz, $CDCl_3$) δ 7.39 (d, *J* = 4.0 Hz, 1H), 7.79 (dd, *J* = 8.4, 2.4 Hz, 1H), 7.54-7.51 (m, 2H), 7.47-7.43 (m, 2H), 7.38-7.33 (m, 1H), 6.82 (dd, *J* = 8.4, 0.8 Hz, 1H), 3.99 (s, 3H). ^{13}C NMR (100

MHz, $CDCl_3$) δ 163.58, 144.96, 137.89, 137.45, 130.07, 128.95, 127.29, 126.66, 110.79, 53.51. EI-MS *m/z* 185 (M^+).

N,*N*-dimethyl-5-phenyl-2-pyrimidinamine (**32ya**)[40] [CAS: 85386-16-9]

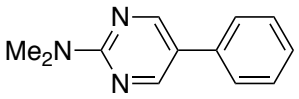

Colorless solid. ^1H NMR (396 MHz, $CDCl_3$) δ 8.57 (s, 2H), 7.50-7.42 (m, 4H), 7.35-7.31 (m, 1H), 3.24 (s, 6H). ^{13}C NMR (100 MHz, $CDCl_3$) δ 161.59, 155.83, 135.89, 129.12, 127.08, 125.78, 121.97, 37.28. EI-MS *m/z* 199 (M^+).

2-methyl-6-phenylquinoline (**32za**)[41] [CAS: 91875-31-9]

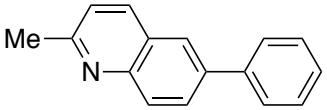

Colorless solid. ^1H NMR (396 MHz, $CDCl_3$) δ 8.10-8.07 (m, 2H), 7.97-7.94 (m, 2H), 7.72-7.70 (m, 2H), 7.49 (tt, *J* = 8.0, 1.6 Hz, 2H), 7.39 (tt, *J* = 7.2, 1.6 Hz, 1H), 7.31 (d, *J* = 8.4 Hz, 1H), 2.77 (s, 3H). ^{13}C NMR (100 MHz, $CDCl_3$) δ 159.01, 147.24, 140.44, 138.40, 136.34, 129.10, 129.03, 128.90, 127.53, 127.35, 126.62, 125.23, 122.38, 25.40. EI-MS *m/z* 219 (M^+).

2,4'-dimethylbiphenyl (**32ab**)[42] [CAS: 611-61-0]

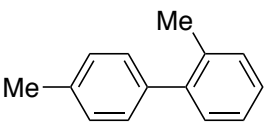

Colorless liquid. ^1H NMR (396 MHz, $CDCl_3$) δ 7.28-7.21 (m, 8H), 2.40 (s, 3H), 2.28 (s, 3H). ^{13}C NMR (100 MHz, $CDCl_3$) δ 141.83, 138.99, 136.34, 135.36, 130.25, 129.83, 129.04, 128.74, 127.04, 125.72, 21.16, 20.50. EI-MS *m/z* 182 (M^+).

4-methoxy-4’-methylbiphenyl (**32ac**)[28] [CAS: 53040-92-9]

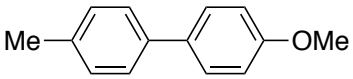

Colorless solid. ^{1}H NMR (396 MHz, $CDCl_3$) δ 7.51 (d, *J* = 8.8 Hz, 2H), 7.45 (d, *J* = 8.0 Hz, 2H), 7.22 (d, *J* = 7.6 Hz, 2H), 7.51 (d, *J* = 8.4 Hz, 2H), 3.85 (s, 3H), 2.38 (s, 3H). ^{13}C NMR (100 MHz, $CDCl_3$) δ 158.88, 137.93, 136.34, 133.72, 129.41, 127.94, 126.56, 114.12, 55.32, 21.04. EI-MS *m/z* 198 (M^+).

5-(4-methylphenyl)-1,3-benzodioxole (**32ad**)[43] [CAS: 145248-86-8]

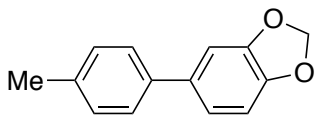

Colorless solid. ^{1}H NMR (396 MHz, $CDCl_3$) δ 7.41 (d, *J* = 8.0 Hz, 2H), 7.21 (d, *J* = 8.4 Hz, 2H), 7.06-7.03 (m, 2H), 6.86 (d, *J* = 8.0 Hz, 1H), 5.99 (s, 2H), 2.38 (s, 3H). ^{13}C NMR (100 MHz, $CDCl_3$) δ 147.99, 146.75, 137.99, 136.57, 135.48, 129.39, 126.66, 120.27, 108.45, 107.46, 101.01, 20.98. EI-MS *m/z* 212 (M^+).

4-methyl-4’-morpholinobiphenyl (**32ae**)[44] [CAS: 2166579-40-2]

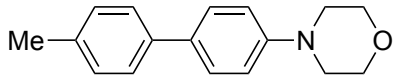

Colorless solid. ^{1}H NMR (396 MHz, $CDCl_3$) δ 7.51 (dt, *J* = 9.2, 2.4 Hz, 2H), 7.46 (dt, *J* = 8.0, 2.4 Hz, 2H), 7.22 (d, *J* = 7.6 Hz, 2H), 6.97 (dt, *J* = 8.4, 3.2 Hz, 2H), 3.88 (t, *J* = 4.4 Hz, 4H), 3.20 (t, *J* = 4.8 Hz, 4H), 2.38 (s, 3H). ^{13}C NMR (100 MHz, $CDCl_3$) δ 150.30, 137.89, 136.18, 132.67, 129.40, 127.57, 126.36, 115.76, 66.87, 49.21, 21.03. EI-MS *m/z* 253 (M^+).

2-(4-methylphenyl)naphthalene (**32af**)[45] [CAS: 59115-49-0]

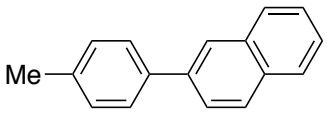

Colorless solid. ^{1}H NMR (396 MHz, $CDCl_3$) δ 8.02 (s, 1H), 7.91-7.85 (m, 3H), 7.74 (dd, *J* = 8.8, 2.0 Hz, 1H), 7.63 (d, *J* = 8.4 Hz, 2H), 7.52-7.45 (m, 2H), 7.30 (d, *J* = 8.4 Hz, 2H), 2.42 (s, 3H). ^{13}C NMR (100 MHz, $CDCl_3$) δ 138.43, 138.17, 137.13, 133.68, 132.45, 129.56, 128.31, 128.10, 127.60, 127.22, 126.20, 125.74, 125.52, 125.39, 21.11. EI-MS *m/z* 218 (M^+).

1-(4-methylphenyl)pyrene (**32ag**)[46] [CAS: 929099-46-7]

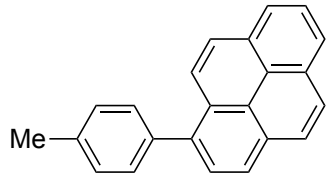

Pale yellow solid. ^{1}H NMR (396 MHz, $CDCl_3$) δ 8.19-8.10 (m, 4H), 8.04 (s, 2H), 7.98-7.93 (m, 3H), 7.51 (d, *J* = 8.0 Hz, 2H), 7.34 (d, *J* = 7.2 Hz, 2H), 2.47 (s, 3H). ^{13}C NMR (100 MHz, $CDCl_3$) δ 138.22, 137.74, 136.91, 131.46, 130.96, 130.44, 129.07, 128.49, 127.61, 127.40, 127.30, 127.27, 125.92, 125.35, 124.98, 124.70, 114.61, 21.27. EI-MS *m/z* 292 (M^+).

4-methyl-4'-fluorobiphenyl (**32ah**)[47] [CAS: 72093-43-7]

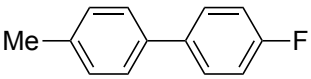

Colorless solid. ^{1}H NMR (396 MHz, $CDCl_3$) δ 7.54-7.50 (m, 2H), 7.44 (d, *J* = 7.6 Hz, 2H), 7.24 (d, *J* = 7.6 Hz, 1H), 7.11 (td, *J* = 8.4, 1.6 Hz, 2H), 2.39 (s, 3H). ^{13}C NMR (100 MHz, $CDCl_3$) δ 162.27 (d, *J* = 245.8 Hz), 137.36, 137.26, 137.03, 129.51, 128.44 (d, *J* = 7.6 Hz), 126.83, 115.52 (d, *J* = 21.1 Hz), 21.06. EI-MS *m/z* 186 (M^+).

4-methyl-4’-trifluoromethoxybiphenyl (**32ai**)[48] [CAS: 1546954-83-9]

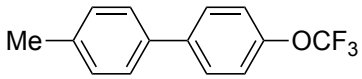

Colorless solid. ^{1}H NMR (396 MHz, $CDCl_3$) δ 7.58 (d, *J* = 8.4 Hz, 2H), 7.45 (d, *J* = 8.0 Hz, 2H), 7.28-7.26 (m, 4H), 2.40 (s, 3H). ^{13}C NMR (100 MHz, $CDCl_3$) δ 148.41, 139.91, 137.51, 136.95, 129.60, 128.21, 126.93, 121.20, 21.09. EI-MS *m/z* 252 (M^+).

4-methyl-4’-trifluoromethylbiphenyl (**32aj**)[48] [CAS: 97067-18-0]

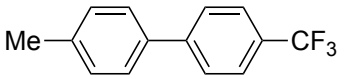

Colorless solid. ^{1}H NMR (396 MHz, $CDCl_3$) δ 7.67 (s, 4H), 7.50 (d, *J* = 8.4 Hz, 2H), 7.28 (d, *J* = 7.6 Hz, 2H), 2.41 (s, 3H). ^{13}C NMR (100 MHz, $CDCl_3$) δ 144.62, 138.14, 136.84, 129.69, 128.99 (q, *J* = 31.1 Hz), 127.15, 127.09, 125.64 (d, *J* = 3.8 Hz), 122.98, 21.13. EI-MS *m/z* 236 (M^+).

4-methyl-4’-formylbiphenyl (**32ak**)[48] [CAS:36393-42-7]

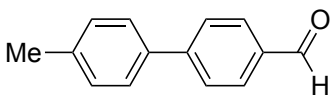

Colorless solid. ^{1}H NMR (396 MHz, $CDCl_3$) δ 10.04 (s, 1H), 7.93 (d, *J* = 8.0 Hz, 2H), 7.73 (d, *J* = 8.4 Hz, 2H), 7.53 (d, *J* = 8.0 Hz, 2H), 7.28 (d, *J* = 8.0 Hz, 2H), 2.41 (s, 3H). ^{13}C NMR (100 MHz, $CDCl_3$) δ 192.02, 147.22, 138.63, 136.87, 135.05, 130.37, 129.85, 127.49, 127.29, 21.29. EI-MS *m/z* 196 (M^+).

1-methyl-5-(4-methylphenyl)indole (**32al**)[49] [CAS: 1607841-66-6]

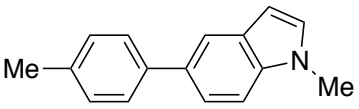

Colorless solid. ^{1}H NMR (396 MHz, $CDCl_3$) δ 7.83 (d, J = 1.2 Hz, 1H), 7.57 (dt, J = 8.0, 1.6 Hz, 2H), 7.49-7.46 (m, 1H), 7.37 (d, J = 8.8 Hz, 1H), 7.26 (d, J = 8.0 Hz, 2H), 7.07 (d, J = 3.2 Hz, 1H), 6,53 (dd, J = 3.2, 1.2 Hz, 1H), 3.62 (s, 3H), 2.41 (s, 3H). ^{13}C NMR (100 MHz, $CDCl_3$) δ 139.72, 136.10, 135.82, 132.76, 129.37, 129.33, 128.92, 127.19, 121.28, 119.13, 109.33, 101.23, 32.87, 21.03. EI-MS *m/z* 221 (M^+).

1-vinylnaphthalene (**32qm**)[50] [CAS: 826-74-4]

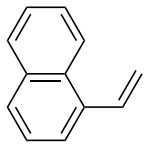

Colorless solid. ^{1}H NMR (396 MHz, $CDCl_3$) δ 8.12 (d, J = 7.6 Hz, 1H), 7.86-7.84 (m, 1H), 7.62 (d, J = 8.4 Hz, 1H), 7.62 (d, J = 7.6 Hz, 1H), 7.54-7.43 (m, 4H), 5.79 (dd, J = 13.2, 1.6 Hz, 1H), 5.47 (dd, J = 11.6, 1.6 Hz, 1H). ^{13}C NMR (100 MHz, $CDCl_3$) δ 135.57, 134.35, 133.54, 131.06, 128.49, 128.07, 126.03, 125.74, 125.61, 123.73, 123.60, 117.10. EI-MS *m/z* 154 (M^+).

1-methyl-4-[(1*E*)-1-propyl-1-penten-1-yl]benzene (**32al**)[51] [CAS: 42353-96-8]

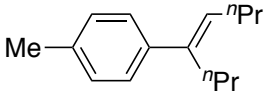

Colorless solid. ^{1}H NMR (396 MHz, $CDCl_3$) δ 7.25 (d, J = 6.0 Hz, 2H), 7.11 (d, J = 7.6 Hz, 2H), 5.64 (t, J = 7.2 Hz, 1H), 7.37 (d, J = 8.8 Hz, 1H), 7.26 (d, J = 8.0 Hz, 2H), 7.07 (d, J = 3.2 Hz, 1H), 2.46 (t, J = 7.6 Hz, 2H), 2.34 (s, 3H), 2.17 (q, J = 7.6 Hz, 2H), 1.51-1.42 (m, 2H), 1.41-1.30 (m, 2H), 0.96 (t, J = 8.0 Hz, 3H), 0.88 (t, J = 7.2 Hz, 3H). ^{13}C NMR (100

MHz, $CDCl_3$) δ140.57, 139.75, 135.94, 128.79, 128.46, 126.19, 31.65, 30.62, 23.10, 21.81, 21.01, 13.96. EI-MS *m/z* 202 (M^+).

Preparation of Substrates

Aryltriethoxysilanes were prepared by following the procedure unless otherwise noted.

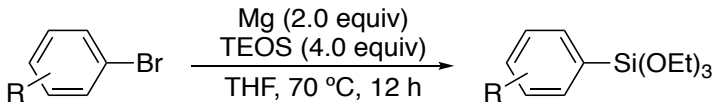

Magnesium turnings (243 mg, 10 mmol) and a solution of tetraethylorthosilicate (TEOS, 4.4 mL, 20 mmol) in dry THF (5 mL) were charged in a Schlenk tube under N_2. To the mixture, a solution of the aryl bromide (5.0 mmol) in dry THF (5 mL) was added dropwise with gentle heating. The resulting solution was stirred at 70 ºC for 12 h. The mixture was then poured into an ice-cold sat. $NH_4Cl_{aq.}$ (10 mL) in a separatory funnel. The aqueous layer was extracted with *t*-BuOMe (2 × 10 mL), and the extracts were combined, washed with brine (20 mL), dried over Na_2SO_4, and concentrated under reduced pressure. The resulting residue was purified by bulb-to-bulb vacuum distillation (4.5 mmHg) or chromatography [silica gel, hexane/EtOAc = 9/1] to give the corresponding aryltriethoxysilane.

2-methylphenyltriethoxysilane[52] [CAS: 18412-55-0]

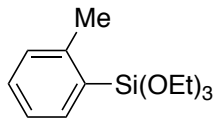

This compound was isolated by bulb-to-bulb vacuum distillation at 170 ºC in 59% yield as a colorless liquid. ^{1}H NMR (396 MHz, $CDCl_3$) δ 7.72 (dd, *J* = 7.6, 1.6 Hz, 1H), 7.32 (td, *J* = 8.4, 1.6 Hz, 1H), 7.19-7.15 (m, 2H), 3.86 (q, *J* = 7.6 Hz, 6H), 2.51 (s, 3H), 1.25 (t, *J* = 7.6 Hz, 9H). ^{13}C NMR (100 MHz, $CDCl_3$) δ 144.50, 136.45, 130.45, 129.80, 129.69, 124.64, 58.48, 22.39, 18.16. EI-MS *m/z* 254 (M^+).

5-(triethoxysilyl)-1,3-benzodioxole[52] [CAS: 376353-50-3]

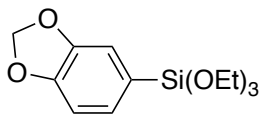

This compound was isolated by bulb-to-bulb vacuum distillation at 200 ºC in 70% yield as a colorless liquid. ^{1}H NMR (396 MHz, $CDCl_3$) δ 7.19 (dd, *J* = 8.0, 0.8 Hz, 1H), 7.11 (s, 1H), 6.86 (d, *J* = 7.6 Hz, 1H), 5.95 (s, 2H), 3.85 (q, *J* = 7.6 Hz, 6H), 1.24 (t, *J* = 7.6 Hz, 9H). ^{13}C NMR (100 MHz, $CDCl_3$) δ 149.44, 147.33, 129.37, 123.75, 114.00, 108.64, 100.61, 58.70, 18.20. EI-MS *m/z* 284 (M^+).

4-morphorinophenyltriethoxysilane [CAS: none]

This compound was isolated by silica gel chromatography [hexane/EtOAc = 4/1] in 48% yield as a colorless liquid. ^{1}H NMR (396 MHz, $CDCl_3$) δ 7.58 (dt, *J* = 8.8, 2.4 Hz, 2H), 6.91 (d, *J* = 8.0 Hz, 2H), 3.88-3.82 (m, 10H), 3.21 (t, *J* = 4.4 Hz, 4H), 1.24 (t, *J* = 7.6 Hz, 9H). EI-MS *m/z*

325 (M^+). IR (ATR): 2971, 2884, 1597, 1509, 1383, 1237, 1164, 1068, 926, 766 cm^{-1}. HRMS (ESI, *m/z*, M^+) calcd for $C_{16}H_{27}NO_4Si$ 325.1709, found 325.1718.

2-(triethoxysilyl)naphthalene [CAS: 17995-18-5]

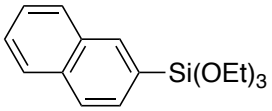

This compound was isolated by bulb-to-bulb vacuum distillation at 210 ºC in 63% yield as a colorless liquid. ^1H NMR (396 MHz, $CDCl_3$) δ 8.22 (s, 1H), 7.89-7.82 (m, 3H), 7.72 (dd, *J* = 8.0, 1.2 Hz, 1H), 7.54- 7.47 (m, 2H), 3.92 (q, *J* = 7.6 Hz, 6H), 1.27 (t, *J* = 7.6 Hz, 9H). ^{13}C NMR (100 MHz, $CDCl_3$) δ 136.28, 134.37, 132.78, 130.34, 128.40, 128.30, 127.71, 127.15, 126.81, 125.90, 58.80, 18.26. EI-MS *m/z* 290 (M^+).

1-(triethoxysilyl)pyrene[53] [CAS: 212609-47-7]

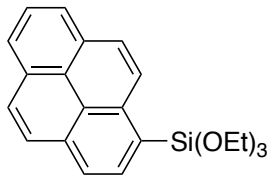

This compound was isolated by silica gel chromatography in 45% yield as a pale yellow liquid. ^1H NMR (396 MHz, $CDCl_3$) δ 8.65 (d, *J* = 9.2 Hz, 1H), 8.49 (d, *J* = 7.6 Hz, 1H), 8.23-8.06 (m, 6H), 8.02 (t, *J* = 7.6 Hz, 1H), 3.95 (q, *J* = 7.6 Hz, 6H), 1.28 (t, *J* = 7.6 Hz, 9H). ^{13}C NMR (100 MHz, $CDCl_3$) δ 136.41, 134.29, 133.05, 131.11, 130.70, 128.43, 128.04, 127.72, 127.42, 126.08, 125.81, 125.35, 125.23, 125.60, 124.44, 124.05, 58.80, 18.25. EI-MS *m/z* 364 (M^+).

4-fluorophenyltriethoxysilane[54] [CAS:3 3715-53-6]

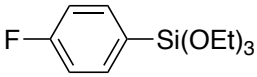

This compound was isolated by bulb-to-bulb distillation at 130 ºC in 55% yield as a colorless liquid. ^{1}H NMR (396 MHz, $CDCl_3$) δ 7.68-7.65 (m, 2H), 7.08 (t, *J* = 9.2 Hz, 2H), 3.86 (q, *J* = 7.6 Hz, 6H), 1.24 (t, *J* = 7.6 Hz, 9H). ^{13}C NMR (100 MHz, $CDCl_3$) δ 164.49 (d, *J* = 248.2 Hz), 136.94 (d, *J* = 7.6 Hz), 126.64, 115.07 (d, *J* = 20.1 Hz), 58.75, 18.19. EI-MS *m/z* 258 (M^+).

4-trifluoromethoxyphenyltriethoxysilane [CAS: none]

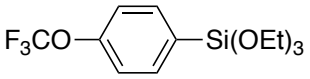

This compound was isolated by bulb-to-bulb distillation at 160 ºC in 51% yield as a colorless liquid. ^{1}H NMR (396 MHz, $CDCl_3$) δ 7.71 (tt, *J* = 8.8, 2.4 Hz, 2H), 7.23-7.21 (m, 2H), 3.87 (q, *J* = 7.6 Hz, 6H), 1.25 (t, *J* = 7.6 Hz, 9H). ^{13}C NMR (100 MHz, $CDCl_3$) δ 151.02, 136.53, 129.87, 120.42 (q, *J* = 256.8 Hz), 120.07, 58.83, 18.17. EI-MS *m/z* 324 (M^+). IR (ATR): 2976, 2888, 1595, 1500, 1390, 1254, 1161, 1072, 958, 780 cm^{-1}. HRMS (ESI, *m/z*, M^+) calcd for $C_{13}H_{19}F_3O_4Si$ 324.1005, found 324.1024.

1-methyl-5-triethoxysilylindole[52] [CAS: 808770-01-6]

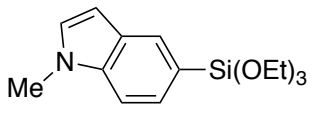

This compound was isolated by bulb-to-bulb distillation at 220 ºC in 63% yield as a colorless liquid. ^{1}H NMR (396 MHz, $CDCl_3$) δ 8.00 (s, 1H), 7.52 (d, *J* = 8.0 Hz, 1H), 7.36 (d, *J* = 8.4 Hz, 2H), 7.04 (d, *J* = 3.2 Hz, 1H), 6.51 (d, *J* = 2.4 Hz, 1H), 3.95 (q, *J* = 7.6 Hz, 6H), 3.79 (s, 3H), 1.25 (t, *J* = 7.6 Hz, 9H). ^{13}C NMR (100 MHz, $CDCl_3$) δ 137.94, 128.82,

128.69, 128.25, 127.34, 119.42, 108.92, 101.34, 58.58, 32.73, 18.25. EI-MS *m/z* 293 (M^+).

4-(*trans*-4-propylcyclohexyl)phenyltriethoxysilane [CAS: none]

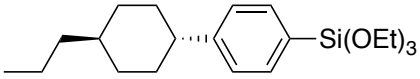

This compound was isolated by bulb-to-bulb distillation at 230 ºC in 48% yield as a colorless liquid. ^{1}H NMR (396 MHz, $CDCl_3$) δ 7.58 (d, *J* = 7.6 Hz, 2H), 7.22 (d, *J* = 8.0 Hz, 2H), 3.86 (q, *J* = 7.6 Hz, 6H), 2.46 (tt, *J* = 12.4, 3.2 Hz, 1H), 1.90-1.84 (m, 4H), 1.49-1.18 (m, 16H), 1.09-0.99 (m, 2H), 0.90 (t, *J* = 7.6 Hz, 3H). ^{13}C NMR (100 MHz, $CDCl_3$) δ 150.14, 134.83, 127.66, 126.47, 58.65, 44.72, 39.70, 36.99, 34.10, 33.52, 20.01, 18.23, 14.41. EI-MS *m/z* 293 (M^+). IR (ATR): 2971, 2920, 1602, 1445, 1389, 1165, 1073, 956, 788, 727 cm^{-1}. HRMS (ESI, *m/z*, M^+) calcd for $C_{21}H_{36}O_3Si$ 364.2434, found 364.2429.

Synthesis of 3-adamantyl-4-methoxyphenyltriethoxysilane

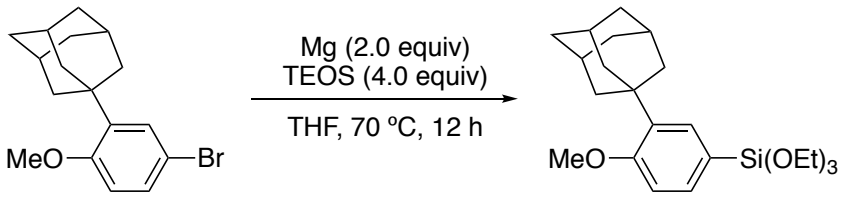

Magnesium turnings (1514 mg, 62.3 mmol) and a solution of tetraethylorthosilicate (TEOS, 27.5 mL, 124.6 mmol) in dry THF (30 mL) were charged in a Schlenk tube under N_2. To the mixture, a solution of 1-bromo-3-

adamantyl-4-methoxybenzene (10 g, 31.2 mmol) in dry THF (40 mL) was added dropwise with gentle heating. The resulting solution was stirred at 70 ºC for 12 h. The mixture was then poured into an ice-cold sat. $NH_4Cl_{aq.}$ (60 mL) in a separatory funnel. The aqueous layer was extracted with *t*-BuOMe (2 × 50 mL), and the extracts were combined, washed with brine (100 mL), dried over Na_2SO_4, and concentrated under reduced pressure. The resulting residue was purified by chromatography [silica gel, hexane/EtOAc = 9/1] to give the titled product (9319 mg, 23.4 mmol) in 75% yield

[CAS: none] Colorless viscous liquid. ^{1}H NMR (396 MHz, $CDCl_3$) δ 7.50-7.48 (m, 2H), 6.88 (d, *J* = 8.8 Hz, 2H), 3.86 (q, *J* = 7.6 Hz, 6H), 3.84 (s, 3H), 2.10-2.06 (m, 9H), 1.77 (s, 6H), 1.25 (t, *J* = 7.6 Hz, 3H). ^{13}C NMR (100 MHz, $CDCl_3$) δ 160.68, 127.68, 134.10, 132.87, 121.13, 111.05, 58.61, 54.69, 40.48, 37.12, 36.99, 29.09, 18.27. IR (ATR): 2971, 2902, 2849, 1589, 1453, 1234, 1072, 954, 778, 718 cm^{-1}. HRMS (ESI, *m/z*, M^+) calcd for $C_{23}H_{36}O_4Si$ 404.2383, found 404.2390.

Synthesis of triethoxysilyldextromethorphan

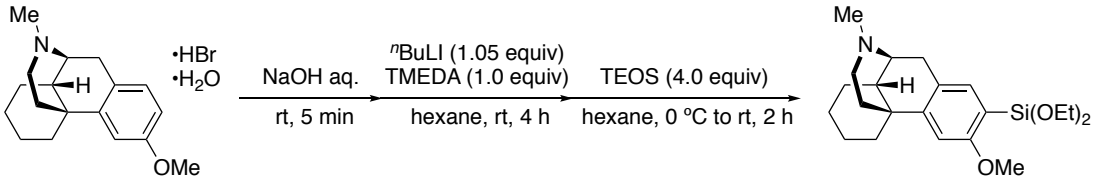

Dextromethorphan hydrobromide (2590 mg, 7.0 mmol) was treated with 1.0 M aqueous solution of NaOH (10 mL) at room temperature for 5 min. The aqueous layer was extracted with CH_2Cl_2 (3 × 5 mL) and the extracts were combined,

washed with brine (20 mL), dried over Na_2SO_4, and concentrated under reduced pressure. The residue (1897 mg, 7.0 mmol) was dissolved in dry hexane (14 mL) under N_2, and *N,N,N',N'*-tetramethylethylenediamine (TMEDA) (812 mg, 7.0 mmol) was added to that solution. To the mixture, ^{n}BuLi in hexane (1.56 M, 7.35 mmol, 4.7 mL) was added dropwise. The resulting solution was stirred at rt for 4 h and then cooled to 0 ºC with an ice bath, followed by adding tetraethylorthosilicate (6.2 mL, 28 mmol). The mixture was warmed to rt and stirred for 2 h. The mixture was then poured into an ice-cold sat. $NH_4Cl_{aq.}$ (20 mL) in a separatory funnel. The aqueous layer was extracted with *t*-BuOMe (2 × 10 mL), and the extracts were combined, washed with brine (40 mL), dried over Na_2SO_4, and concentrated under reduced pressure. The resulting residue was purified by chromatography [silica gel, CH_2Cl_2/EtOH = 3/1] to give the corresponding product (1970 mg, 4.6 mmol) in 65% yield.

[CAS: none] Colorless solid. Mp. 73 ºC. ^{1}H NMR (396 MHz, $CDCl_3$) δ 7.33 (s, 1H), 6.70 (s, 1H), 3.81 (q, *J* = 7.6 Hz, 2H), 3.79 (s, 3H), 2.98 (d, *J* = 18.4 Hz, 1H), 2.80 (bs, 1H), 2.56 (dd, *J* = 18.0, 7.6 Hz, 1H), 2.42-2.34 (m, 5H), 2.06, (tt, *J* = 12.0, 2.8 Hz, 1H), 1.81 (bd, *J* = 12.4 Hz, 1H), 1.73 (tt, *J* = 12.8, 4.8 Hz, 1H), 1.64 (bd, *J* = 11.6 Hz, 1H), 1.52 (bd, *J* = 11.6 Hz, 1H), 11.41-1.24 (m, 14H), 1.14-1.09 (m, 1H). ^{13}C NMR (100 MHz, $CDCl_3$) δ 163.12, 144.46, 136.68, 129.39, 116.30, 106.22, 58.67, 57.98, 55.21, 47.19, 45.48, 42.76, 41.88, 37.55, 36.71, 26.69, 26.53, 23.30, 22.25, 18.22. IR (ATR): 2970, 2923, 1740, 1597, 1382, 1229, 1074, 953,

883, 779 cm^{-1}. HRMS (FAB, *m/z*, MH^+) calcd for $C_{24}H_{40}NO_4Si$ 434.2727, found 434.2722.

Synthesis of [(1*E*)-1-propyl-1-penten-1-yl]triethoxysilane[55]

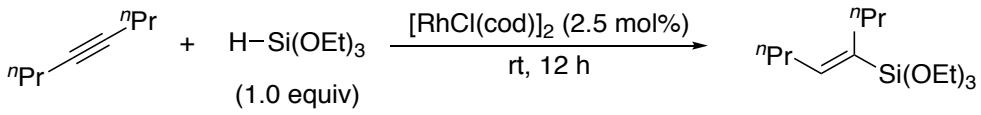

$[RhCl(cod)]_2$ (123 mg, 0.25 mmol), 4-octyne (1102 mg, 10.0 mnol), and triethoxysilane (1642 mg, 10.0 mmol) were charged in a round-bottom flask (30 mL) under N_2. The mixture was stirred at rt for 12 h. Then, the resulting mixture was purified by bulb-to-bulb vacuum distillation (150 ºC) to give [(1*E*)-1-propyl-1-penten-1-yl]triethoxysilane (1318 mg, 4.8 mmol) in 48% yield.

[CAS: 2059119-15-0] Colorless liquid. ^1H NMR (396 MHz, $CDCl_3$) δ 6.09 (t, *J* = 7.6 Hz, 1H), 3.80 (q, *J* = 7.6 Hz, 6H), 2.14-2.08 (m, 4H), 1.46-1.35 (m, 4H), 1.22 (t, *J* = 7.6 Hz, 9H), 0.93-0.89 (m, 6H). ^{13}C NMR (100 MHz, $CDCl_3$) δ 145.92, 132.74, 58.30, 31.39, 30.43, 22.97, 22.47, 18.20, 14.39, 13.92.

Synthesis of an aryl bromide-tethered Norfloxacin

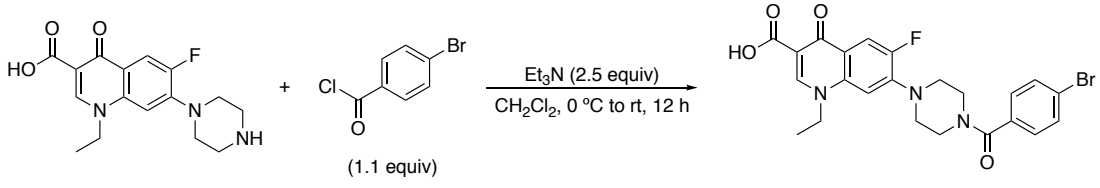

Norfloxacin (1595 mg, 5.0 mmol) was suspended in dry DCM (20 mL) under N_2. To the suspension, triethylamine (1.75 mL, 12.5 mmol) was added, and then the mixture was cooled to 0 ºC. 4-Bromobenzoyl chloride (1207 mg, 5.5 mmol) in dry DCM (10 mL) was added dropwise to that reaction mixture. After the addition, the mixture was warmed to rt and stirred for 12 h. The resulting mixture was then poured into aqueous solution of HCl (2M, 10 mL) in a separatory funnel. The aqueous layer was extracted with DCM (2 × 10 mL), and the extracts were combined, washed with brine (30 mL), dried over Na_2SO_4, and concentrated under reduced pressure. The resulting residue was stirred in EtOH (5 mL) with refluxing for 5 min, then the residue was filtered off, rinsed with cold EtOH (2 × 2 mL), followed by dried under reduced pressure to give the titled product (1561 mg, 3.1 mmol) in 62% yield.

Colorless solid. Mp. 251 ºC. ^{1}H NMR (396 MHz, $CDCl_3$) δ 8.67 (s, 1H), 8.07 (d, J = 12.8 Hz, 1H), 7.61-7.58 (m, 2H), 7.36-7.33 (m, 2H), 6.85 (d, J = 6.8 Hz, 1H), 4.33 (q, J = 7.6 Hz, 2H), 4.00-3.71 (br, 4H), 3.33 (br, 4H), 1.59 (t, J = 7.6 Hz, 3H). ^{13}C NMR (100 MHz, $CDCl_3$) δ 176.93, 169.51, 166.94, 147.25, 145.53 (d, J = 9.9 Hz), 136.98, 133.81, 131.92, 128.91, 124.59, 121.22, 113.17, 112.94, 108.53, 104.25, 49.75, 14.48. IR (ATR): 3050, 2969, 1719, 1624, 1432, 1366, 1230, 1204, 1003, 747 cm^{-1}. HRMS (FAB, *m/z*, MH^+) calcd for $C_{23}H_{22}BrFN_3O_4$ 502.0778, found 502.0761.

References

(1) (a) C. Torborg, M. Belle *Adv. Synth. Catal.* **2009**, *351*, 3027–3043. (b) J. Magano, J. R. Dunetz *Chem. Rev.* **2011**, *111*, 2177–2250. (c) A. F. P. Biajoli, C. S. Schwalm, J. Limberger, T. S. Claudino, A. L. Monteiro *J. Braz. Chem. Soc.* **2014**, *25*, 2186–2214. (d) S. Xu, E. H. Kim, A. Wei, E.-i. Negishi *Sci. Technol. Adv. Mater.* **2014**, *15*, 044201 (23 pp).

(2) (a) K. Tamao, K. Sumitani, M. Kumada *J. Am. Chem. Soc.***1972**, *94*, 4374–4376. (b) R. J. P. Corriu, J. P. Masse *J. Chem. Soc., Chem. Commun*. **1972**, 144a.

(3) (a) E. Negishi, A. O. King, N. Okukado *J. Org. Chem.* **1977**, *42*, 1821–1823. (b) E. Negishi *Acc. Chem. Res.* **1982**, *15*, 340–348. (c) P. Knochel, R. D. Singer *Chem. Rev.* **1993**, *93*, 2117–2188.

(4) (a) M. Kosugi, K. Sasazawa, Y. Shimizu, T. Migita *Chem. Lett.* **1977**, *6*, 301–302. (b) D. Milstein, J. K. Stille *J. Am. Chem. Soc.* **1978**, *100*, 3636–3638. (c) J. K. Stille *Angew. Chem. Int. Ed. Engl.* **1986**, *25*, 508–524.

(5) (a) N. Miyaura. K. Yamada, A. Suzuki *Tetrahedron Lett.* **1979**, *20*, 3437–3440. (b) N. Miyaura, T. Yanagi, A. Suzuki *Synth. Commun.* **1981**, *11*, 513–519. (c) N. Miyaura, A. Suzuki *Chem. Rev.* **1995**, *95*, 2457–2483.

(6) (a) Y. Hatanaka, T. Hiyama *J. Org. Chem.* **1988**, *53*, 918–920. (b) S. E. Denmark, J. H.-C. Liu *Angew. Chem. Int. Ed.* **2010**, *49*, 2978–2986. (c) Y. Nakao, T. Hiyama *Chem. Soc. Rev.* **2011**, *40*, 4893–4901. (d) T. Komiyama, Y. Minami, T. Hiyama *ACS Catal.* **2017**, *7*, 631–651.

(7) (a) D. G. Brown, J. Boström *J. Med. Chem.* **2016**, *59*, 4443–4458. (b) I. Maluenda, O. Navarro *Molecules* **2015**, *20*, 7528–7557.

(8) In the preparation of pharmaceuticals, contamination of the resulting products by palladium metal must be less than 10 ppm. The ICH Q3D guideline can be viewed here: http://www.ich.org/products/guidelines/quality/article/qualityguidelines.html (accessed May 20, 2019).

(9) For representative examples see; (a) A. Hosomi, S. Kohra, Y. Tominaga *Chem. Pharm. Bull.* **1988**, *36*, 4622–4625. (b) S. E. Denmark, J. Y. Choi *J. Am. Chem. Soc.* **1999**, *121*, 5821–5822. (c) S. Riggleman, P. DeShong *J. Org. Chem.* **2003**, *68*, 8106–8109. (d) Y. Nakao, H. Imanaka, A. K. Sahoo, A. Yada, T. Hiyama *J. Am. Chem. Soc.* **2005**, *127*, 6952–6953. (e) S. E. Denmark, R. C. Smith, W.-T. Chang, J. M. Muhuhi *J. Am. Chem. Soc.* **2009**, *131*, 3104–3118. (f) D. Martinez-Solorio Melillo, L. Sanchez, Y. Liang, E. Lam, K. N. Houk, A. B. Smith III *J. Am. Chem. Soc.* **2016**, *138*, 1836–1839.

(10) A successful Hiyama coupling reaction using a 10 ppm loading of a palladium catalyst has been reported, but was limited to only one substrate; see: E. Alacid, C. Nájera, *Adv. Synth. Catal.* **2006**, *348*, 945–952.

(11) M. E. Mowery, P. DeShong *Org. Lett.* **1999**, *1*, 2137–2140.

(12) (a) I. Blaszczyk, M. A. Trzeciak *Tetrahedron* **2010**, *66*, 9502–9507. (b) M. Osińska, A. Gniewek, M. A. Trzeciak *J. Mol. Catal. A: Chem.* **2016**, *418–419*, 9–18.

(13) D. A. Alonso, C. Nájera, C. Pacheco *Adv. Synth. Catal.* **2002**, *344*, 172–183.

(14) M. G. Organ, S. Avola, I. Dubovyk, N. Hadei, E. A. B. Kantchev, C. J. O'Brien, C. Valente *Chem. Eur. J.* **2006**, *12*, 4749–4755.

(15) T. E. Barder, S. D. Walker, J. R. Martinelli, S. L. Buchwald *J. Am. Chem. Soc.* **2005**, *127*, 4685–4696.

(16) For information on adapalene, see: https://www.accessdata.fda.gov/drugsatfda_docs/nda/2016/020380s10_toc.cfm (accessed May 20, 2019).

(17) For information on norfloxacin, see: https://www.accessdata.fda.gov/drugsatfda_docs/label/2016/019384s067lbl.pdf (accessed May 20, 2019)

(18) For information on dextromethorphan, see; https://www.accessdata.fda.gov/drugsatfda_docs/nda/2004/021620s000_MucinexTOC.cfm (accessed May 20, 2019)

(19) Y. Goto, T. Ogawa, S. Sawada, S. Sugimori *Mol. Cryst. Liq. Cryst.* **1991**, *209*, 1–7.

(20) G. Hamasaka, F. Sakurai, Y. Uozumi *Chem. Commun.* **2015**, *51*, 3886–3888.

(21) O. Weber, V. Voehringer, H.-G. Lerchen, F.-T. Hafner, J. Keldenich, K.-H. Schlemmer, U. Krenz, B. Riedl, WO 2008025509, May 6, 2008.

(22) J. Zanon, A. Klapars, S. L. Buchwald *J. Am. Chem. Soc.* **2003**, *125*, 2890–2891.

(23) S. Hibi, K. Ueno, S. Nagato, K. Kawano, K. Ito, Y. Norimine, O. Takenaka,

T. Handa, M. Yonaga *J. Med. Chem*. **2012**, *55*, 10584–10600.

(24) S. Ishida, M. Ito, H. Horiuchi, H. Hiratsuka, S. Shiraishi, S. Kyushin *Dalton Trans.* **2010**, *39*, 9421–9426.

(25) A. Nagaki, K. Hirose, Y. Moriwaki, K. Mitamura, K. Matsukawa, N. Ishizuka, J. Yoshida *Catal. Sci. Technol.* **2016**, *6*, 4690–4694.

(26) C. Liu, X. Rao, Y. Zhang, X. Li, J. Qiu, Z. Jin Eur. *J. Org. Chem.* **2013**, 4345.

(27) S. Shi, Y. Zhang *J. Org. Chem.* **2007**, 7*2*, 5927–5930.

(28) R. Martinez, I. M. Pastor, M. Yus *Eur. J. Org. Chem.* **2014**, 872–877.

(29) S. M. Raders, J. V. Kingston, J. G. Verkade *J. Org. Chem.* **2010**, *75*, 1744–1747.

(30) T. Yanase, Y. Monguchi, H. Sajiki *RSC Adv.* **2012**, *2*, 590–594.

(31) S. Crosignani, J. Gonzalez, D. Swinnen *Org. Lett.* **2004**, *6*, 4579–4582.

(33) B. Singh, R. Paira, G. Biswas, B. K. Shaw, S. K. Mandai *Chem. Commun.* **2018**, *54*, 13220–13223.

(33) Q. Zhou, Y.-N. Wang, Z.-Q. Guo, Z.-H. Zhu, Z.-M. Li, X.-F. Hou *Organometallics* **2015**, *34*, 1021–1028.

(34) L. Wang, Z.-X. Wang *Org. Lett.* **2007**, *9*, 4335–4338.

(35) W. Li, P. Sun *J. Org. Chem.* **2012**, *77*, 8362–8366.

(36) Q-F Xu-Xu, Q.-Q. Liu, X. Zhang, S.-L. You *Angew. Chem. Int. Ed.* **2018**, *57*, 15204–15208.

(37) S. D. Ramgren, L. Hie, Y. Ye, N. K. Garg *Org. Lett.* **2013**, *15*, 3950–3953.

(38) J. W. B. Fyfe, N. J. Fazakerley, A. J. B. Watson *Angew. Chem. Int. Ed.* **2017**,

56, 1249–1253.

(39) M. Kuriyama, S. Matsuo, M. Shinozawa, O. Onomura *Org. Lett.* **2013**, *15*, 2716–2719.

(40) H. A. M. Adnen, K. Jameleddine, B. H. Bechir *Mol. Diver.* **2008**, *12*, 61–64.

(41) Y. Qiu, Y. Liu, W. Hong, Z. Li, Z. Wang, Z. Yao, S. Jiang *Org. Lett.* **2011**, *13*, 3556–3559.

(42) W. Erb, M. Albini, J. Rouden, J. Blanchet *J. Org. Chem.* **2014**, *79*, 10568–10580.

(43) C. Savarin, L. S. Liebeskind *Org. Lett.* **2001**, *3*, 2149–2152.

(44) S. Asghar, S. B. Tailor, D. Elorriaga, R. B. Bedford *Angew. Chem. Int. Ed.* **2017**, *56*, 16367–16370.

(45) M. J. Iglesias, A. Prieto, M. C. Nicasio *Org. Lett.* **2012**, *14*, 4318–4321.

(46) A. S. K. Hashmi, C. Lothschütz, R. Döpp, M. Rudolph, T. D. Ramamurthi, F. Rominger *Angew. Chem. Int. Ed.* **2009**, *48*, 8243–8246.

(47) T. Agrawal, S. P. Cook *Org. Lett.* **2014**, *16*, 5080–5083.

(48) Y.-Z. Luan, T. Zhang, W.-W. Yao, K. Lu, L.-Y. Kong, Y.-T. Lin, M. Ye *J. Am. Chem. Soc.* **2017**, *139*, 1786–1789.

(49) T. Markovic, B. N. Rocke, D. C. Blakemore, V. Mascitti, M. C. Wills *Org. Lett.* **2017**, *19*, 6033–6035.

(50) Y. Nishida, N. Hosokawa, M. Murai, K. Takai *J. Am. Chem. Soc.* **2015**, *137*, 114–117.

(51) E. Shirakawa, T. Yamagami, T. Kimura, S. Yamaguchi, T. Hayashi *J. Am.*

Chem. Soc. **2005**, *127*, 17164–17165.

(52) A. S. Manoso, C. Ahn, A. Soheili, C. J. Handy, R. Correia, W. M. Seganish, P. DeShong *J. Org. Chem.* **2004**, *69*, 8305–8314.

(53) M. Ueda, I. Yahagi, M. Kitano, EP 861845, September 2, 1998.

(54) J. Yu, J. Liu, G. Shi, C. Shao, Y. Zhang *Angew. Chem. Int. Ed.* **2015**, *54*, 4079–4082.

(55) H. Miura, K. Endo, R. Ogawa, T. Shishido *ACS Catal*. **2017**, *7*, 1543–1553.

Chapter 3

Mechanistic Studies on the Hiyama Coupling Reaction at Perts Per Million Levels of Pd

Manuscript in preparation

Shun Ichii, Go Hamasaka and Yasuhiro Uozumi

Introduction

This author has discovered that the Hiyama coupling reaction of aryl bromides with aryltrialkoxysilanes proceeded smoothly in the presence of a 5 mol ppm loading amount of the palladium NNC-pincer complex **9** in propylene glycol to give the corresponding biaryls in excellent yields (Chapter 2). In this chapter, this author conducted some mechanistic studies on the Hiyama coupling reaction in glycol solvents to understand the reason for the high efficiency of the present method.

A catalytic cycle of the Hiyama cross-coupling reaction is shown in Scheme 1.

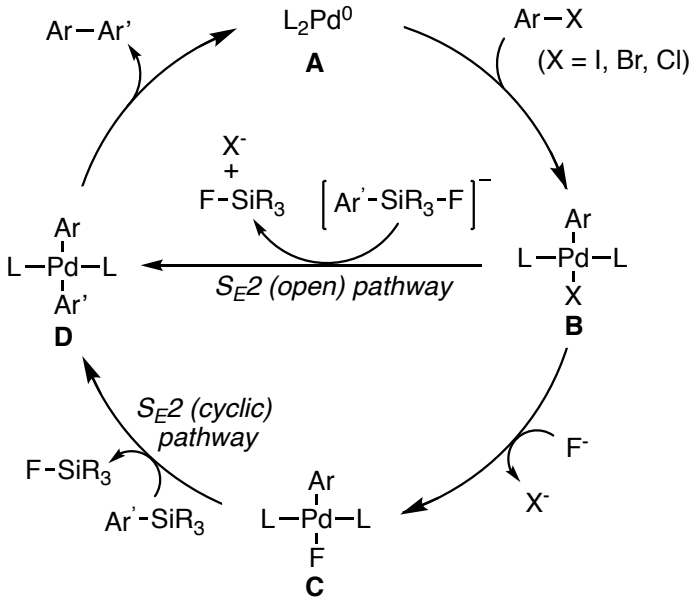

Scheme 1. Catalytic Cycle of the Hiyama Cross-Coupling Reaction

The first step is the oxidative addition of Pd(0) species **A** to the aryl halide (Ar-X) to form the Arylpalladium halide **B**. Subsequently, transmetalation occurs

through two possible reaction pathways: between **B** and the arylfluorosilicate (S_E2 (open) pathway, **B** to **D**) and between the arylpalladium fluoride **C** and the arylsilane (S_E2 (cyclic) pathway, **C** to **D**) to generate the diarylpalladium species **D**.[1] Finally, reductive elimination of **D** affords the coupling product (Ar-Ar') and regenerates palladium (0) species **A**.

As described in the Chapter 2, total reaction efficiency of the Hiyama cross-coupling was strongly affected by the solvent used, where 1,2-diols brought about a significant increase in the reaction efficiency. Taking the reactivity of a 1,2-diol with trialkoxysilane (e.g. -$Si(OMe)_3$) into account, this author hypothesized that a highly active silicon intermediate should be generated in situ with a 1,2-diol under the standard conditions shown in Chapter 2 (Table 1, entry 9), which significantly facilitates transmetalation step forming **D** from **B**.

Results and Discussion

To gain insight into the reason for the high efficiency of the present method, this author initially performed ^{29}Si NMR and ESI-MS analyses of the reaction mixture (Scheme 2). After the reaction of trimethoxy(phenyl)silane (**31a**) with potassium fluoride in ethylene glycol for two hours, the resulting mixture was analyzed by ^{29}Si NMR spectroscopy and ESI-MS. In the ^{29}Si NMR spectra, the signal of **31a** at –57.8 ppm completely disappeared, and a new signal was observed at −93.7 ppm (Scheme 2a, Figure 1a and 1b).

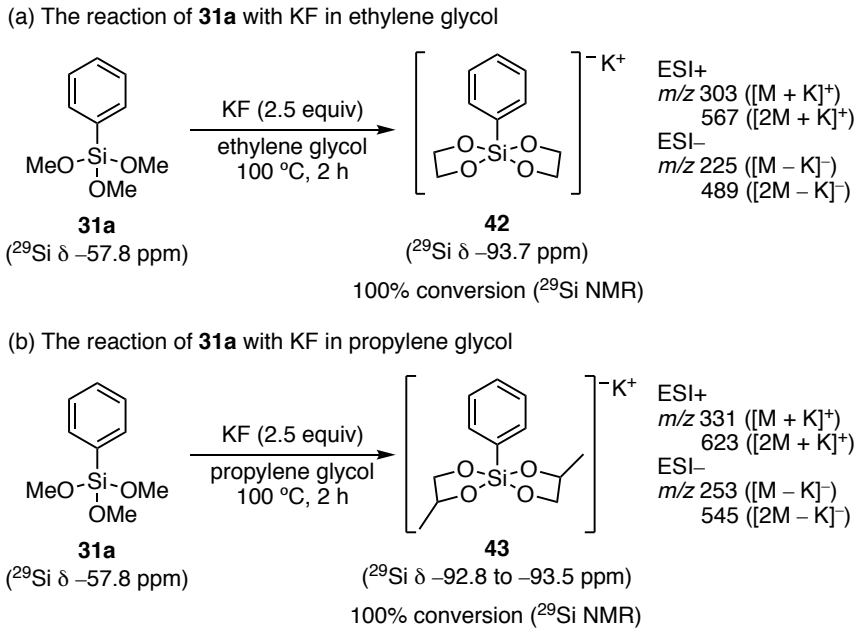

Scheme 2. ^{29}Si NMR and ESI-MS Experiments for a Mixture of Trimethoxy(phenyl)silane with KF in Glycol Solvents

ESI-MS experiments on the resulting product clearly revealed the formation of an ethylene glycol-derived pentacoordinate spirosilicate **42** (Scheme 2a). The

propylene glycol-derived pentacoordinate spirosilicate **43** also formed by performing the reaction in propylene glycol under similar reaction conditions (Scheme 2b, Figure 1c).

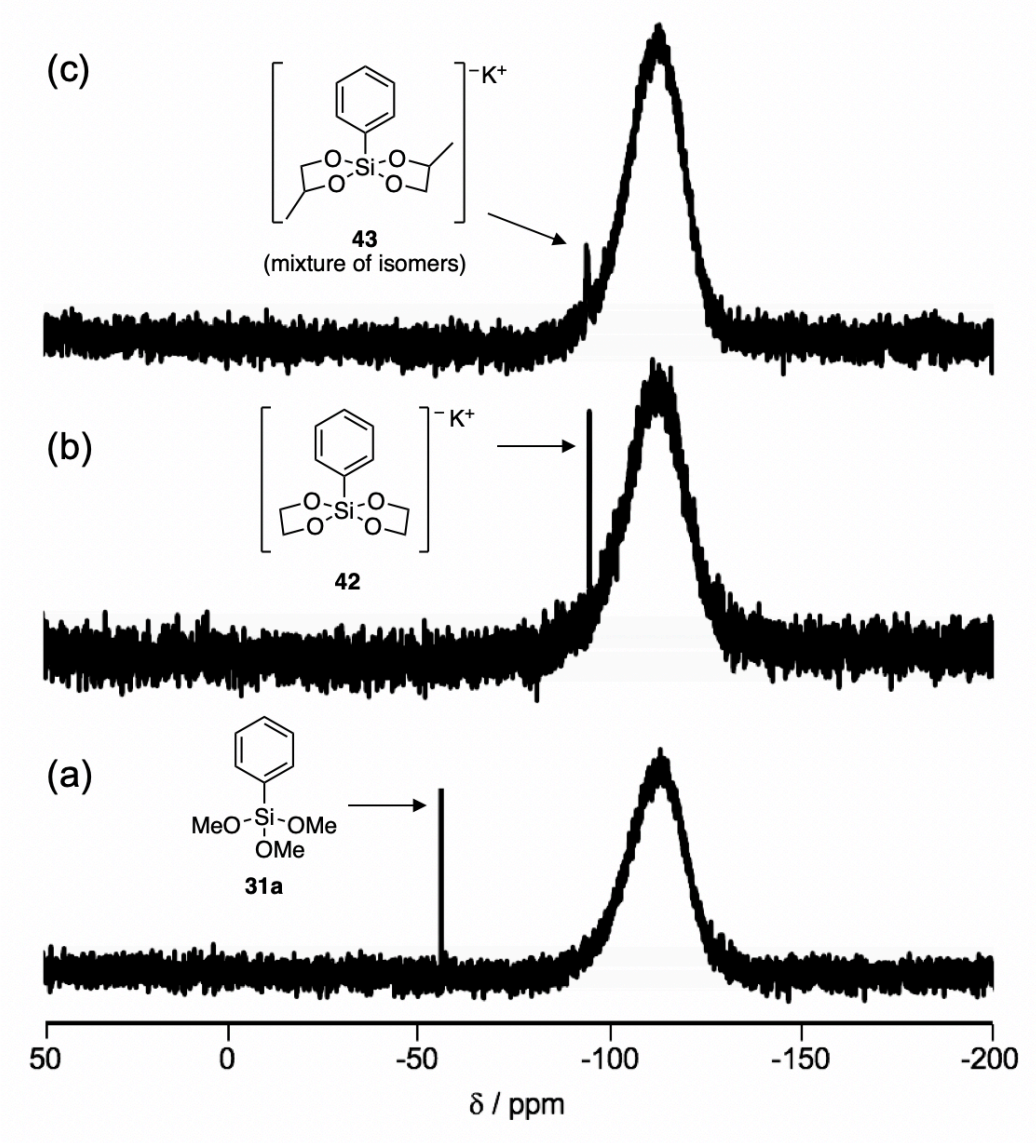

Figure 1. ^{29}Si NMR Spectra of the Reaction Mixture (a) trimethoxy(phenyl)silane (**31a**) (b) ethylene glycol-derived silicate **42** (c) propylene glycol-derived silicate **43**

The ethylene glycol-derived spirosilicate **42** was readily isolated and recrystallized from MeOH/toluene. A single-crystal X-ray diffraction analysis of silicate **42** clearly confirmed its structure (Figure 2).

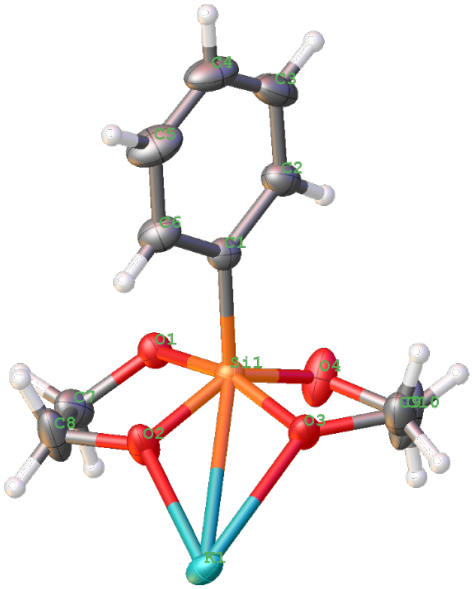

Formula	$C_{10}H_{13}O_4SiK$
Fw	264.39
crystal color, habit	colorless, plate
crystal size, mm^3	0.635 × 0.485 × 0.246
crystal system	tetragonal
space group	P-42$_1$c
***a*, Å**	12.2643(2)
***b*, Å**	12.2643(2)
***c*, Å**	16.3182(5)
α, deg	90.0
β, deg	90.0
γ, deg	90.0
***V*, Å^3**	2454.47(11)
Z	8
***F*(000)**	1104.0
***d*$_{calc}$, g/cm^3**	1.431
***μ*(MoKα), mm^{-1}**	0.526
***T*, K**	123(2)
***R*$_1$**	0.0395
w*R*$_2$	0.0895
GOF	1.054

Figure 2. An ORTEP drawing of the pentacoordinate spirosilicate (**42**) (50% probability ellipsoids). O = red, C = grey, Si = orange and K = turquoise green**.**

From these results, the spirosilicates-generated in situ appear to be key intermediates in permitting the Hiyama coupling reaction to proceed efficiently. The structures and reactivities of related catechol-derived pentacoordinate spirosilicates have been studied extensively,[2] and silicates have recently attracted attention as precursors of alkyl radical in photocatalytic reactions.[3] Hiyama coupling reactions in the presence of organobis(catecholato)silicates have also

been independently reported by the groups of Hosomi[4] and DeShong.[5] Nevertheless, the reactivity of glycol-derived pentacoordinate spirosilicates in C–C bond-forming reactions remains unexplored.

To understand the reactivity of the pentacoordinate spirosilicate intermediates formed in situ, this author conducted preliminary theoretical studies on the transmetalation step. By electrochemical methods, Jutand and co-workers elucidated the roles of fluoride ion in the Hiyama coupling reaction.[6] Fluoride ions react with [Ar–Pd–X], formed by oxidative addition of ArX to Pd(0) species, to generate [Ar–Pd–F] species. Transmetalation occurs between [Ar–Pd–F] and $PhSi(OMe)_3$ via a four-membered cyclic transition state, whereas the fluorosilicate $[PhSi(OMe)_3F]^-$ is not reactive. DFT calculations on the transmetalation of $[CH_2=CH–Pd–F]$ with $CH_2=CHSiMe_3$ have been performed by Sakaki and Hiyama and their co-workers.[7] In accord with these reports, this author set up model reactions of $[Ph–Pd–F(PPh_3)]$ (**44**) with the silicate intermediate **42** and with $PhSi(OMe)_3$ (**31a**). Geometry optimization and frequency analysis were performed by the B3LYP method[8] with the basis sets 6-31G(d,p) for C and H; 6-31+G(d,p) for O, F, Si, P, and K; and LanL2DZ for Pd, in conjunction with the Gaussian 16 program.[9] Gibbs free energies in the solution phase were calculated by single-point energy calculations at the B3YLP/6-311++G(2d,p) level for C, H, O, F, Si, P, and K and at the SDD level for Pd in the SMD solvation model (DMF) for the optimized structures.

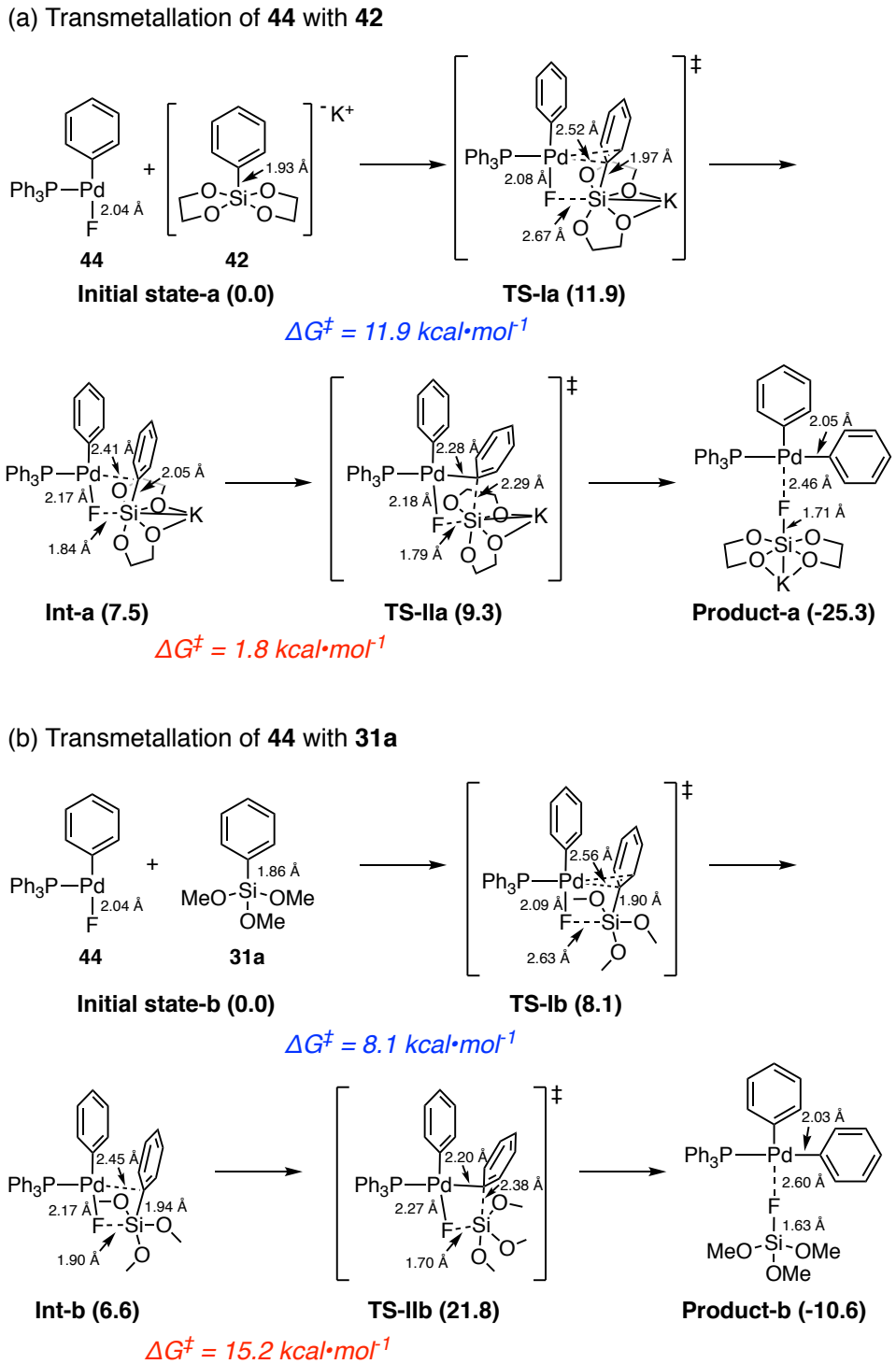

Figure 3. Results of Theoretical Studies on the Transmetalation Step. (a) transmetalation of an arylpalladium fluoride **44** with the pentacoordinate spirosilicate **42**. (b) transmetalation of an arylpalladium fluoride **44** with trimethoxy(phenyl)silane (**31a**).

First, the phenyl group of the arylsilanes **31a** and **42** coordinates to the palladium center, and the fluorine ligand of **44** begins to interact with the silyl groups to form the hexacoordinate spirosilicate **Int-a** and the pentacoordinate silicate **Int-b**, respectively. Here, a slightly higher activation barrier is required for the formation of **TS-Ia** (11.9 kcal/mol) compared with that for **TS-Ib** (8.1 kcal/mol), due to the steric effect of the larger silicate moiety of **42**. Subsequently, a palladium–carbon bond starts to form via **TS-IIa** and **TS-IIb**. The silicon center adopts a hexacoordinated octahedral structure in **TS-IIa**, whereas the geometry around the silicon center in **TS-IIb** is understood to be trigonal bipyramidal. Notably, the palladium–carbon bond formation from **Int-a** occurs with a very low activation barrier of 1.8 kcal/mol. In sharp contrast, this process with trimethoxy(phenyl)silane (**31a**) requires a significantly higher activation barrier of 15.2 kcal/mol. Consequently, these calculation results strongly support the assumption that the glycol-derived pentacoordinate spirosilicates are quite reactive in the transmetalation step.

To further evaluate the reactivity of the glycol-derived silicate intermediates, stoichiometric reactions between arylpalladium halides and various silicon reagents were demonstrated. First, the reaction of an arylpalladium fluoride complex **45** with ethylene glycol-derived spirosilicate **42**, trimethoxy(phenyl)silane (**31a**), or trimethoxy(phenyl)silane-tetrabutylammounium fluoride complex **46**, which is known as an active silicon intermediate in the traditional Hiyama cross-coupling reaction, were carried out

in DMF at 25 ºC (Figure 4). The reaction progress was monitored by ^{19}F NMR using 4-trifluoromethylbiphenyl (**32ha**) as an internal standard. The reaction of spirosilicate **42** with arylpalladium fluoride **45** completed within 9 minutes to give the coupling product **32ga** in 85% yield (Figure 4, red line).

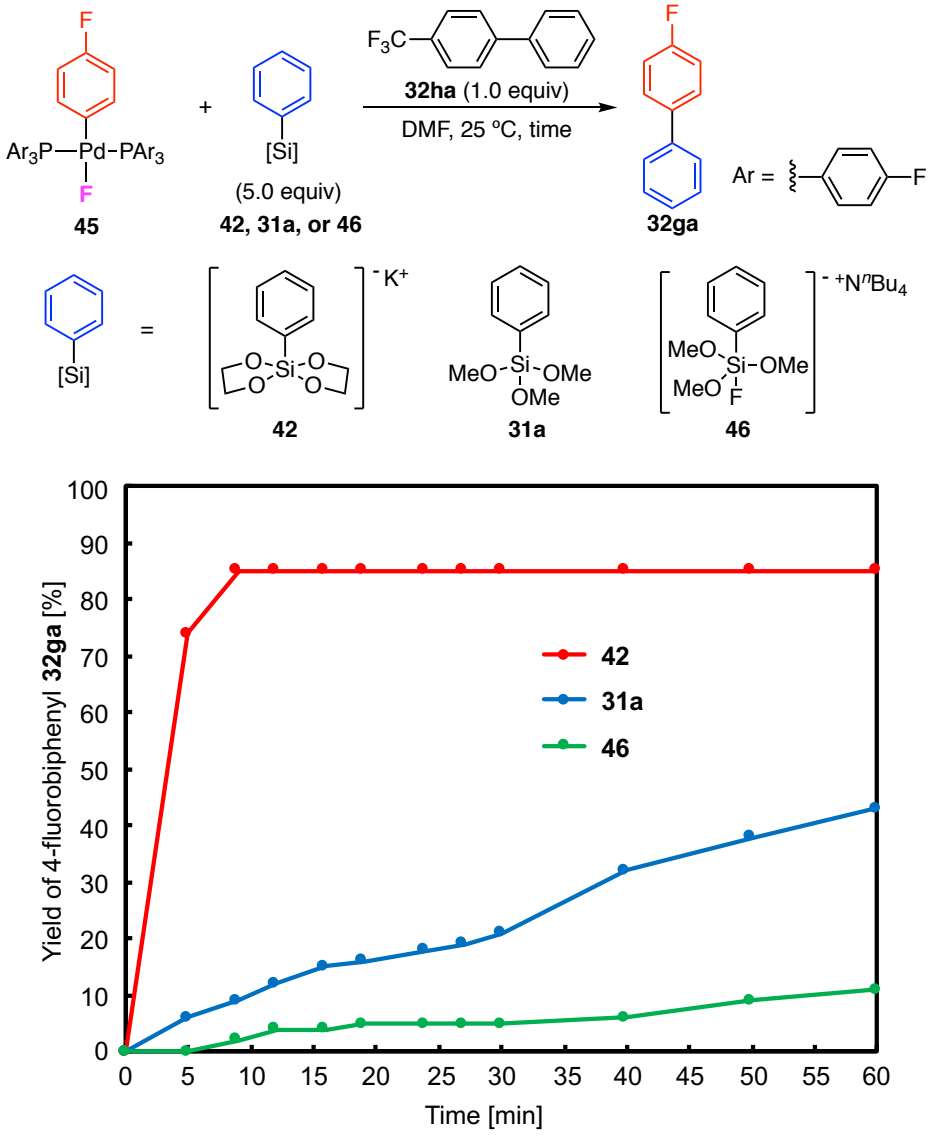

Figure 4. Stoichiometric Reactions between an Arylpalladium Fluoride **45** and Silicon Reagents **42**, **31a**, or **46**.

When trimethoxy(phenyl)silane (**31a**) was used as the silicon reactant, the reaction proceeded much slower than that of **42** to afford **32ga** in 9% yield after 9 minutes and in 43% yield even on prolonging the reaction time to 60 minutes (Figure 4, blue line). Moreover, the fluorosilicate **46** was found to be much less effective, giving **32ga** in 11% yield only after 60 minutes (Figure 4, green line). Thus, these results experimentally revealed that the glycol-derived spirosilicates are quite reactive silicon reagents in the transmetalation step via the S_E2 (cyclic) pathway and are in good agreement with computational results (Figure 3).

Considering another possible reaction pathway, arylpalladium bromide species formed by oxidative addition of Ar-Br to Pd(0) species can directly react with silicon reagents via S_E2 (open) pathway. Therefore, this author also performed a stoichiometric reaction of an arylpalladium bromide complex **47** with ethylene glycol-derived spirosilicate **42** (Scheme 3).

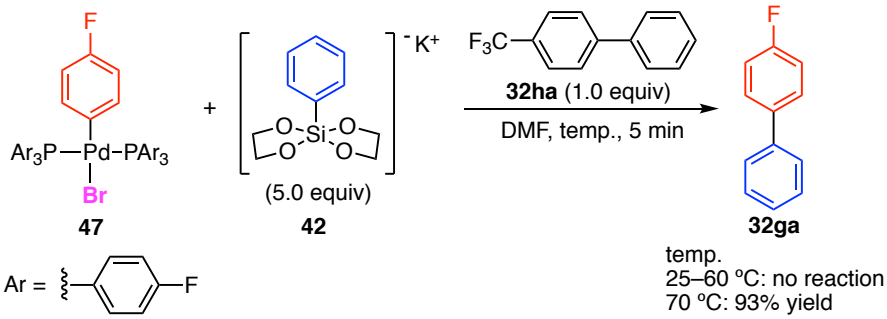

Scheme 3. Stoichiometric Reaction of an Arylpalladium Bromide **47** with the Spirosilicate **42** under Thermal Conditions.

The reaction progress was monitored by ^{19}F VT-NMR using **32ha** as an internal

standard. The reaction of **47** with **42** did not proceed at all at below 60 ºC, whereas **47** was rapidly converted into the coupling product **32ga** in 93% yield at 70 ºC within 5 minutes. This observation indicates that the spirosilicates can react with arylpalladium bromide species under thermal conditions (70 ºC).

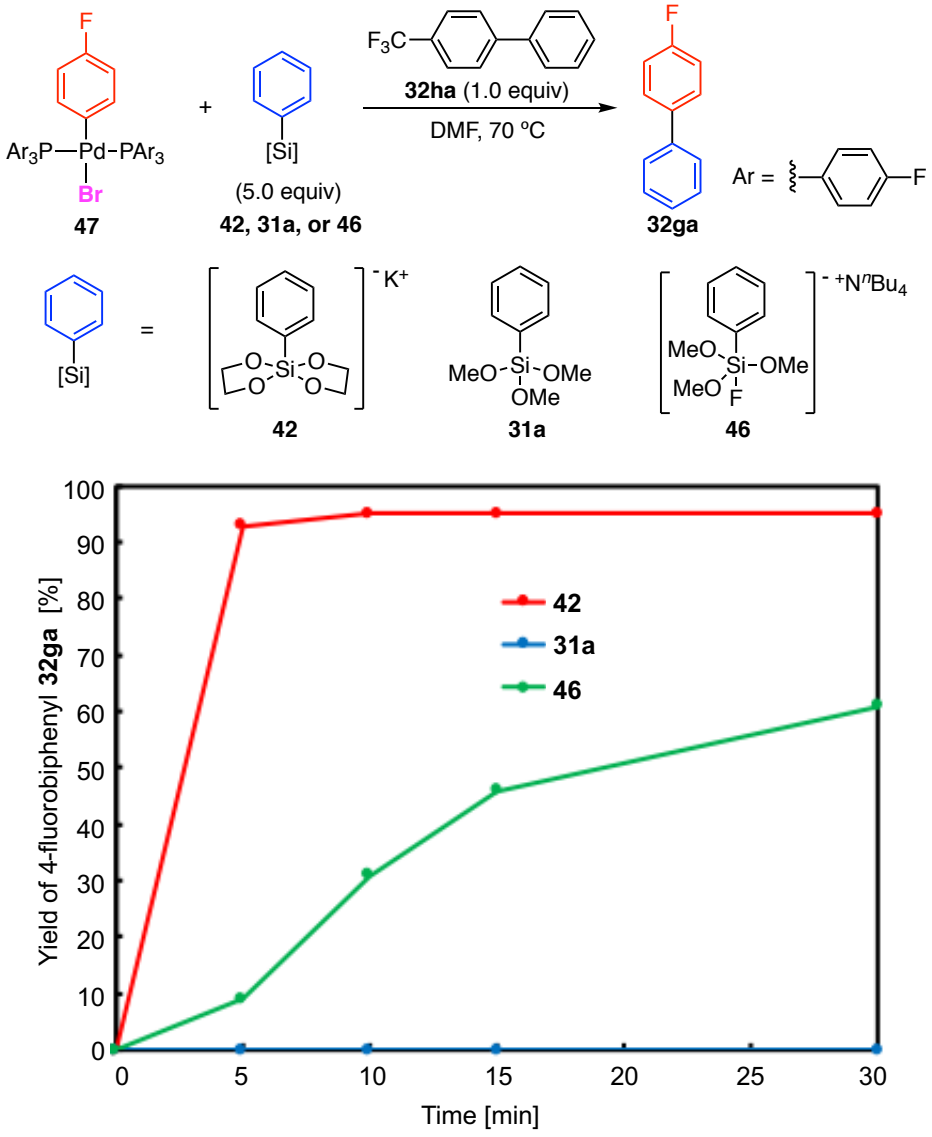

Figure 5. Stoichiometric Reactions between an Arylpalladium Bromide **47** and Silicon Reagents **42**, **31a**, or **46**.

In accord with the obtained result in Figure 4, this author performed the similar experiments using trimethoxy(phenyl)silane (**31a**) and fluorosilicate **46** instead of spirosilicate **42 (**Figure 5). Trimethoxy(phenyl)silane (**31a**) was found to be completely inactive in the S_E2 (open) reaction (Figure 5, blue line). On the other hand, the fluorosilicate **46** reacted with the palladium bromide **47** much slower than **42** to furnish the product **32ga** in 9% yield after 5 minutes and in 61% yield after 30 minutes (figure 5, green line). From these results, the glycol-derived spirosilicates also significantly facilitate the transmetalation step via the S_E2 (open) pathway.

Based on the above mentioned observations, this author proposes pathways of the transmetalation step as summarized in Scheme 4. In the present method (Scheme 4a), spirosilicate intermediate **42** is generated in situ by the reaction of trimethoxyphenylsilane (**31a**) with the glycol solvent in the presence of potassium fluoride. Spirosilicate **42** reacts with an arylpalladium bromide species **A**, formed by oxidative addition of aromatic bromide to Pd(0) species, under thermal conditions via S_E2 (open) pathway, and also undergoes the transmetalation with an arylpalladium fluoride species **B**, generated by ligand exchange of the arylpalladium bromide with potassium fluoride, even at room temperature via S_E2 (cyclic) pathway. Therefore, the transmetalation of the spirosilicate proceeds very smoothly via both S_E2 (open) and S_E2 (cyclic) pathways.

In the case of the conventional Hiyama coupling reaction (Scheme 4b), trimethoxyphenylsilane (**31a**) and its fluorosilicate **46** are considered to be in an

equilibrium in the presence of TBAF.[10] **31a** undergoes the transmetalation with **B** via S_E2 (cyclic) pathway, but it is completely inactive in the S_E2 (open) pathway. The fluorosilicate **46** reacts with **A** under thermal conditions, whereas **46** is inactive in S_E2 (cyclic) pathway. The equilibrium between **31a** and **46** mainly distributes to the fluorosilicate **46**,[10] indicating that the general Hiyama coupling reaction mostly proceeds via S_E2 (open) pathway. Moreover, transmetalation of the glycol-derived spirosilicates occurs significantly faster than that of the conventional Hiyama coupling in both S_E2 (open) and S_E2 (cyclic) pathways ($\boldsymbol{k_1} > \boldsymbol{k_3}$, $\boldsymbol{k_2} > \boldsymbol{k_4}$). Consequently, the present method exhibits the high efficiency to realize the Hiyama coupling reaction at ppm levels of a palladium catalyst.

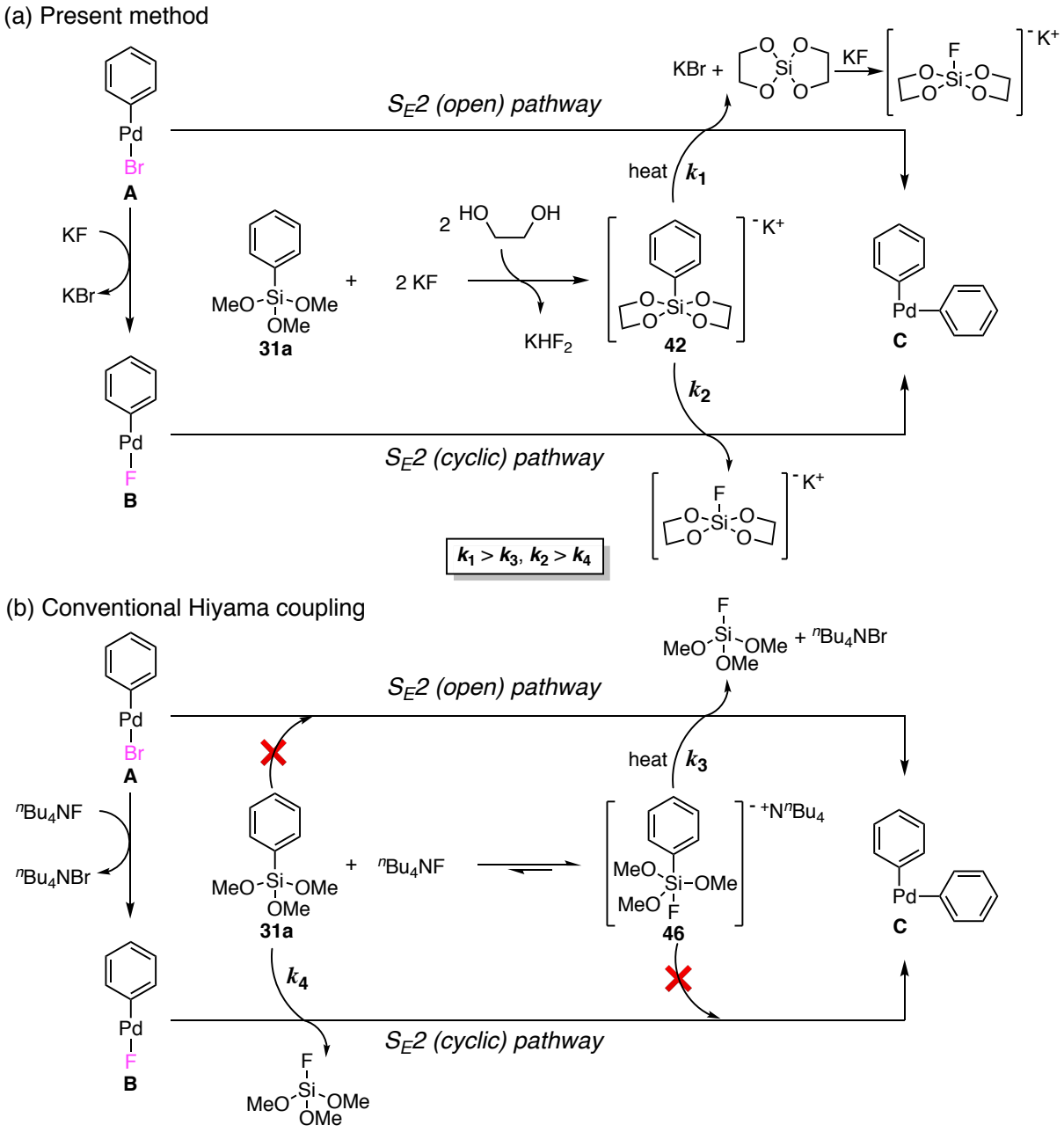

Scheme 4. Proposed Reaction Pathways of Transmetalation Step

Conclusion

In summary, several mechanistic investigations were carried out to understand the reason for the high efficiency of the Hiyama coupling reaction in glycol solvents. ESI-MS and ^{29}Si NMR analyses of the reaction mixture suggested that aryltrialkoxysilanes reacted with glycol solvents in the presence of potassium fluoride as a base to afford glycol-derived pentacoordinate spirosilicate intermediates in situ. A single-crystal x-ray analysis of the spirosilicate clearly confirmed its structural nature. Preliminary theoretical studies and stoichiometric reactions on the transmetalation between arylpalladium halides and silicon reagents substantiated that the glycol-derived pentacoordinate spirosilicate intermediates are quite reactive silicon reactants in the transmetalation step.

Experimental Section

General Methods. All reactions with oxygen- or moisture-sensitive reagents were performed under a nitrogen atmosphere, nitrogen gas was dried by passage through P_2O_5. Silica gel was purchased from Kanto chemical (Silica gel 60N, spherical neutral, particle size 40-50μm) or Yamazen corporation (Hi-FlashTM Column Silica gel 40 mm 60 Å). NMR spectra were recorded on a JEOL JNM ECS-400 spectrometer (396 MHz for ^{1}H, 100 MHz for ^{13}C). Chemical shifts are reported in δ (ppm) referenced to an internal tetramethylsilane standard for ^{1}H NMR. Chemical shifts of ^{13}C NMR are given related to solvent peak as an internal standard ($CDCl_3$: δ 77.0 or DMSO-d_6: δ 39.5). Chemical shifts of ^{29}Si NMR were obtained related to tetramethylsilane (δ -0.0) as an external standard. Chemical shifts of ^{19}F NMR were obtained related to CF_3CO_2H (δ -75.0) as an external standard. ^{1}H, ^{13}C, ^{29}Si, and ^{19}F NMR spectra were recorded in $CDCl_3$ or DMSO-d_6 at 25 °C. ESI-TOF-MS spectra were recorded on a JEOL JMS-T100LC spectrometer and a JEOL JMS-T100GC spectrometer. X-ray crystal structure analysis was performed on Synergy Custom (Rigaku Oxford Diffraction). Elemental analyses were performed on a J-SCIENCE LAB MICRO CORDER JM10. Commercially available chemicals (purchased from Sigma-Aldrich, TCI, Kanto chemical, Wako Pure Chemical Industries, Nacalai tesque, and Merck).

Formation of Glycol-Derived Pentacoordinate Spirosilicates

Ethylene glycol-derived pentaccoordinate spirosilicate (**42**)

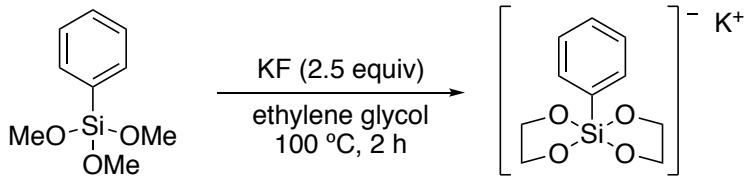

KF (157 mg, 2.7 mmol), phenyltrimethoxysilane (**31a**) (0.2 mL, 1.1 mmol), and ethylene glycol (0.8 mL) were added into a J-Young NMR tube at 25 ºC under N_2 flow. The mixture was heated at 100 ºC for 2h. The resulting sample was cooled to 25 ºC and analyzed by ^{29}Si NMR measurement using tetramethylsilane as an external standard. After the NMR experiment, 10 mg of the mixture was diluted with dry MeOH (10 mL) under N_2. The resulting solution was analyzed by ESI-MS measurements. ^{29}Si NMR (79 MHz, none) -93.72. ESI-TOF-MS positive: *m/z* 303 ($[M+K]^+$), 567 ($[2M+K]^+$), negative: *m/z* 225 ($[M-K]^-$), 489 ($[2M-K]^-$).

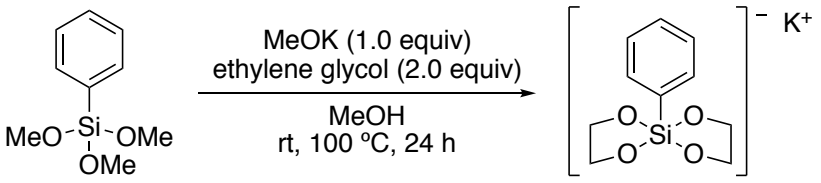

An authentic sample was also prepared according to a following procedure. To a mixture of phenyltrimethoxysilane (**31a**) (1190 mg, 6.0 mmol), and ethylene glycol (745 mg, 12 mmol) in dry MeOH (5 mL) was added potassium methoxide (30% in MeOH, 1.5 mL, 6.0 mmol) under N_2 atmosphere. The reaction mixture

was stirred at room temperature for 24 h. After removal of the solvent under reduced pressure, the resulting residue was suspended in dry Et_2O (10 mL), filtered off, and dried over under reduced pressure to give **42** (1345 mg, 5.1 mmol). [CAS: none] Colorless solid. Mp. >300 ºC. ^{1}H NMR (396 MHz, DMSO-d_6) δ 5.59 (dd, J = 7.2, 1.6 Hz, 2H), 7.19-7.05 (m, 3H), 3.51-3.43 (m, 4H), 3.51-3.27 (m, 4H). ^{13}C NMR (100 MHz, DMSO-d_6) δ 147.70, 135.74, 126.77, 126.41, 60.08. ^{29}Si NMR (79 MHz, DMSO-d_6) δ -93.11. ESI-TOF-MS positive: *m/z* 303 ($[M+K]^+$), 567 ($[2M+K]^+$), negative: *m/z* 225 ($[M-K]^-$), 489 ($[2M-K]^-$). Anal. Calcd for $C_{10}H_{13}KO_4Si•2H_2O$: C, 39.98: H, 5.70%. Found: C, 39.93, H, 5.38%.

Single-crystal X-ray crystallographic data of **42**

A crystal of pentacoordinate spirosilicate (**42**) was mounted in a loop. Data collection was performed at 123 K on a ROD, Synergy Custom system (Rigaku Oxford Diffraction) equipped with confocal monochromated Mo-Kα radiation, and data were processed using CrysAlisPro 1.171.39.43c (Rigaku Oxford Diffraction). Numerical and empirical absorption correction were performed in the data processing.

These crystal structures were solved by dual-space iterative method (SHELXT, ver. 2018/3)[11] and refined by the full-matrix least squares techniques on F^2 (SHELXL, ver. 2018/3)[34] embedded in Olex2 program.[12] All non-hydrogen atoms were refined anisotropically. All hydrogen atoms were grown using the appropriate crystallographic treatments and refined isotropically using the riding

model with Uiso constrained to be 1.5 times Ueq of the carrier atom. The diffused electron densities resulting from the residual solvent molecules were removed from the data set using the SQUEEZE routine of PLATON66 and refined further using the generated data. Crystallographic data have been deposited with Cambridge Crystallographic Data Centre: Deposition number CCDC 1911672 for pentacoordinate spirosilicate (**42**). These data can be obtained free of charge from the Cambridge Crystallographic Data Centre via www.ccdc.cam.ac.uk/data_request/cif.

Propylene glycol-derived pentaccordinate spirosilicate (**43**)

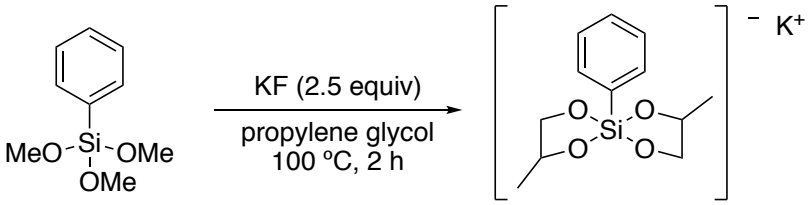

KF (157 mg, 2.7 mmol), phenyltrimethoxysilane (**31a**) (0.2 mL, 1.1 mmol), and propylene glycol (0.8 mL) were added into a J-Young NMR tube at 25 ºC under N_2 flow. The mixture was heated at 100 ºC for 2h. The resulting sample was cooled to 25 ºC and analyzed by ^{29}Si NMR measurement using tetramethylsilane as an external standard. After the NMR experiment, 10 mg of the mixture was diluted with dry MeOH (10 mL) under N_2. The resulting solution was analyzed by ESI-MS measurements. ^{29}Si NMR (79 MHz, none) mixture of diastereomers δ -92.80, -92.93, -93.12, -93.49. ESI-TOF-MS positive: *m/z* 331 ($[M+K]^+$), 623 ($[2M+K]^+$), negative: *m/z* 253 ($[M-K]^-$), 545 ($[2M-K]^-$).

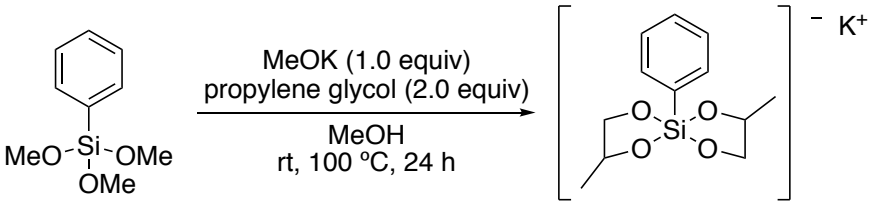

An authentic sample was also prepared according to a following procedure. To a mixture of phenyltrimethoxysilane (**31a**) (396 mg, 2.0 mmol), and propylene glycol (316 mg, 4 mmol) in dry MeOH (4 mL) was added potassium methoxide (30% in MeOH, 0.5 mL, 2.0 mmol) under N_2 atmosphere. The reaction mixture was stirred at room temperature for 24 h. After removal of the solvent under reduced pressure, the resulting residue was suspended in dry Et_2O (5 mL), filtered off, and dried over under reduced pressure to give **43** (440 mg, 1.5 mmol).

[CAS: none] Colorless solid. Mp. 272 ºC. ^{1}H NMR (396 MHz, DMSO-d_6) mixture of diastereomers, δ 7.70-7.64 (m, 2H), 7.10-7.08 (m, 3H), 3.74-2.63 (m, 6H), 1.04-0.89 (m, 6H). ^{13}C NMR (100 MHz, DMSO-d_6) mixture of diastereomers, δ 149.00, 148.42, 128.24, 148.06, 147.68, 135.71, 135.53, 135.45, 135.33, 126.74, 126.65, 126.62, 126.55, 126.48, 126.35, 126.24, 126.09, 67.98, 67.59, 67.23, 67.02, 66.84, 66.69, 66.54, 66.29, 66.08, 65.90, 65.70, 64.91, 64.51, 64.26, 63.99, 22.90, 22.54, 22.44, 22.32, 22.07, 21.96, 21.84. ^{29}Si NMR (79 MHz, DMSO-d_6) mixture of diastereomers, δ -92.75, -92.88, -93.24, -93.70. ESI-TOF-MS positive: *m/z* 303 ($[M+K]^+$), 623 ($[2M+K]^+$), negative: *m/z* 225 ($[M-K]^-$), 545 ($[2M-K]^-$). Anal. Calcd for $C_{12}H_{17}KO_4Si•1.5H_2O$: C, 45.12: H, 6.31%. Found: C, 45.35, H, 6.10%.

Computational Procedure

All calculations were carried out with the *Gaussian16* program. Geometry optimizations and frequency calculations for all molecules were performed at the B3LYP level of theory and with the basis sets 6-31G(d,p) for C and H, 6-31+G(d,p) for F, Si, K, O, and P, and LanL2DZ for Pd. Single -point energies were obtained by calculations at B3LYP level of theory and with the basis sets 6-311++G(2d,p) for C, H, O, F, Si, P and K and SDD for Pd using the SMD solvation model (DMF). The computations were performed using Research Center for Computational Science, Okazaki, Japan.

Cartesian Coordinates

Pentacoordinate Spirosilicate (**42**)

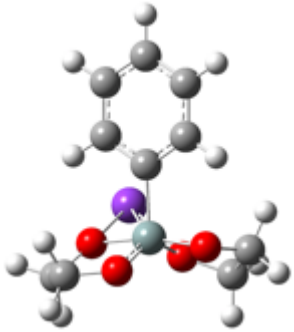

Zero-point correction = 0.223511 (Hartree/Particle)
Thermal correction to Energy = 0.239063
Thermal correction to Enthalpy = 0.240007
Thermal correction to Gibbs Free Energy = 0.179480
Sum of electronic and zero-point Energies = -1579.156409
Sum of electronic and thermal Energies = -1579.140857
Sum of electronic and thermal Enthalpies = -1579.139913
Sum of electronic and thermal Free Energies = -1579.200440

Single point energy = -1579.67104402

K	-0.23858600	-1.25365200	2.40142500
Si	-0.78626600	0.28544900	-0.47256700
O	-1.56611700	-0.08063300	-1.94664800
O	-1.07473700	-1.46921900	0.02746300
O	-1.37472400	0.67982600	1.16887300
O	-0.89003400	1.98754200	-0.85119400
C	1.13073700	0.10615200	-0.41609600
C	1.79448500	-1.11799500	-0.17872900
C	-1.93693100	-2.14330700	-0.86561800
C	3.97166400	-0.06289800	-0.26520100
C	3.34670800	1.15787700	-0.52947300
C	1.95419700	1.23565100	-0.60416400
C	-1.00306700	2.83140900	0.26355600
C	-1.75161600	-1.45440400	-2.22123700
C	3.18925500	-1.20625600	-0.09782900
C	-1.77247300	2.03832800	1.32540900
H	-2.98508200	-2.05303400	-0.53306100
H	-1.68468200	-3.21239300	-0.91334100
H	-2.62272500	-1.58101100	-2.87476200
H	-0.86867100	-1.86004600	-2.74028900
H	5.05528200	-0.12515300	-0.20838100
H	3.94671400	2.05093500	-0.68637500
H	1.48472100	2.18624700	-0.83452100
H	1.20079700	-2.02548500	-0.09912000
H	3.66333100	-2.17023800	0.07438800
H	-2.85703700	2.11794300	1.16323200
H	-0.00805500	3.11201400	0.65623500
H	-1.52686600	3.75555300	-0.01217100
H	-1.54973300	2.38031100	2.34537300

Trimethoxy(phenyl)silane (**31a**)

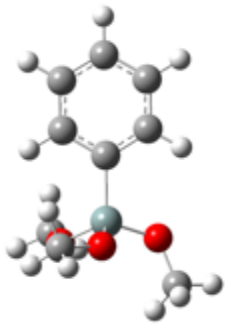

Zero-point correction = 0.219933 (Hartree/Particle)

Thermal correction to Energy = 0.235765
Thermal correction to Enthalpy = 0.236709
Thermal correction to Gibbs Free Energy = 0.174549
Sum of electronic and zero-point Energies = -866.468362
Sum of electronic and thermal Energies = -866.452530
Sum of electronic and thermal Enthalpies = -866.451586
Sum of electronic and thermal Free Energies = -866.513746

Single point energy = -866.893903

C	1.71507000	-1.03753200	0.17467900
C	0.94584700	0.12377900	-0.03274800
C	1.62582900	1.33653800	-0.25277700
C	3.02039800	1.38558900	-0.26894000
C	3.76424400	0.22104600	-0.06597500
C	3.11020500	-0.99212300	0.15632200
H	1.21890300	-1.98812100	0.35712000
H	1.05391600	2.24718000	-0.40551300
H	3.52712400	2.33176400	-0.43784700
H	4.85006900	0.25946200	-0.07840200
H	3.68524400	-1.89962400	0.31870000
Si	-0.91598500	0.03585500	-0.05418300
O	-1.46478000	1.56120500	0.25798600
O	-1.56864800	-0.41745300	-1.50477300
O	-1.45832400	-1.10010800	1.03219800
C	-2.81113200	1.99578500	0.06571100
H	-3.50137900	1.44693400	0.71749800
H	-2.85627800	3.05781500	0.31968900
H	-3.12109900	1.85990900	-0.97549000
C	-1.53428200	-1.72913100	-2.05839300
H	-2.08640700	-1.70759900	-3.00147900
H	-0.50375100	-2.04510900	-2.26508800
H	-2.00368400	-2.45393200	-1.38416700
C	-1.19032700	-1.08451900	2.43188700
H	-1.57119100	-2.01706800	2.85651900
H	-0.11438000	-1.01697000	2.63450100
H	-1.69440000	-0.24236100	2.92063300

PhPdF(PPh_3) (**44**)

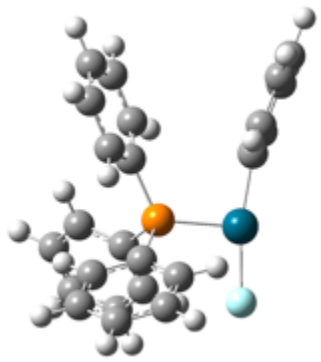

Zero-point correction = 0.367359 (Hartree/Particle)
Thermal correction to Energy = 0.392372
Thermal correction to Enthalpy = 0.393316
Thermal correction to Gibbs Free Energy = 0.307633
Sum of electronic and zero-point Energies = -1494.212308
Sum of electronic and thermal Energies = -1494.187296
Sum of electronic and thermal Enthalpies = -1494.186352
Sum of electronic and thermal Free Energies = -1494.272034

Single point energy = -1496.110598

Pd	-0.60640600	-1.63019500	-0.81130000
P	0.55534700	0.10521900	0.04911700
F	1.04157700	-2.74056400	-1.28669800
C	-2.40319600	-0.84606400	-0.46522700
C	-3.16775100	-1.41000200	0.56949100
C	-4.52744500	-1.10377300	0.69540100
C	-5.13174300	-0.21547500	-0.19618900
C	-4.37331600	0.36505400	-1.21552800
C	-3.01441100	0.06107600	-1.34413900
C	-0.32248000	1.63891800	0.54314400
C	-1.27801200	1.58202200	1.57288100
C	-1.97398000	2.72733600	1.95096400
C	-1.73958600	3.94045600	1.29730600
C	-0.80540400	4.00173700	0.26446000
C	-0.09689200	2.85782300	-0.11255500
C	1.47405000	-0.47364000	1.53066400
C	1.65099900	0.32391100	2.67143300
C	2.40367500	-0.15523400	3.74607200
C	2.98308300	-1.42311600	3.68556700
C	2.80985000	-2.21629000	2.54806600

C	2.05602200	-1.75330600	1.47002400
C	1.85016600	0.62100600	-1.14502600
C	1.75612000	0.24653700	-2.49171300
C	2.73687800	0.64916600	-3.39994200
C	3.81827700	1.41778900	-2.96922700
C	3.92563100	1.78118900	-1.62402600
C	2.94881500	1.38282600	-0.71266900
H	-2.70970000	-2.09734800	1.27810400
H	-5.11011600	-1.55632200	1.49405700
H	-6.18579000	0.02746500	-0.09420500
H	-4.83781700	1.05917700	-1.91154500
H	-2.43694900	0.53003200	-2.13687200
H	-1.49041000	0.63982500	2.06712300
H	-2.70867500	2.66983900	2.74845500
H	-2.28904100	4.83071300	1.58912100
H	-0.62252600	4.93911100	-0.25268900
H	0.62967000	2.91898900	-0.91503200
H	1.20291000	1.31029800	2.72868400
H	2.53432600	0.46471100	4.62846800
H	3.56617000	-1.79367800	4.52396700
H	3.25783500	-3.20444000	2.49924100
H	1.91064000	-2.36758400	0.58087500
H	0.93690900	-0.38680800	-2.81560900
H	2.66096300	0.34643400	-4.43985100
H	4.58387200	1.72404100	-3.67629100
H	4.77343200	2.36778700	-1.28230300
H	3.04848100	1.65383900	0.33424100

TS-Ia

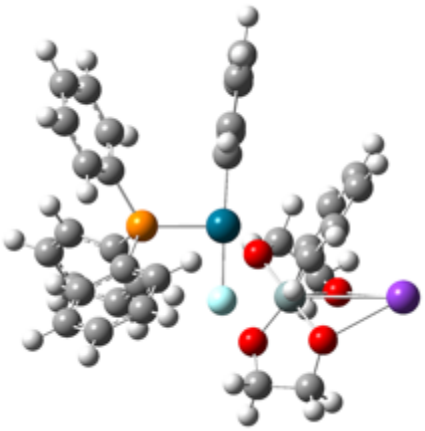

Zero-point correction = 0.591066 (Hartree/Particle)

Thermal correction to Energy = 0.632792
Thermal correction to Enthalpy = 0.633736
Thermal correction to Gibbs Free Energy = 0.510832
Sum of electronic and zero-point Energies = -3073.374913
Sum of electronic and thermal Energies = -3073.333187
Sum of electronic and thermal Enthalpies = -3073.332243
Sum of electronic and thermal Free Energies = -3073.455147

Single point energy = -3075.762598

Pd	0.03164800	0.42922900	-0.34764400
P	2.11633800	-0.49232300	-0.06903000
F	-0.68325700	-1.44851200	-0.90221600
C	0.62458600	2.25545500	0.21069600
C	0.38537600	2.66707100	1.53120900
C	0.66978300	3.97780100	1.92973800
C	1.20272700	4.89258200	1.01733500
C	1.45150800	4.48703300	-0.29544100
C	1.17100700	3.17466300	-0.69470800
C	3.59715900	0.57907500	0.14029200
C	3.70616500	1.38616800	1.28625000
C	4.79862600	2.23470800	1.45050100
C	5.79207500	2.30153000	0.46985000
C	5.68625700	1.51393800	-0.67572500
C	4.59616200	0.65539200	-0.84127400
C	2.11066100	-1.61959900	1.38357000
C	3.25045200	-1.82735700	2.17759100
C	3.20392400	-2.72199100	3.24857500
C	2.02443400	-3.41332200	3.53206400
C	0.89058400	-3.20908600	2.74297700
C	0.92315000	-2.31574000	1.67131900
C	2.51792000	-1.56176500	-1.51108300
C	1.96115900	-1.26905900	-2.76326200
C	2.28567100	-2.04545700	-3.87644800
C	3.15852900	-3.12681200	-3.74611500
C	3.70569400	-3.43302700	-2.49811500
C	3.38727500	-2.65564100	-1.38394700
H	-0.03725300	1.96478100	2.24564500
H	0.47457800	4.28334200	2.95553300
H	1.42687400	5.90961600	1.32828700
H	1.87280600	5.18905800	-1.01160900
H	1.38662500	2.87296300	-1.71676700
H	2.92940500	1.36314000	2.04280100

H	4.86822100	2.85198400	2.34131600
H	6.64050000	2.96775700	0.59796300
H	6.45203500	1.56150400	-1.44479800
H	4.52747100	0.04580100	-1.73557800
H	4.16938400	-1.28853700	1.97045100
H	4.08917800	-2.87458900	3.85990900
H	1.98949500	-4.10574800	4.36895700
H	-0.03491800	-3.73418800	2.95894900
H	0.03372900	-2.16316400	1.06651200
H	1.25364700	-0.45080600	-2.85177000
H	1.84367300	-1.81399900	-4.84130100
H	3.40424100	-3.73589400	-4.61155800
H	4.37621000	-4.28071400	-2.38884000
H	3.80517000	-2.90829000	-0.41436300
C	-2.45688900	0.78082200	-0.58374900
Si	-2.89692500	-0.83991400	0.45201800
C	-2.17175200	0.78297800	-1.97404400
C	-2.73017200	2.04622500	-0.00156000
K	-5.50614100	0.57503300	-0.85384100
O	-1.95841700	-0.29614700	1.83885900
O	-4.38233900	-0.34976600	1.29327100
O	-3.84694000	-1.38542700	-0.99972300
O	-2.58486600	-2.48315200	0.81852300
C	-2.20503800	1.96142700	-2.73612600
H	-1.96639000	-0.16936200	-2.44978600
C	-2.78673500	3.21816300	-0.75676200
H	-2.91508900	2.10086900	1.06673400
C	-2.72606700	0.06078400	2.96165300
C	-4.18036200	-0.38825700	2.70273800
C	-4.08536900	-2.78261900	-0.97860800
C	-2.90800000	-3.39658000	-0.21317400
C	-2.52937300	3.17714200	-2.13405100
H	-1.98374200	1.92249300	-3.79998900
H	-3.00480200	4.16683900	-0.27290700
H	-2.33039100	-0.40948000	3.87374300
H	-2.68872700	1.15527000	3.11363600
H	-4.33639800	-1.41458300	3.06365000
H	-4.90582200	0.26856400	3.20045600
H	-5.03481300	-3.00645800	-0.45910300
H	-4.15486200	-3.16785100	-2.00518700
H	-2.04054200	-3.51776600	-0.87439800
H	-3.17092000	-4.36643400	0.22759600
H	-2.56276600	4.09002000	-2.72287900

Int-a

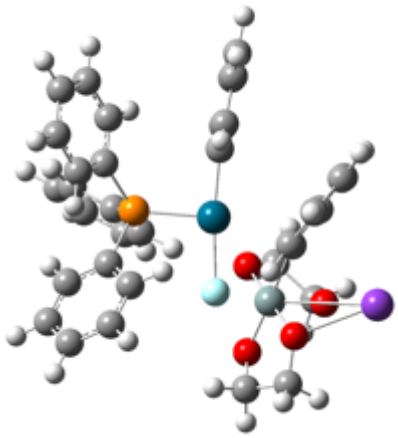

Zero-point correction = 0.591491 (Hartree/Particle)
Thermal correction to Energy = 0.633310
Thermal correction to Enthalpy = 0.634254
Thermal correction to Gibbs Free Energy = 0.511852
Sum of electronic and zero-point Energies = -3073.386660
Sum of electronic and thermal Energies = -3073.344840
Sum of electronic and thermal Enthalpies = -3073.343896
Sum of electronic and thermal Free Energies = -3073.466298

Single point energy = -3075.769729

Pd	-0.01417300	0.49850600	-0.21094100
P	2.03858300	-0.56568100	-0.10073300
F	-1.17544900	-1.30460200	-0.54895900
C	0.85001500	2.23950400	0.20398000
C	0.98170900	2.61794100	1.54714100
C	1.46171200	3.89154100	1.87424000
C	1.82044400	4.78979900	0.86585300
C	1.69763000	4.40847600	-0.47195900
C	1.22057600	3.13542500	-0.80482000
C	3.56899500	0.28779000	-0.66813400
C	4.08782700	1.36300000	0.07486500
C	5.22924800	2.03435200	-0.35990100
C	5.86165700	1.65547700	-1.54671700
C	5.34720600	0.59787100	-2.29596500
C	4.20933700	-0.08533100	-1.85992000
C	2.39038600	-1.13966500	1.60779500
C	3.69765300	-1.30670600	2.09278800
C	3.90912800	-1.80378400	3.37998800
C	2.82094300	-2.14189400	4.18694300

C	1.52027200	-1.97832600	3.70634600
C	1.29499500	-1.47478800	2.42354300
C	1.96054100	-2.09487900	-1.12029900
C	1.21346400	-2.08867400	-2.30755500
C	1.17230700	-3.22292000	-3.11892200
C	1.86465800	-4.37638200	-2.74622300
C	2.59948100	-4.39379000	-1.55920300
C	2.64872800	-3.25949800	-0.74795000
H	0.70640400	1.92672400	2.33926300
H	1.55495100	4.17785700	2.91914600
H	2.19537500	5.77724100	1.12104400
H	1.97868800	5.09936900	-1.26332600
H	1.14025900	2.84936300	-1.84939600
H	3.59685600	1.68288200	0.98734100
H	5.61873500	2.86089300	0.22707800
H	6.74866600	2.18359600	-1.88480000
H	5.83136200	0.29569900	-3.22021400
H	3.82442200	-0.91040800	-2.44898600
H	4.54909800	-1.04515600	1.47279600
H	4.92354200	-1.92610000	3.74919600
H	2.98749800	-2.52895900	5.18844700
H	0.66984400	-2.23742400	4.32995100
H	0.27197800	-1.33749600	2.07274700
H	0.64406400	-1.20608300	-2.58043400
H	0.58437900	-3.20893900	-4.03184700
H	1.82297200	-5.26260800	-3.37302200
H	3.13079500	-5.29231400	-1.25890900
H	3.21331100	-3.28594100	0.17828100
C	-2.36300100	1.01942800	-0.41774000
Si	-2.74493200	-0.86495000	0.29426700
C	-2.15081200	1.26644200	-1.80298200
C	-2.55556100	2.17758400	0.38285300
K	-5.34710900	0.85855900	-0.73912500
O	-1.80336500	-0.59742400	1.77864200
O	-4.21302200	-0.26313600	1.21392800
O	-3.72855500	-1.09411400	-1.22816100
O	-3.00819400	-2.56467000	0.65703100
C	-2.19355100	2.55604700	-2.35539400
H	-2.02372000	0.41073500	-2.45990700
C	-2.60650000	3.46474200	-0.15418200
H	-2.69760300	2.04838900	1.45145800
C	-2.57002500	-0.32072200	2.92673100
C	-4.05368800	-0.57217200	2.58417600

C	-4.30441400	-2.38559300	-1.30330700
C	-3.42333200	-3.31186900	-0.45379800
C	-2.43470900	3.65696900	-1.53255900
H	-2.04362000	2.69669100	-3.42355900
H	-2.76580700	4.32180200	0.49587200
H	-2.25266800	-0.95486700	3.76904900
H	-2.42361700	0.73073100	3.23518400
H	-4.30815100	-1.62661700	2.76234900
H	-4.71433400	0.05831700	3.19741700
H	-5.33310400	-2.37715700	-0.89110200
H	-4.36299300	-2.71390600	-2.35172700
H	-2.55557000	-3.64621000	-1.04867500
H	-3.97737000	-4.20422000	-0.12888200
H	-2.47314000	4.65856100	-1.95307300

TS-IIa

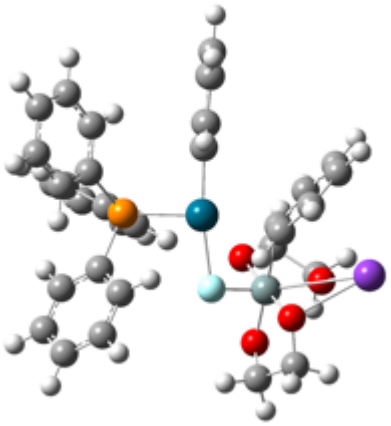

Zero-point correction = 0.591073 (Hartree/Particle)
Thermal correction to Energy = 0.632249
Thermal correction to Enthalpy = 0.633193
Thermal correction to Gibbs Free Energy = 0.513159
Sum of electronic and zero-point Energies = -3073.384398
Sum of electronic and thermal Energies = -3073.343222
Sum of electronic and thermal Enthalpies = -3073.342278
Sum of electronic and thermal Free Energies = -3073.462311

Single point energy = -3075.766840

Pd	-0.05419800	0.39906600	-0.19842300
P	2.10779400	-0.47803100	-0.13232000
F	-1.12945600	-1.47177800	-0.52645300
C	0.65263200	2.21631400	0.21367400
C	0.85645700	2.58036600	1.55236700

C	1.27115600	3.87771500	1.87753500
C	1.48653300	4.82179500	0.87081100
C	1.28592300	4.46025500	-0.46352800
C	0.87576800	3.16363700	-0.79328200
C	3.52636800	0.46960500	-0.82952100
C	3.95499300	1.65093000	-0.19801000
C	5.00453100	2.39578200	-0.73390400
C	5.63192100	1.98535700	-1.91263000
C	5.20554400	0.82169200	-2.55210700
C	4.16140000	0.06548100	-2.01424500
C	2.59351000	-0.90181700	1.58923800
C	3.92670300	-0.89732800	2.02815000
C	4.23652200	-1.27868500	3.33518000
C	3.22130300	-1.67201700	4.20906500
C	1.89386900	-1.67947300	3.77538900
C	1.57180300	-1.29183700	2.47348200
C	2.14002500	-2.07916800	-1.04033900
C	1.34654200	-2.22569600	-2.18827700
C	1.37671700	-3.41443700	-2.91853200
C	2.18777800	-4.47170000	-2.50291200
C	2.97041700	-4.33793500	-1.35431200
C	2.94841400	-3.14844800	-0.62510500
H	0.69640300	1.85510700	2.34580700
H	1.42563000	4.14617900	2.92005600
H	1.80796200	5.82862600	1.12337500
H	1.45086900	5.18747000	-1.25520600
H	0.72865500	2.89902800	-1.83629200
H	3.46661900	1.99415000	0.70734200
H	5.32498100	3.30391000	-0.23177500
H	6.44654000	2.57068100	-2.32961200
H	5.68645300	0.49384600	-3.46934100
H	3.84464600	-0.84043800	-2.51913800
H	4.72202100	-0.59108400	1.35618700
H	5.27083500	-1.26822700	3.66753300
H	3.46444400	-1.96879700	5.22559800
H	1.09973400	-1.98235700	4.45152000
H	0.53033300	-1.28686400	2.15374400
H	0.68777600	-1.41944100	-2.49448400
H	0.75308800	-3.51792400	-3.80157000
H	2.20262000	-5.40053400	-3.06604800
H	3.59585700	-5.16110200	-1.02088400
H	3.55296900	-3.05704700	0.27137600
C	-2.24070400	1.01804800	-0.41913300

Si	-2.64568300	-1.09956800	0.34540100
C	-2.34330700	1.24577100	-1.81577400
C	-2.60370900	2.11165100	0.40547100
K	-5.26048600	0.74668900	-0.68232600
O	-1.69558000	-0.83644900	1.80199200
O	-4.08375200	-0.43757100	1.23377100
O	-3.61685600	-1.21198000	-1.17444200
O	-2.95436600	-2.78657100	0.65974600
C	-2.82879900	2.44676800	-2.35280000
H	-2.08609300	0.43531300	-2.49190000
C	-3.10228400	3.31242500	-0.10693900
H	-2.51454800	2.00453200	1.48248300
C	-2.43824100	-0.47203100	2.94219800
C	-3.93082200	-0.68234400	2.61838500
C	-4.24396400	-2.48071200	-1.28936500
C	-3.40125300	-3.47527600	-0.47983700
C	-3.22028000	3.48097800	-1.49498600
H	-2.89546600	2.58014600	-3.43057200
H	-3.37625800	4.12457400	0.56274600
H	-2.13745100	-1.08187200	3.80660200
H	-2.24449500	0.58419700	3.19807100
H	-4.22574600	-1.71614500	2.84898700
H	-4.56596800	0.00237000	3.19842400
H	-5.26897400	-2.44393900	-0.87106800
H	-4.31821500	-2.76353600	-2.34918900
H	-2.54766600	-3.82154300	-1.08691100
H	-3.99103000	-4.35469700	-0.18647600
H	-3.59279200	4.41826500	-1.90145000

Product-a

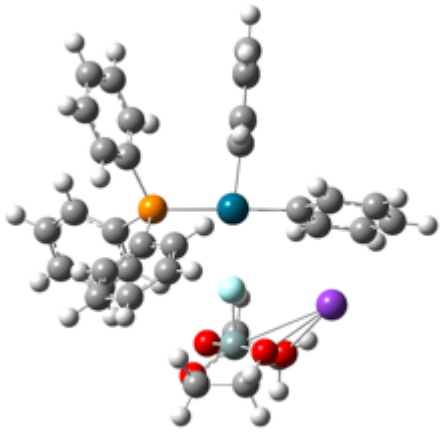

Zero-point correction = 0.591532 (Hartree/Particle)
Thermal correction to Energy = 0.634283

Thermal correction to Enthalpy = 0.635227
Thermal correction to Gibbs Free Energy = 0.507645
Sum of electronic and zero-point Energies = -3073.441510
Sum of electronic and thermal Energies = -3073.398760
Sum of electronic and thermal Enthalpies = -3073.397816
Sum of electronic and thermal Free Energies = -3073.525398

Single point energy = -3075.821899

Pd	0.18038000	1.10059200	0.08112700
P	1.72838100	-0.83948800	0.02943800
F	-1.71847500	-0.45664000	0.06928600
C	1.57479500	2.53344100	0.13759600
C	1.89674000	3.16420700	1.34850300
C	2.91750200	4.11984600	1.40292900
C	3.62029700	4.47081100	0.24813800
C	3.29266200	3.85939000	-0.96286400
C	2.27446200	2.90097600	-1.01985000
C	3.51684400	-0.49590400	-0.26474400
C	4.17517200	0.39495800	0.60022000
C	5.52733900	0.68376700	0.42409600
C	6.23981600	0.10006800	-0.62637200
C	5.59299300	-0.77719300	-1.49651100
C	4.24006300	-1.07726000	-1.31649200
C	1.73316800	-1.95787700	1.49665000
C	2.90737700	-2.51695100	2.02584700
C	2.84586600	-3.37265900	3.12821400
C	1.61491200	-3.68677200	3.70639700
C	0.44288100	-3.13827300	3.18147000
C	0.49826800	-2.27178800	2.08945700
C	1.25950700	-1.94245900	-1.37467200
C	0.79288600	-1.34350100	-2.55615200
C	0.46231400	-2.12353700	-3.66495000
C	0.57670200	-3.51461700	-3.60030800
C	1.02046800	-4.12018800	-2.42293700
C	1.36212500	-3.34000700	-1.31600100
H	1.35127500	2.91732500	2.25484200
H	3.15415900	4.59687700	2.35127600
H	4.40943500	5.21647200	0.29100900
H	3.83114400	4.12303800	-1.87013800
H	2.04264800	2.43373300	-1.97329500
H	3.62740100	0.87615200	1.40354600
H	6.01922900	1.37671600	1.10022600

H	7.29173300	0.33203800	-0.76730200
H	6.13901800	-1.23499000	-2.31668900
H	3.75123700	-1.76574900	-1.99723200
H	3.86997900	-2.28563200	1.58247300
H	3.76268900	-3.79512200	3.53028400
H	1.57014400	-4.35622600	4.56107000
H	-0.52484200	-3.37732400	3.61166800
H	-0.43197300	-1.86475800	1.70779300
H	0.68261100	-0.26306900	-2.59928100
H	0.10784500	-1.64655200	-4.57445600
H	0.31412700	-4.12362900	-4.46076300
H	1.10047300	-5.20181200	-2.36274200
H	1.70018800	-3.82039400	-0.40362200
C	-1.12430500	2.67697900	-0.01586500
Si	-3.11370000	-1.41429500	0.28548200
C	-1.32135900	3.42811200	-1.19289700
C	-1.96744100	2.97270100	1.07564300
K	-3.85980500	1.51485200	-1.03300600
O	-2.76008300	-1.82322400	1.93144100
O	-4.34820200	-0.31123300	0.83608200
O	-3.63736600	-1.03080600	-1.38421700
O	-2.97178000	-3.04298400	-0.15213700
C	-2.33072200	4.39701200	-1.29272300
H	-0.66574500	3.26999100	-2.04577800
C	-2.97553200	3.94417800	0.98921600
H	-1.84447100	2.43486800	2.01285800
C	-3.20276300	-0.84013700	2.83859500
C	-4.51052000	-0.29213900	2.25402600
C	-3.92562500	-2.19058400	-2.14051300
C	-3.06044000	-3.30756400	-1.54376300
C	-3.16895200	4.65630600	-0.20095500
H	-2.44817500	4.96459600	-2.21357400
H	-3.60198200	4.15261200	1.85388300
H	-3.35339800	-1.28551700	3.82925900
H	-2.45798400	-0.03139100	2.93557300
H	-5.36106400	-0.93246100	2.52539600
H	-4.72387200	0.73101800	2.58817500
H	-4.99522300	-2.44438200	-2.05536300
H	-3.69678800	-2.01971500	-3.20044700
H	-2.05443200	-3.29994600	-1.98464300
H	-3.50166700	-4.29942600	-1.69429100
H	-3.93806900	5.42139600	-0.26625300

TS-Ib

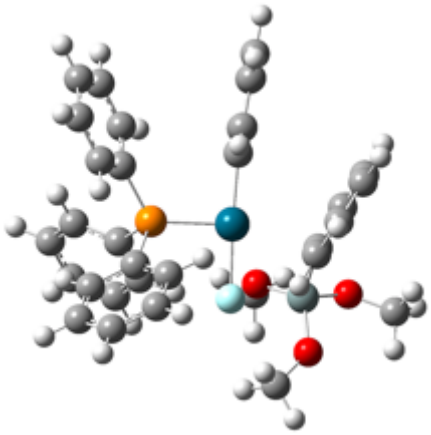

Zero-point correction = 0.588132 (Hartree/Particle)
Thermal correction to Energy = 0.629891
Thermal correction to Enthalpy = 0.630835
Thermal correction to Gibbs Free Energy = 0.506477
Sum of electronic and zero-point Energies = -2360.689924
Sum of electronic and thermal Energies = -2360.648165
Sum of electronic and thermal Enthalpies = -2360.647221
Sum of electronic and thermal Free Energies = -2360.771579

Single point energy = -2362.991526

Pd	0.39246900	0.39352900	0.26766600
P	-1.72119700	-0.49146100	0.02409400
F	1.16194700	-1.48087900	0.79194400
C	-0.21133900	2.21642700	-0.29015300
C	0.03071800	2.62559400	-1.61006500
C	-0.26070200	3.93346800	-2.01390100
C	-0.80795100	4.84450500	-1.10734600
C	-1.06268900	4.43967500	0.20447400
C	-0.77214000	3.13189900	0.60948500
C	-3.18437600	0.60090900	-0.19257700
C	-3.28848800	1.39167800	-1.35025500
C	-4.37440800	2.24629900	-1.52508200
C	-5.36545700	2.33487000	-0.54368900
C	-5.26450100	1.56290000	0.61281600
C	-4.18119700	0.69797500	0.78931100
C	-1.78042500	-1.67838000	-1.37899200
C	-2.92640500	-1.85750000	-2.16941100
C	-2.92915600	-2.80767000	-3.19320500
C	-1.79493200	-3.58542700	-3.42951800

C	-0.65447800	-3.41014400	-2.64182000
C	-0.63619000	-2.45923100	-1.62073900
C	-2.10465700	-1.49889900	1.51455400
C	-1.54822400	-1.13959000	2.74995300
C	-1.85711300	-1.86704700	3.89985800
C	-2.71488400	-2.96563200	3.82376300
C	-3.26356300	-3.33659500	2.59423800
C	-2.96099100	-2.60815200	1.44314600
H	0.45748900	1.92897500	-2.32797600
H	-0.05953400	4.23769500	-3.03852400
H	-1.03768400	5.85892800	-1.42182400
H	-1.49483300	5.13930900	0.91611100
H	-0.98937100	2.83226900	1.63137600
H	-2.51267400	1.35343900	-2.10716800
H	-4.44045900	2.85162200	-2.42419400
H	-6.20835100	3.00632500	-0.67974800
H	-6.02849400	1.62784400	1.38219600
H	-4.11650300	0.10081400	1.69212600
H	-3.81255100	-1.25637000	-1.99508300
H	-3.81883900	-2.93737100	-3.80297500
H	-1.79901200	-4.32370200	-4.22661800
H	0.23109600	-4.01202700	-2.82408300
H	0.25470300	-2.31301500	-1.01436800
H	-0.85601400	-0.30479000	2.80019200
H	-1.41619500	-1.58346700	4.85104500
H	-2.94831200	-3.53693100	4.71767700
H	-3.92373200	-4.19662900	2.52822300
H	-3.38274800	-2.90992800	0.48952000
C	2.45354000	0.87244300	1.84690400
C	2.90948800	0.77126500	0.50698300
C	3.25168800	1.98224200	-0.14970900
C	3.15623700	3.21172000	0.49234500
C	2.72006500	3.27949000	1.82166200
C	2.36758700	2.11418000	2.49550600
H	2.22724800	-0.03795100	2.39114300
H	3.62441900	1.94070300	-1.16872600
H	3.42853600	4.12070500	-0.03599700
H	2.65963100	4.24038000	2.32478800
H	2.03677700	2.15802400	3.52956300
Si	3.47222100	-0.85533400	-0.29364300
O	3.96639800	-2.02432500	0.75597400
O	2.53988100	-1.29664100	-1.59267000
O	4.91085800	-0.42468000	-1.04412700

C	3.31678000	-3.11731300	1.39274400
H	2.80016500	-3.74869600	0.66291700
H	4.09346500	-3.70638800	1.89098900
H	2.58002100	-2.77011200	2.11894100
C	3.06593500	-1.83165000	-2.80477700
H	2.22903400	-1.95191700	-3.49908800
H	3.81349600	-1.16496100	-3.24576900
H	3.52923100	-2.81251600	-2.63934800
C	6.14096200	-0.22584300	-0.36545400
H	6.91372400	-0.02466600	-1.11409700
H	6.08864400	0.63466400	0.31689900
H	6.42389700	-1.11372000	0.21158300

Int-b

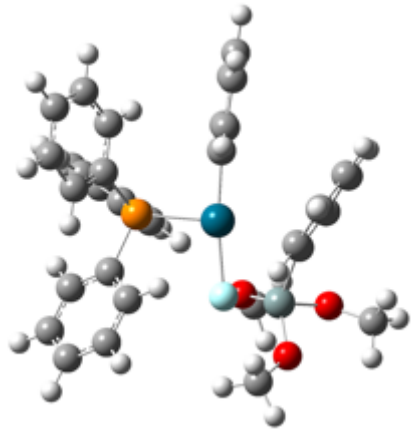

Zero-point correction = 0.589088 (Hartree/Particle)
Thermal correction to Energy = 0.630585
Thermal correction to Enthalpy = 0.631529
Thermal correction to Gibbs Free Energy = 0.510053
Sum of electronic and zero-point Energies = -2360.694233
Sum of electronic and thermal Energies = -2360.652737
Sum of electronic and thermal Enthalpies = -2360.651792
Sum of electronic and thermal Free Energies = -2360.773268

Single point energy = -2362.993909

Pd	-0.41370500	0.47630300	-0.37481100
P	1.63220700	-0.56883500	-0.04831100
F	-1.60935300	-1.29013700	-0.77595100
C	0.44805000	2.21701400	0.06204900
C	0.56475000	2.61491300	1.39987700
C	1.04835000	3.89133200	1.71249900
C	1.42586300	4.77040700	0.69492000

C	1.31840900	4.36869800	-0.63832700
C	0.83796300	3.09371600	-0.95675900
C	3.16744700	0.19161400	-0.72409300
C	3.67182400	1.38063700	-0.16689600
C	4.82103200	1.97069200	-0.69067100
C	5.47398300	1.39709300	-1.78429600
C	4.97375500	0.22489500	-2.35025400
C	3.82955000	-0.37823200	-1.82307500
C	1.93860900	-0.84624900	1.74029600
C	3.22307000	-0.83069300	2.30442200
C	3.39264400	-1.08661900	3.66685700
C	2.28613900	-1.36346300	4.47102600
C	1.00658200	-1.38666000	3.91106200
C	0.82511300	-1.12750500	2.55195500
C	1.57904200	-2.24741100	-0.79463900
C	0.90462800	-2.43858900	-2.01000700
C	0.89212600	-3.69492200	-2.61635200
C	1.53922700	-4.77274200	-2.00935500
C	2.20159700	-4.59209000	-0.79363600
C	2.22385300	-3.33567000	-0.18691600
H	0.28339300	1.93831100	2.20179300
H	1.12989600	4.19316000	2.75370400
H	1.80303400	5.75954400	0.93921500
H	1.61342800	5.04487500	-1.43697000
H	0.77148300	2.79190800	-1.99763600
H	3.16783900	1.84938100	0.67079800
H	5.20019200	2.88614700	-0.24631900
H	6.36620600	1.86296200	-2.19255000
H	5.47377100	-0.22888700	-3.20095600
H	3.45691400	-1.29352700	-2.26898200
H	4.08915300	-0.61382500	1.68811400
H	4.39013600	-1.06848800	4.09649300
H	2.42023600	-1.55931200	5.53106700
H	0.14266500	-1.60133700	4.53296100
H	-0.17582500	-1.15258300	2.12310400
H	0.36971600	-1.61284900	-2.46717700
H	0.36291300	-3.83309100	-3.55437400
H	1.51983900	-5.75262700	-2.47754800
H	2.69915400	-5.42936400	-0.31300300
H	2.73569900	-3.20619800	0.76101100
C	-2.51507200	1.27394900	-1.75129900
C	-2.82154500	0.94232300	-0.40307100
C	-3.08363800	2.03118600	0.47103300

C	-3.05755700	3.34873800	0.02945000
C	-2.77967200	3.63813600	-1.31439100
C	-2.50968900	2.60356100	-2.20334700
H	-2.35994800	0.47373800	-2.46967400
H	-3.34876500	1.81405400	1.50113300
H	-3.26898400	4.15761900	0.72336200
H	-2.78000100	4.66837600	-1.65929100
H	-2.30604800	2.81764400	-3.24913800
Si	-3.21062600	-0.87707100	0.14986700
O	-4.03262400	-1.88522100	-0.91234900
O	-2.37202400	-1.47762100	1.49165700
O	-4.61550400	-0.45946700	1.05057200
C	-3.53707700	-2.73345700	-1.92977600
H	-2.79436800	-3.44233200	-1.54748900
H	-4.38707300	-3.29468300	-2.33375600
H	-3.07501600	-2.16598100	-2.74767200
C	-2.99157200	-1.84865500	2.71639100
H	-2.22016900	-2.30627500	3.34785800
H	-3.42071600	-0.98514400	3.23510700
H	-3.79159300	-2.58031300	2.56036300
C	-5.85315300	-0.11094000	0.47158100
H	-6.55760000	0.13239800	1.27631600
H	-5.77064700	0.77333300	-0.18164500
H	-6.26520900	-0.93537300	-0.12341400

TS-IIb

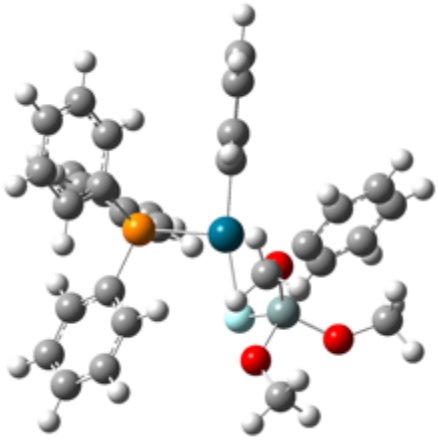

Zero-point correction = 0.587823 (Hartree/Particle)
Thermal correction to Energy = 0.629158
Thermal correction to Enthalpy = 0.630102
Thermal correction to Gibbs Free Energy = 0.508090
Sum of electronic and zero-point Energies = -2360.671407
Sum of electronic and thermal Energies = -2360.630072

Sum of electronic and thermal Enthalpies = -2360.629128
Sum of electronic and thermal Free Energies = -2360.751140

Single point energy = -2362.969718

Pd	-0.49011900	-0.30755100	-0.15396400
P	1.75875500	0.45115100	-0.15165400
F	-1.66489000	1.50540100	-0.85126400
C	0.08701100	-2.05907400	0.60313500
C	0.59829500	-3.08135800	-0.20361700
C	0.96765800	-4.30631700	0.36694700
C	0.82579800	-4.51834300	1.73974500
C	0.31028000	-3.49808600	2.54277700
C	-0.05790800	-2.27158000	1.97968500
C	2.76500200	0.25121800	1.37868600
C	3.14124800	-1.03774700	1.79764200
C	3.86872400	-1.21013600	2.97454800
C	4.21712900	-0.10692400	3.75729900
C	3.83655700	1.17326500	3.35531200
C	3.11669700	1.35421600	2.17210000
C	2.75798400	-0.33097100	-1.48543600
C	4.14397400	-0.52667900	-1.38988500
C	4.85213400	-1.08439900	-2.45669900
C	4.18702000	-1.44632300	-3.62921600
C	2.80761200	-1.25350300	-3.73334300
C	2.09627600	-0.70501800	-2.66630400
C	1.83029200	2.25442800	-0.52435100
C	0.84035300	3.09444100	0.01159200
C	0.87410700	4.46836800	-0.23121400
C	1.88814700	5.01649000	-1.01755300
C	2.87118900	4.18713500	-1.56211300
C	2.84498400	2.81356200	-1.31839200
H	0.71777500	-2.93369800	-1.27231900
H	1.36349100	-5.09435000	-0.26919200
H	1.11044800	-5.47045900	2.17891000
H	0.19253200	-3.65261900	3.61261000
H	-0.45993600	-1.48744200	2.61453600
H	2.86647400	-1.90627400	1.20908000
H	4.15519800	-2.21137700	3.28263400
H	4.77998500	-0.24587300	4.67588900
H	4.10190000	2.03729900	3.95774200
H	2.83092100	2.35564100	1.86924000
H	4.67059200	-0.25159800	-0.48184600

H	5.92441800	-1.23458200	-2.36934100
H	4.74017900	-1.88058100	-4.45700600
H	2.28325800	-1.53720400	-4.64120200
H	1.02033900	-0.57014600	-2.74168700
H	0.02704300	2.68106500	0.59747100
H	0.09398800	5.10029300	0.18154700
H	1.90813400	6.08468300	-1.21390800
H	3.65891600	4.60753700	-2.18084600
H	3.61022900	2.17832100	-1.75196300
C	-3.11514300	-1.96966000	0.34122000
C	-2.56053500	-0.97191300	-0.49269600
C	-2.66065500	-1.19474700	-1.89031700
C	-3.27430300	-2.33262200	-2.42124100
C	-3.81377500	-3.29224600	-1.55927400
C	-3.74316200	-3.10359500	-0.17522300
H	-3.04818700	-1.84086300	1.41708100
H	-2.26776000	-0.44663800	-2.57623000
H	-3.33466800	-2.47195200	-3.49801200
H	-4.29155300	-4.18075300	-1.96434400
H	-4.16625500	-3.84772700	0.49525700
Si	-3.01529200	1.27065100	0.15582400
O	-2.78441600	0.66947300	1.70556000
O	-3.02616200	2.94382100	0.45860800
O	-4.51504500	1.17616300	-0.54571100
C	-2.97417400	1.41925600	2.90391300
H	-4.04129800	1.52622000	3.13652500
H	-2.49855100	0.86279900	3.71757600
H	-2.52714000	2.41508800	2.83440500
C	-4.17760700	3.73164300	0.68511200
H	-3.85897500	4.77496100	0.78985100
H	-4.88544500	3.65968800	-0.14843900
H	-4.70771000	3.44563300	1.60635800
C	-5.47809400	0.14083800	-0.63863600
H	-5.61991900	-0.36746300	0.32107000
H	-6.42366900	0.60634600	-0.93471900
H	-5.19618900	-0.59898800	-1.39260300

Product-b

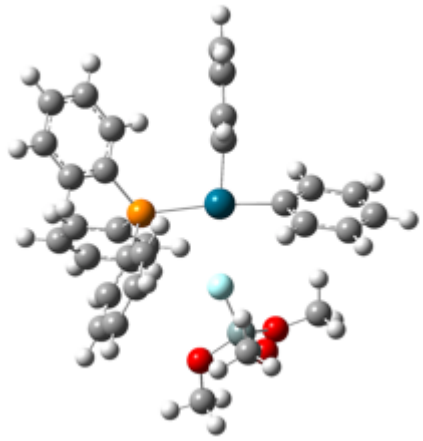

Zero-point correction = 0.587222 (Hartree/Particle)
Thermal correction to Energy = 0.630696
Thermal correction to Enthalpy = 0.631640
Thermal correction to Gibbs Free Energy = 0.498240
Sum of electronic and zero-point Energies = -2360.716356
Sum of electronic and thermal Energies = -2360.672883
Sum of electronic and thermal Enthalpies = -2360.671938
Sum of electronic and thermal Free Energies = -2360.805338

Single point energy = -2363.021455

Pd	-0.01086900	1.14701900	-0.05663800
P	1.45358000	-0.85791800	-0.01725000
F	-1.92738300	-0.60902600	-0.04877600
C	1.36278500	2.59439000	0.07686700
C	1.78832500	3.03752900	1.33785000
C	2.83245400	3.96337900	1.45116800
C	3.45345200	4.47011300	0.30801900
C	3.01932000	4.04730400	-0.94994600
C	1.97837700	3.11976700	-1.06747200
C	3.24624800	-0.75371700	-0.44198400
C	4.00404700	0.27863500	0.13677500
C	5.36908300	0.38541800	-0.12930800
C	5.99379200	-0.52617000	-0.98304400
C	5.24738600	-1.54918000	-1.56901000
C	3.88175900	-1.66522800	-1.29991800
C	1.44412000	-1.76265600	1.59047900
C	2.42254600	-2.70774000	1.93846500
C	2.36090500	-3.36773200	3.16655400
C	1.32459600	-3.09083500	4.06149900

C	0.35120900	-2.14785500	3.72761400
C	0.41233300	-1.48398900	2.50082400
C	0.78450200	-2.06642000	-1.24309200
C	0.65034200	-1.63455500	-2.57520800
C	0.11679700	-2.48091800	-3.54599800
C	-0.31024200	-3.76608000	-3.19754000
C	-0.19823000	-4.19629800	-1.87510500
C	0.34691800	-3.35313000	-0.90201300
H	1.31592700	2.65853000	2.24026200
H	3.15465900	4.28963800	2.43743800
H	4.25996900	5.19287000	0.39615600
H	3.48719200	4.44264000	-1.84853900
H	1.65103200	2.81068800	-2.05550200
H	3.52678400	1.00731500	0.78326800
H	5.93924600	1.19204900	0.32192800
H	7.05552200	-0.43612400	-1.19472000
H	5.72539300	-2.26114000	-2.23616600
H	3.31195800	-2.46353400	-1.76393700
H	3.23700600	-2.92260700	1.25331100
H	3.12561900	-4.09451500	3.42595000
H	1.28140100	-3.60294200	5.01858500
H	-0.45147700	-1.91973000	4.42284400
H	-0.33807000	-0.74046400	2.24793800
H	0.96692700	-0.63211800	-2.85159900
H	0.03112100	-2.13663200	-4.57288700
H	-0.72789500	-4.42562900	-3.95301300
H	-0.53300700	-5.19094000	-1.59466000
H	0.42090500	-3.69798500	0.12359700
C	-2.19872100	2.68251500	-1.31558200
C	-1.37765300	2.64789200	-0.17263600
C	-1.66689800	3.54976400	0.86463700
C	-2.75206500	4.42954800	0.78040600
C	-3.56622000	4.43831100	-0.35476200
C	-3.28433700	3.56244400	-1.40551000
H	-1.99855600	2.01546400	-2.15189600
H	-1.03473800	3.57855200	1.74811100
H	-2.95580500	5.11494200	1.60023300
H	-4.40391800	5.12720900	-0.42463200
H	-3.90296100	3.56744600	-2.30028000
Si	-3.44983200	-1.12485800	0.21721000
O	-4.28935700	-0.94621900	-1.17840300
O	-3.23538000	-2.67151000	0.70744500
O	-4.18764000	-0.28481400	1.39835600

C	-3.83166000	-1.31725000	-2.48145500
H	-3.60049800	-2.38710800	-2.52924100
H	-4.63454100	-1.09180800	-3.18680800
H	-2.93867000	-0.74742300	-2.75730600
C	-4.25722200	-3.48857400	1.28199900
H	-3.79658800	-4.43767200	1.56527100
H	-4.68278700	-3.01452000	2.17247100
H	-5.05827400	-3.68434000	0.55951500
C	-4.73834000	1.03965100	1.30000000
H	-5.28853300	1.22590000	2.22477600
H	-3.94198400	1.77991200	1.19256000
H	-5.42124300	1.10956100	0.44851000

Procedures for the Stoichiometric Reactions between Arylpalladium Complexes and Silicon Reagents

Stoichiometric Reactions between Arylpalladium Fluoride (**45**) and Silicon Reagents

Arylpalladium fluoride (**45**, 4.11 mg, 0.005 mmol) and 4-trifluoromethylbiphenyl (1.11 mg, 0.005 mmol) were charged into a J-Young tube and transferred into a glove box. A silicon reagent (**42**, **31a**, or **46**, 0.025 mmol) and dry DMF (0.5 mL) were sequentially added into the J-Young tube. After shaken the reaction mixture vigorously, the reaction progress was measured by ^{19}F NMR at 25 ºC. NMR yields of 4-fluoromethylbiphenyl (δ = -116.17 ppm) were determined related to the integration of 4-trifluoromethylbiphenyl (δ = -61.40 ppm) as an internal standard.

Stoichiometric Reactions between Arylpalladium Brimide (**47**) and Silicon Reagents

Arylpalladium bromide (**47**, 4.56 mg, 0.005 mmol) and 4-trifluoromethylbiphenyl (1.11 mg, 0.005 mmol) were charged into a J-Young tube and transferred into a glove box. A silicon reagent (**42**, **31a**, or **46**, 0.025 mmol) and dry DMF (0.5 mL) were sequentially added into the J-Young tube. After shaken the reaction mixture vigorously, the reaction progress was measured by ^{19}F VT-NMR at 70 ºC. NMR yields of 4-fluoromethylbiphenyl (δ = -116.17 ppm) were determined related to the integration of 4-trifluoromethylbiphenyl (δ = -61.40 ppm) as an internal standard.

Preparation of Palladium Complexes and [^{n}Bu$_4$N][PhSiF(OMe)$_3$]

Synthesis of an arylpalladium fluoride complex (**45**)

To a mixture of Pd_2dba_3•$CHCl_3$ (200 mg, 0.194 mmol) and tris(4-fluorophenyl)phosphine (492 mg, 1.55 mmol) in dry toluene (5.0 mL) was added 4-fluoroiodobenzene (46 μL, 0.4 mmol) under N_2. The mixture was stirred at 35 ºC for 12 h under N_2. After the mixture was cooled to 25 ºC, the resulting solution was concentrated under reduced pressure to give a crude product that was purified by recrystallization from hot hexane to give a white solid (297 mg). In a glove box, the white solid (200 mg) was dissolved in dry toluene (8.0 mL), and silver fluoride (79 mg, 0.62 mmol) was added to the solution. The mixture was stirred vigorously at 25 ºC under in dark. After 6 h, the resulting mixture was passed through a pad of Celite®. The resulting solution was concentrated under reduced pressure, and the obtained yellow solid was redissolved in a minimum amount of

$CHCl_3$ (ca. 0.5 mL). The solution was added dropwise into hexane (20 mL) to give a colorless solid which was subsequently filtered and washed with hexane (1 mL× 3) to furnish the titled product (107 mg, 0.13 mmol) in 64% yield.

[CAS: none] Colorless solid. Mp. 100-105 ºC (decomp.). ^{1}H NMR (396 MHz, $CDCl_3$) δ 7.54-7.47 (m, 12H), 7.00 (t, *J* = 8.8 Hz, 12H), 6.45 (t, *J* = 8.0 Hz, 2H), 6.13 (t, *J* = 8.8 Hz, 2H). ^{13}C NMR (100 MHz, $CDCl_3$) δ 164.10 (d, *J* = 253.9 Hz), 160.18 (d, *J* = 242.4 Hz), 136.31 (q, *J* = 7.7 Hz), 126.00 (t, *J* = 23.0 Hz), 115.82 (dt, *J* = 79.4, 5.7 Hz), 114.26 (d, *J* = 19.2 Hz). ^{19}F NMR (372 MHz, $CDCl_3$) δ -108.47, -123.35, -277.94. ^{31}P NMR (160 MHz, $CDCl_3$) δ 18.17. IR (ATR): 3073, 1588, 1493, 1394, 1228, 1160, 1096, 1012, 811, 725 cm^{-1}. Anal. Calcd for $C_{42}H_{28}F_8P_2Pd\cdot 1/2H_2O$: C, 58.52: H, 3.39. Found: C, 58.23: H, 3.39.

Synthesis of an arylpalladium bromide complex (**47**)

To a mixture of Pd_2dba_3•$CHCl_3$ (100 mg, 0.097 mmol) and tris(4-fluorophenyl)phosphine (246 mg, 0.776 mmol) in dry toluene (3.0 mL) was added 4-fluorobromobenzene (22 μL, 0.2 mmol) under N_2. The mixture was stirred at 85 ºC for 12 h under N_2. After the mixture was cooled to 25 ºC, the resulting solution was passed through a pad of silica gel using $CHCl_3$ as an eluent and concentrated under reduced pressure to give a crude product that was purified by recrystallization from hot hexane to give the titled product (137 mg, 0.15 mmol) in 75% yield.

[CAS: none] Colorless solid. Mp. 185 ºC (decomp.). ^{1}H NMR (396 MHz, $CDCl_3$)

δ 7.47-7.41 (m, 12H), 6.99 (t, *J* = 8.8 Hz, 12H), 6.50-6.45 (m, 2H), 6.17 (t, *J* = 9.2 Hz, 2H). ^{13}C NMR (100 MHz, $CDCl_3$) δ 163.92 (d, *J* = 253.9 Hz), 160.40 (d, *J* = 243.3 Hz), 148. 61 (d, *J* = 2.8 Hz), 136.53 (q, *J* = 7.7 Hz), 135.87 (q, *J* = 5.8 Hz), 126.35 (td, *J* = 23.9, 2.8 Hz), 115.56 (dt, *J* = 21.1, 5.7 Hz), 114.94 (d, *J* = 19.2 Hz). ^{19}F NMR (372 MHz, $CDCl_3$) δ -108.45, -122.75. ^{31}P NMR (160 MHz, $CDCl_3$) δ 22.73. IR (ATR): 3059, 1587, 1493, 1393, 1228, 1159, 1093, 1011, 809, 719 cm^{-1}. Anal. Calcd for $C_{42}H_{28}BrF_7P_2Pd \cdot CHCl_3$: C, 49.98: H, 2.83. Found: C, 50.11: H, 2.92.

Preparation of [^{n}Bu$_4$N][PhSiF(OMe)$_3$] (**46**)[10]

In a glove box, trimethoxy(phenyl)silane (**31a**, 39.7 mg, 0.2 mmol) was added to a tetrabutylammonium fluoride solution in THF (1M, 0.2 mL, 0.2 mmol). The resulting mixture was stirred at room temperature for 30 minutes to give a [^{n}Bu$_4$N][PhSiF(OMe)$_3$] solution in THF which was used in the stoichiometric reactions without isolation and purification.

References

(1) (a) Y. Hatanaka, T. Hiyama *J. Am. Chem. Soc.* **1990**, *112*, 7793–7794. (b) T. Hiyama, Y. Hatanaka *Pure & Appkl. Chem.* **1994**, *7*, 1471–1478. (c) Y. Hatanaka, T. Hiyama *Synlett* **1991**, 845–853. (d) S. E. Denmark, R. F. Swais, D. Wehrli *J. Am. Chem. Soc.* **2004**, *126*, 4865–4875. (e) S. E. Denmark, R. F. Swais, *J. Am. Chem. Soc.* **2004**, *126*, 4876–4882.

(2) (a) R. R. Holmes *Chem. Rev.* **1990**, *90*, 17–31. (b) C. Chult, R. J. P. Corriu, C. Reye, J. C. Young *Chem. Rev.* **1993**, *93*, 1371–1448.

(3) For selected examples: (a) V. Corcé, L.-M. Chamoreau, E. Derat, J.-P. Goddard, C. Ollivier, L. Fensterbank *Angew. Chem. Int. Ed.* **2015**, *54*, 11414–11418.; *Angew. Chem.* **2015**, *127*, 11576–11580. (b) M. Jouffroy, D. N. Primer, G. A. Molander *J. Am. Chem. Soc.* **2016**, *138*, 475–478. (c) K. Lin, R. J. Wiles, C. B. Kelly, G. H. M. Davis, G. A. Molander *ACS Catal.* **2017**, *7*, 5129–5133. (d) A. Cartier, E. Levernier, V. Corcé, T. Fukuyama, A.-L. Dhimane, C. Ollivier, I. Ryu, L. Fensterbank *Angew. Chem. Int. Ed.* **2019**, *58*, 1789–1793.; *Angew. Chem.* **2019**, *131*, 1803–1807.

(4) A. Hosomi, S. Kohra, Y. Tominaga *Chem. Pharm. Bull.* **1988**, *36*, 4622–4625.

(5) (a) W. M. Seganish, P. DeShong *J. Org. Chem.* **2004**, *69*, 1137–1143. (b) W. M. Seganish, P. DeShong *Org. Lett.* **2004**, *6*, 4379–4381.

(6) C. Amatore, L. Grimaud, G. Le Duc, A. Jutand *Angew. Chem. Int. Ed.* **2014**, *53*, 6982–6985.; *Angew. Chem.* **2014**, *126*, 7102–7105.

(7) A. Sugiyama, Y. Ohnishi, M. Nakaoka, Y. Nakao, H. Sato, S. Sakaki, Y.

Nakao, T. Hiyama *J. Am. Chem. Soc.* **2008**, *130*, 12975–12985.

(8) (a) A. D. Becke *J.Chem.Phys.* **1993**, *98*, 5648–5652. (b) C. Lee, W. Yang, R. G. Parr, *Phys. Rev. B* **1988**, *37*, 785–789.

(9) Frisch, M. J.; Trucks, G. W.; Schlegel, H. B.; Scuseria, G. E.; Robb, M. A.; Cheeseman, J. R.; Scalmani, G.; Barone, V.; Petersson, G. A.; Nakatsuji, H.; Li, X.; Caricato, M.; Marenich, A. V.; Bloino, J.; Janesko, B. G.; Gomperts, R.; Mennucci, B.; Hratchian, H. P.; Ortiz, J. V.; Izmaylov, A. F.; Sonnenberg, J. L.; Williams-Young, D.; Ding, F.; Lipparini, F.; Egidi, F.; Goings, J.; Peng, B.; Petrone, A.; Henderson, T.; Ranasinghe, D.; Zakrzewski, V. G.; Gao, J.; Rega, N.; Zheng, G.; Liang, W.; Hada, M.; Ehara, M.; Toyota, K.; Fukuda, R.; Hasegawa, J.; Ishida, M.; Nakajima, T.; Honda, Y.; Kitao, O.; Nakai, H.; Vreven, T.; Throssell, K.; Montgomery, J. A., Jr.; Peralta, J. E.; Ogliaro, F.; Bearpark, M. J.; Heyd, J. J.; Brothers, E. N.; Kudin, K. N.; Staroverov, V. N.; Keith, T. A.; Kobayashi, R.; Normand, J.; Raghavachari, K.; Rendell, A. P.; Burant, J. C.; Iyengar, S. S.; Tomasi, J.; Cossi, M.; Millam, J. M.; Klene, M.; Adamo, C.; Cammi, R.; Ochterski, J. W.; Martin, R. L.; Morokuma, K.; Farkas, O.; Foresman, J. B.; Fox, D. J. Gaussian, Inc., Wallingford CT, 2016.

(10) K. H. Shukla, P. DeShong *J. Org. Chem.* **2008**, *73*, 6283–6291.

(11) O. V. Dolomanov, L. J. Bourhis, R. J. Gildea, J. A. K. Howard and H. Puschmann *J. Appl. Cryst.* **2015**, *42*, 339–341.

(12) G. M. Sheldrick *Acta Crystallogr. Sect. C* **2015**, *71*, 3–8.

General Conclusion

The research reported in this thesis has focused on the development of highly efficient methods for realizing Carbon-Carbon bond forming reactions using mol ppb to mol ppm levels of a palladium catalyst.

In Chapter 1, this author has developed an efficient Mizoroki-Heck reaction using a palladium NNC-pincer complex. The Mizoroki-Heck reaction of various aryl halides with alkenes proceeded in the presence of an NNC-pincer palladium complex at 1 to 10 mol ppm loadings to give the corresponding internal alkenes in excellent yields. A mol ppb loading amount of the catalyst was found to promote the reaction of iodobenzene with *n*-butyl acrylate under the neat conditions to afford *n*-butyl cinnamate in 87% yield, where total turnover number and turnover frequency reached up to 870,000,000 and 3,356 s^{-1}, respectively. Reaction rate analyses, transmission electron microscopic measurement of the reaction mixture, and catalyst poisoning tests suggested that the palladium NNC-pincer complex served as a precursor for the generation of a monomeric (single atomic) palladium species. The catalyst was applied in a ten-gram-scale synthesis of the UV-B sunscreen agent octinoxate (2-ethylhexyl 4-methoxycinnamate).

In Chapter 2, the Hiyama cross-coupling reaction using a ppm loading mount of a palladium NNC-pincer complex has been developed. A palladium NNC-pincer complex at a 5 mol ppm loading efficiently catalyzed the Hiyama coupling

reaction of aromatic bromides with aryltrialkoxysilanes in the presence of potassium fluoride in propylene glycol to furnish the corresponding biaryls in up to 99% yield with wide functional group tolerance including a variety of heteroaromatics. To demonstrate the further utility of the reaction system, this method was applied to a multi-gram scale synthesis of adapalene and a synthesis of a liquid-crystalline compound, as well as to the derivatization of triethoxysilylated dextromethorphan and an aryl bromide-tethered norfloxacin.

In Chapter 3, to gain insight into the reason for the high efficiency of the Hiyama cross-coupling reaction, detailed mechanistic studies were conducted. ESI-MS and ^{29}Si NMR analyses of the reaction mixture suggested that aryltrialkoxysilanes reacted with glycol solvents in the presence of potassium fluoride as a base to afford glycol-derived pentacoordinate spirosilicate intermediates in situ. A single-crystal x-ray analysis of the spirosilicate clearly confirmed its structural nature. Preliminary theoretical studies and stoichiometric reactions on the transmetalation between arylpalladium halides and silicon reagents substantiated that the glycol-derived pentacoordinate spirosilicate intermediates are quite reactive silicon reactants in the transmetalation step.

Collectively, these results showed the high utility of the palladium NNC-pincer complex as a catalyst for reducing the catalyst loading in several carbon-carbon bond forming reactions. The in situ-generation of a catalytically active species as

well as highly active reactants is the key concept to realize the efficient coupling reactions. This author believes that these work in this thesis may provide a promising way to reduce the catalyst loading to mol ppm amounts or less in industrial processes.

Acknowledgement

This thesis summarizes my Ph.D. research from April 2015 to March 2020 at the Department of Functional Molecular Science, School of Physical Sciences, The Graduate University for Advanced Studies (SOKENDAI) under the supervision of Professor Yasuhiro Uozumi.

First, I would like to express my greatest appreciation to my supervisor, Professor Yasuhiro Uozumi for his guidance, patience, encouragement, and continuous support of my research. I have learned a lot not only science but also human nature from him.

Also, I am deeply grateful to Professor Toshiaki Mase, Assistant Professors Dr. Takao Osako and Dr. Go Hamasaka for their encouragement, incisive advice, and valuable discussions.

I would like to express my appreciation to current members and alumni of Uozumi group, Dr. Makoto Nagaosa, Dr. Shiguang Pan, Dr. Shuichi Hirata, Dr. David Roy, Dr. Anggi Eka Putra, Dr. Shuo Yan, Dr. Kim Kiseong, Dr. Yuya Sugiyama, Dr. Guanshuo Shen, Ms. Ryoko Niimi and Mr. Kazuki Tani for their helpful discussions and cooperation. I am also grateful the kind help of technician staffs, Ms. Kaoru Torii, Ms. Aya Tazawa, Mr. Tatsushi Tsuchimoto, and Mr. Kotaro Yamamura. I also wish to thank the assistance of secretaries, Ms. Tokiyo Sasaki, Ms. Mayuko Taniwake, Ms. Kozue Hazama, and Ms. Tomoko Fukushima.

I would like to thank Dr. Pondchanok Chinapang, and Professors Mio Kondo and Shigeyuki Masaoka for performing the X-ray crystallography. I appreciate

Professors Masanari Nagasaka and Hikaru Takaya for taking X-ray absorption spectra at UVSOR. I also would like to thank Mr. Seiji Makita and Ms. Kiyoe Fujikawa for the help in elemental analysis and FAB-MS.

I would like to express my gratitude to Professor Timothy M. Swager for hosting my visit at Massachusetts Institute of Technology, and to him, Dr. Nathan A. Romero, Mr. Kosuke Yoshinaga, and Mr. Kohei Yumino, and other members in Swager's group for their support during my stay at MIT.

I express my appreciation to the financial support during my Ph.D. research from IMS SRA, Course-by-course Education Program (SOKENDAI), and the JSPS (Research Fellowship for Young Scientists, DC1, Grant Number 17J05446).

Finally, I am deeply grateful to my father Masatsugu Ichii, mother Shoko Ichii, and sisters Asako Ichii and Mako Ichii, all friends, and all relatives for their care, encouragement, and financial support.

Shun Ichii

List of Publications

Chapter 1

Go Hamsaka, Shun Ichii, and Yasuhiro Uozumi

"A Palladium NNC-Pincer Complex as an Efficient Catalyst Precursor for the Mizoroki-Heck Reaction"

Adv. Synth. Catal. **2018**, *360*, 1833-1840.

Chapter 2

Shun Ichii, Go Hamasaka and Yasuhiro Uozumi

"The Hiyama Cross-Coupling Reaction at Parts Per Million Levels of Pd: In Situ Formation of Highly Active Spirosilicates in Glycol Solvents"

Chem. Asian J. **2019**, *14*, 3850-3854.

Chapter3

Shun Ichii, Go Hamasaka and Yasuhiro Uozumi

Manuscript in preparation

Other Publications

Yang Zhu, Takahiro Nakanishi, Kazuyoshi Kanamori, Kazuki Nakanishi, Shun Ichii, Kohji Iwaida, Yu Masui, Toshiyuki Kamei, Toyoshi Shimada, Akihito Kumamoto, Yumi H. Ikuhara, Mina Jeon, George Hasegawa, Masamoto Tafu, Chang Won Yoon, and Tewodros Asefa

"Amine/Hydrido Bifunctional Nanoporous Silica with Small Metal Nanoparticles Made Onsite: Efficient Dehydrogenation Catalyst"

ACS Appl. Mater. Interfaces **2017**, *9*, 36–41.

Nirmalya Moitra, Shun Ichii, Toshiyuki Kamei, Kazuyoshi Kanamori, Yang Zhu, Kazuyuki Takeda, Kazuki Nakanishi, and Toyoshi Shimada

"Surface Functionalization of Silica by Si−H Activation of Hydrosilanes"

J. Am. Chem. Soc. **2014**, *136*, 11570–11573.